

X-BAND HIGH POWER SOLID STATE RF SWITCH

A THESIS SUBMITTED TO
THE GRADUATE SCHOOL OF NATURAL AND APPLIED SCIENCES
OF
MIDDLE EAST TECHNICAL UNIVERSITY

BY

KUTLAY GÜZEL

IN PARTIAL FULFILLMENT OF THE REQUIREMENTS
FOR
THE DEGREE OF MASTER OF SCIENCE
IN
ELECTRICAL AND ELECTRONICS ENGINEERING

SEPTEMBER 2012

Approval of the thesis:

X-BAND HIGH POWER SOLID STATE RF SWITCH

submitted by **KUTLAY GÜZEL** in partial fulfillment of the requirements for the degree of **Master of Science in Electrical and Electronics Engineering Department, Middle East Technical University** by,

Prof. Dr. Canan Özgen
Dean, Graduate School of **Natural and Applied Sciences** _____

Prof. Dr. İsmet Erkmen
Head of Department, **Electrical and Electronics Engineering** _____

Assoc. Prof. Dr. Şimşek Demir
Supervisor, **Electrical and Electronics Engineering Dept., METU** _____

Examining Committee Members:

Prof. Dr. Canan Toker
Electrical and Electronics Engineering Dept., METU _____

Assoc. Prof. Dr. Şimşek Demir
Electrical and Electronics Engineering Dept., METU _____

Prof. Dr. Nevzat Yıldırım
Electrical and Electronics Engineering Dept., METU _____

Prof. Dr. Gönül Turhan Sayan
Electrical and Electronics Engineering Dept., METU _____

Dr. Mustafa Akkul
ASELSAN Inc. _____

Date: 10.09.2012

I hereby declare that all information in this document has been obtained and presented in accordance with academic rules and ethical conduct. I also declare that, as required by these rules and conduct, I have fully cited and referenced all material and results that are not original to this work.

Name, Last name : Kutlay Güzel

Signature :

ABSTRACT

X-BAND HIGH POWER SOLID STATE RF SWITCH

Güzel, Kutlay

M.S., Department of Electrical and Electronics Engineering

Supervisor: Assoc. Prof. Dr. Şimşek Demir

September 2012, 89 pages

RF/Microwave switches are widely used in microwave measurement systems, telecommunication and radar applications. The main purposes of RF switches are Tx-Rx switching, band select and switching the signal between different paths. Thus, they are key circuits especially in T/R modules. Wideband operation is an important criterion in EW applications. High power handling is also a key feature especially for radars detecting long range.

In this study, different types of high power solid state switches operating at X-Band are designed, fabricated and measured. The main objectives are small size and high power handling while keeping good return loss and low insertion loss. The related studies are investigated and analyzed. Solutions for increasing the power handling are investigated, related calculations are done. Better bias conditions are also analyzed. The measurement results are compared with simulations and analysis. Circuit designs and simulations are performed using AWR[®] and CST[®].

Keywords: Solid State Switch, High Power RF Switch, PIN Diode, SPDT

ÖZ

X-BANT YÜKSEK GÜÇLÜ KATI HAL RF ANAHTAR

Güzel, Kutlay

Yüksek Lisans, Elektrik ve Elektronik Mühendisliği Bölümü

Tez Yöneticisi: Doç. Dr. Şimşek Demir

Eylül 2012, 89 sayfa

RF/Mikrodalga anahtarlar mikrodalga ölçüm sistemlerinde, telekomunikasyon ve radar uygulamalarında sıklıkla kullanılmaktadır. RF anahtarların başlıca amacı Tx-Rx anahtarlama, bant seçimi ve işaretin farklı kanallar arasında anahtarlanmasıdır. Bu yüzden anahtarlar özellikle T/R modüllerde kullanılan başlıca devrelerden biridir. Elektronik harp uygulamalarında geniş bant operasyon önemli bir kriterdir. Özellikle uzak mesafeleri algılayabilen radarlarda yüksek güç dayanımı da önemli bir özelliktir.

Bu çalışmada X-Bant'ta çalışabilen farklı tipte yüksek güçlü anahtarlar tasarlanmış, üretilmiş ve ölçülmüştür. Temel hedef iyi geri dönüş kaybı ve düşük araya girme kaybını korurken küçük boyut ve yüksek güç dayanımını elde edebilmektir. İlgili çalışmalar araştırılmış ve analiz edilmiştir. Güç dayanımını artırmak için çözümler araştırılmış, ilgili hesaplamalar yapılmıştır. Daha iyi besleme durumları analiz edilmiştir. Ölçüm sonuçları benzetim ve analizlerle karşılaştırılmıştır. Devre tasarımları ve benzetimleri AWR® ve CST® kullanılarak yapılmıştır.

Anahtar Kelimeler: Katı Hal Anahtar, Yüksek Güçlü RF Anahtar, PIN Diyot, SPDT

To my Father

ACKNOWLEDGEMENTS

I would like to express my sincere gratitude to my advisor Assoc. Prof. Dr. Şimşek Demir for his valuable supervision, support and encouragement throughout this thesis study.

I would like to thank ASELSAN Inc. for financing my studies and providing all the resources and facilities.

I present my special thanks to my manager Dr. Mustafa Akkul for sharing his precious experience. I also would like to thank Tuncay Erdöl and Dr. Taylan Eker for their guidance. With his suggestions, Dr. Eker made me gain different point of view and I could easily find solutions whenever I stuck.

I would like to thank Volkan Dikiş, Evren Ünsal and Ömer Öçal for their interest and attention during the PCB production. I also express my thanks to Arda Özgen for his great effort to design and manufacture the cases for high power measurements within a very short period of time. With their experience and talent, Murat Mutluol, Kenan Sayar and Sedat Pehlivan assembled all the microwave components in clean room with great fastidiousness, so I would like to acknowledge my gratitude to them.

Special thanks to my friends Mustafa İncebacak, Zafer Tanç, Hakkı İlhan Altan and Mustafa Barış Dinç for their encouragement and technical support.

I am grateful to Elif Demirel for her patience, morale support and help. She stood next to me throughout my graduate study giving me the strength to successfully finish this thesis work.

Lastly, I would like to express my sincere thanks to my mother Hafize and my brother Tolgay for their understanding and support during this work.

TABLE OF CONTENTS

ABSTRACT	iv
ÖZ	v
ACKNOWLEDGEMENTS	vii
TABLE OF CONTENTS	viii
LIST OF TABLES	x
LIST OF FIGURES	xi
LIST of ABBREVIATIONS	xiv
CHAPTERS	
1. INTRODUCTION	1
1.1 Microwave Switch Types and State of RF Switches	2
1.2 Literature Review	4
1.3 Outline of Thesis	5
2. PIN DIODE AND PIN DIODE SWITCH BACKGROUND	7
2.1 PIN Diode Fundamentals	7
2.1.1 Forward Biased PIN Diode	8
2.1.2 Reverse Biased PIN Diode	9
2.1.3 Power Handling and Thermal Issues	10
2.1.4 Switching Speed	11
2.2 PIN Diode Switch Topologies	12
2.2.1 Series Switch	12
2.2.2 Shunt Switch	14
2.2.3 Series-Shunt Switch	17
2.3 High Power PIN Diode Switching	18
2.3.1 PIN Diodes for High Power Applications	19
3. HIGH POWER PIN DIODE SWITCH DESIGN FOR X-BAND	21
3.1 PIN Diode Selection	21
3.2 Characterization of the PIN Diodes	22
3.3 Shunt SPDT Switch Design	23
3.3.1 Shunt SPDT Switch Design Using MPN7315	24

3.3.2	Shunt SPDT Switch Design Using MPN7453A	30
3.3.3	Shunt SPDT Switch Design Using MPN7453B	34
4.	FABRICATION AND MEASUREMENTS OF X-BAND HIGH POWER SWITCHES	40
4.1	Dielectric Substrate Choice.....	40
4.2	Fabrication of the High Power Switches.....	42
4.3	Small Signal S-Parameter Measurements	44
4.4	Establishing the Minimum Reverse Bias	49
4.5	Self Generated DC Voltage Measurements	53
4.6	High Power Measurements	56
4.7	Second Harmonic and IP3 Measurements	60
4.8	Summary of Results and Comparison with Simulations.....	64
5.	CRITICAL DESIGN RULES FOR HIGH POWER SWITCH APPLICATIONS	68
5.1	PIN Diode Failure	68
5.2	Failure of RF Choke Inductor	71
5.3	Increasing the Power Handling	75
5.4	Increasing the Power Handling and Isolation while Keeping DC Current Consumption Low	82
6.	CONCLUSION	86
	REFERENCES.....	88

LIST OF TABLES

TABLES

Table 3.1: Electrical Parameters of Selected PIN Diodes.....	22
Table 4.1: Expected and Measured Self Generated DC Voltages Under Expected Power Handlings	56
Table 4.2: Expected Power Handlings and Power Dissipations	58
Table 4.3: Breakdown Voltages and Peak Pulsed Power Handlings of the Switches	60
Table 4.4: IP3 and Second Harmonic Suppression of the High Power Switches	63
Table 4.5: Summary of General Performance of Switches at X-Band	67

LIST OF FIGURES

FIGURES

Figure 2.1: Forward Bias Lumped Element Model	8
Figure 2.2: Reverse Bias Lumped Element Model	9
Figure 2.3: Series SPST PIN Diode Switch	13
Figure 2.4: Series SPDT Switch	14
Figure 2.5: Shunt SPST PIN Diode Switch	15
Figure 2.6: Shunt SPDT Switch	17
Figure 2.7: Series-Shunt SPST PIN Diode Switch	18
Figure 3.1: Measurement for PIN Diode Characterization	22
Figure 3.2: Measured Structure for Sample PIN Diode Characterization	23
Figure 3.3: Shunt SPDT Switch Using MPN7315	24
Figure 3.4: Simulation Result of X-Band Switch with MPN7315	25
Figure 3.5: Lumped Equivalent Model of Forward Biased Shunt MPN7315	26
Figure 3.6: Lumped Equivalent Model Compared with Measured Shunt MPN7315 at 48mA Forward Current	27
Figure 3.7: Lumped Equivalent Model of Reverse Biased Shunt MPN7315	27
Figure 3.8: Lumped Equivalent Model Compared with Measured Shunt MPN7315 at -10V	28
Figure 3.9: Lumped Equivalent Switch Compared with Switch Designed Using De- embedded Sample MPN7315 Measurements	29
Figure 3.10: Shunt SPDT Switch Using MPN7453A	30
Figure 3.11: Simulation Result of X-Band Switch with MPN7453A	31
Figure 3.12: Lumped Equivalent Model of Forward Biased Shunt MPN7453A	31
Figure 3.13: Lumped Equivalent Model Compared with Measured Shunt MPN7453A at 65mA Forward Current	32
Figure 3.14: Lumped Equivalent Model of Reverse Biased Shunt MPN7453A	32
Figure 3.15: Lumped Equivalent Model Compared with Measured Shunt MPN7453A at -10V	33

Figure 3.16: Lumped Equivalent Switch Compared with Switch Designed Using De-embedded Sample MPN7453A Measurements	34
Figure 3.17: Shunt SPDT Switch Using MPN7453B	35
Figure 3.18: Simulation Result of X-Band Switch with MPN7453B	35
Figure 3.19: Lumped Equivalent Model of Forward Biased Shunt MPN7453B	36
Figure 3.20: Forward State Lumped Equivalent Compared with Measured Shunt MPN7453B	36
Figure 3.21: Lumped Equivalent Model of Reverse Biased Shunt MPN7453B	37
Figure 3.22: Lumped Equivalent Compared with Measured Shunt MPN7453B at -25V	38
Figure 3.23: Lumped Equivalent Switch Compared with Switch Designed Using De-embedded Sample MPN7453B Measurements	38
Figure 4.1: Sample T-junction	43
Figure 4.2: X-Band Switch with MPN7315	44
Figure 4.3: Measured S-parameters of SPDT Switch with MPN7315	45
Figure 4.4: X-Band Switch with MPN7453A	46
Figure 4.5: Measured S-parameters of SPDT Switch with MPN7453A	47
Figure 4.6: X-Band Switch with MPN7453B	48
Figure 4.7: Measured S-parameters of SPDT Switch with MPN7453B	49
Figure 4.8: Self Generated DC Voltage Measurement Setup	53
Figure 4.9: MPN7315 Measured Self Generated DC Voltage vs Expected	54
Figure 4.10: MPN7453A Measured Self Generated DC Voltage vs Expected	54
Figure 4.11: MPN7453B Measured Self Generated DC Voltage vs Expected	55
Figure 4.12: High Power Measurement Setup	56
Figure 4.13: Constructed Switch Module	57
Figure 4.14: Switch Module Attached on the Heat-Sink	57
Figure 4.15: Temperature Rise of Carriers at Their Expected Power Handlings	58
Figure 4.16: Setup for Measurements of Peak Pulsed Power	59
Figure 4.17: Reverse Voltage vs Output IP3 of Switch with MPN7315	61
Figure 4.18: Reverse Voltage vs Second Harmonic of Switch with MPN7315	62
Figure 4.19: Reverse Voltage vs Loss of Switch with MPN7315	62
Figure 4.20: Reverse Voltage vs Second Harmonic of Switch with MPN7453B	63
Figure 4.21: Simulation and Measurement Comparison of Switch with MPN7315	64

Figure 4.22: Simulation and Measurement Comparison of Switch with MPN7453A	65
Figure 4.23: Simulation and Measurement Comparison of Switch with MPN7453B	65
Figure 5.1: Excess Incident Power Applied on a PIN Diode Switch.....	69
Figure 5.2: Excess Instantaneous Voltage Applied on a PIN Diode.....	70
Figure 5.3: Simulation of Currents Through Biasing Arms at 9W Switch.....	72
Figure 5.4: Currents Through Biasing Arms at 9W Switch.....	73
Figure 5.5: Currents Through Biasing Arms at 80W Switch.....	74
Figure 5.6: RF Choke Inductor after High Current Passed Through It.....	75
Figure 5.7: S-parameters of a Regular Shunt Switch with two MPN7315s at Each Arm	76
Figure 5.8: Impedances of Arms at Regular Shunt Switch.....	78
Figure 5.9: Impedances of Arms at Shunt Switch Matched with Small DC Block Capacitors.....	78
Figure 5.10: Higher Power Switch Designed Using Two MPN7315s at Each Arm .	79
Figure 5.11: Simulated Small Signal S-parameters of the Switch in Figure 5.10	79
Figure 5.12: Currents Through the Forward Biased PIN Diodes at Small Signal	80
Figure 5.13: Measured S-parameters of the Switch with Higher Power Handling....	81
Figure 5.14: Shunt SPDT Switch with Increased Isolation	82
Figure 5.15: Isolations Compared for Different Number of Shunt Diodes	83
Figure 5.16: SPDT Switch with Increased Power Handling and Isolation with Low DC Current Consumption	84
Figure 5.17: S-Parameters of SPDT Switch Given in Figure 5.16	85

LIST of ABBREVIATIONS

ABBREVIATIONS

CMOS	: Complementary Metal Oxide Semiconductor
CW	: Continuous Wave
DC	: Direct Current
FET	: Field-Effect Transistor
GaAs	: Gallium Arsenide
GaN	: Gallium Nitride
IC	: Integrated Circuit
IP3	: Third-Order Intercept Point
I-region	: Intrinsic Region
MEMS	: Micro-Electromechanical Systems
MESFET	: Metal Semiconductor Field-Effect Transistor
MMIC	: Monolithic Microwave Integrated Circuit
PCB	: Printed Circuit Board
PHEMT	: Pseudomorphic High Electron Mobility Transistor
RF	: Radio Frequency
SOI	: Silicon-on-Insulator
SOS	: Silicon-on-Sapphire
SPDT	: Single-Pole-Double-Throw
SPNT	: Single-Pole-N-Throw
SPST	: Single-Pole-Single-Throw
TWTA	: Travelling Wave Tube Amplifier
Tx/Rx	: Transmit/Receive
VSWR	: Voltage Standing Wave Ratio

CHAPTER 1

INTRODUCTION

In general, switches have been one of the key components in our daily lives. The main purpose of a switch is changing the connection paths.

The first electrical switches entered our lives with the invention of electricity. Routing the signal from generator to buildings, turning the lights on and off, shutting down the electricity are all performed using switches. Switches also found place in RF and microwave applications. RF and microwave switches are extensively used in wireless systems for the main purpose of signal routing. An RF switch allows performing different tests on the system without making connects or disconnects. The applications of switches in radar and communication systems are mainly Tx/Rx switching, band selection and routing the signal between different RF paths.

In radar systems which are designed for detecting targets at long distances, the effective isotropic radiated power is increased to increase the probability of detection. In other words, the transmitted power is pulled up to high levels. For such applications, the switch at the high power side should be able to handle that amount of power. In a high power Tx/Rx application, relatively large circulators can be replaced with high power switches of much smaller size. Switches can also provide better isolation compared to single junction circulators so that the low noise amplifier at the receiver chain is protected during transmit. High power switches can also be seen in applications where the high power signal is routed to antennas with different polarizations.

1.1 Microwave Switch Types and State of RF Switches

RF and microwave switches can be categorized into two main groups :

- Electromechanical Switches
- Solid State Switches

Electromechanical switches generally have low insertion loss and good isolation. They can handle signals at very high power levels. However, their switching speed is slow. Their repeatability is not perfect and they suffer from lifetime. They are also sensitive to vibration. Electromechanical switches are making some new in-roads in the form of micro-electromechanical-systems (MEMS) devices [1]. Recent generation MEMS switches have solved many of the reliability and reproducibility problems making them competitive in several applications.

Solid state switches have higher ON resistance when compared to their electromechanical counterparts, thus their insertion loss is higher. Their power handling is also worse than electromechanical switches. However, they provide fast switching speeds. They are resistant to shock and vibration. They are also much more reliable. They exhibit longer lifetime. They can also be realized in small size.

PIN diodes were the first widely used solid state switching technology. Providing lower insertion loss and better power handling capability than most IC FETs they are still in wide use today. An important figure of merit for switches, $R_{on}C_{off}$ product, is usually in the range of 100-200fs for PIN diode switches, which is another fact that makes PIN diodes preferable. However; depending on the thickness of the intrinsic region, PIN diode switches have a limit on operation at low frequencies. Another limitation of PIN diode switches is their power consumption. Since PIN diodes are current controlled devices, they consume more power than voltage controlled FET switches.

GaAs FET switches have started being widely used since the 80s. FET transistors operate as voltage controlled variable resistors. This property makes them useful for applications requiring low power consumption like mobile applications. Their ON resistance is a little larger so their insertion loss is generally higher than their PIN diode counterparts. With the development of PHEMT MMIC devices, lower ON resistance than that of MESFET MMICs is obtained; however, they suffer from gate lag which causes the switching time increase to several microseconds while MESFETs can provide switching speeds down to tens of picoseconds. CMOS SOI (silicon-on-insulator) and CMOS SOS (silicon-on-sapphire) do not suffer from gate lag but they still suffer from low switching speeds since they are designed to optimize the tradeoff between low frequency operation and switching speed. With the recent developments, SOS and SOI FET switches have been competing with GaAs switches as their cut-off frequency, breakdown voltages and insulating substrate quality improved [1]. Their linearity also has been improved allowing them to operate at higher power levels. However, the high power territory is still dominated by the PIN diode switches.

With the use of GaN, the power levels obtained from a single MMIC have been improved in high power amplifier applications. Some GaN suppliers started to release their high power switch products. Although many GaN suppliers have good processing background, processing of GaN is not as mature as GaAs. With the increasing demand for high power switches with less current consumption, GaN seems to be the future technology for especially military and satellite applications [1].

To summarize the state of RF and microwave switches, the GaAs MMIC is the most widely used technology in medium and low power levels. Although SOS and SOI switches have been improved, high power switching at high frequencies is still dominated by PIN diodes. GaN switches stand as the promising technology for the future in high power applications.

1.2 Literature Review

In high power switch applications, main limitations are the power handling of critical components and excess temperature rise. There are two mechanisms that limit the power handling of solid state devices used in a switch. One is the large voltage swing on the *OFF* device, the other is the current handling of the *ON* device. Also, the switch should be heat sunk well in order to cope with the excess heat dissipated on the structure.

Series connected PIN diode's power handling is generally poor [2]. In most high power PIN diode switch applications, all-shunt configuration is chosen since it is easier to heat sink the shunt diode rather than series diode [3]**Error! Reference source not found.** Having better heat sink, observed temperature rise is far less on the most critical component PIN diode.

In order to prevent failure during the large voltage swing, PIN diode should have large breakdown voltage as Sherman [4][4] pointed out. Tenenholtz [5] states that effective breakdown voltage can be increased by connecting two pairs of diodes back to back in a series-shunt configuration.

In a shunt Tx/Rx switch, the shunt diode in receive arm will be carrying the same RF current as the antenna during transmit, thus this diode should have good power dissipation capability [2]. In order to decrease the dissipated power on this device, a PIN diode with low *ON* resistance should be chosen. Vertical epitaxial structure is expected to provide much lower resistance when forward biased than planar ion implanted PIN diodes [6]. This structure also has higher power handling capability than MESFETs. Thus, in most applications with high power handling, very special epitaxial PIN diodes are designed.

A good solution in such high power applications can be reducing the power dissipation in critical components rather than improving heat sink. Multi-section transformers can be used to transform to a lower impedance at the diode which

increases the bandwidth while reducing the RF voltage at the diode allowing the use of faster diodes [7]. Using two shunt PIN diodes in one arm which are connected at the same node can be an alternative solution for reducing the power dissipation. Utilizing this technique, the RF current on the forward biased diode is shared by two diodes, which significantly lowers the power dissipation on each diode. This technique is used in most high power MMIC switches like [8].

Shunt switches do not offer wideband operation due to the quarter wavelength transmission lines used. However; shunt switches offer better heat sink which is very important in high power applications. Thus, it is generally difficult to construct a wideband high power switch. Some matching methods used in small signal may not be applicable at high power. Inserting a matching section at the output ports, high power PIN diodes can be matched within a large bandwidth as in [3].

Similar solutions can be applied for FET switches. FETs chosen for such high power switching application should have large gate peripheries to handle the required RF current as in [9]. It is also stated in [10] that using dual-gate FETs, the gate periphery can be increased. Also, use of dual-gate FETs allows the designer to distribute RF voltage swing into two devices, thus the voltage swing requirement can be satisfied easily.

With the use of promising future technology GaN in such applications, higher power RF signals can be switched. Although this technology is not mature yet, there are several high power GaN MMIC switches in the market [11], [12].

1.3 Outline of Thesis

In Chapter 2, general properties of PIN diodes are described. PIN diode switches of different topologies are analyzed and general performance characteristics are presented. Also, high power performance of each topology is discussed.

In Chapter 3, PIN diodes for the applications are chosen. Each PIN diode is measured and characterized. Three PIN diode switches with different power handling capabilities are designed to operate at X-Band. Related simulation results are given.

Fabrication process and measurements of designed switches are given in Chapter 4. Measurements include S-parameters, power handling, harmonics and switching speed. Measured frequency response is compared with simulations. In this chapter, a theory on establishing the minimum reverse bias voltage in high power PIN diode applications is given in detail. Minimum reverse bias need is found using this theory and measurements done. Nonlinear characteristics at this reverse bias are analyzed.

In Chapter 5, failure mechanisms of a high power PIN diode switch are given. In addition, a method for increasing the power handling by decreasing the power dissipation on critical components is analyzed. This method is justified with high power measurements. Another design with higher power handling and higher isolation is introduced as future work. The main point of this final design is to obtain low DC power consumption although the number of PIN diodes increased.

A brief conclusion about this thesis study is given in the final chapter.

CHAPTER 2

PIN DIODE AND PIN DIODE SWITCH BACKGROUND

2.1 PIN Diode Fundamentals

PIN diode is a device whose impedance at RF and microwave frequencies is controlled by the DC current passing through it. The name PIN comes from the initials of the layers in the structure, namely a high-resistivity intrinsic region placed between positive and negative regions. At RF and microwave frequencies, PIN diodes can be considered as current controlled resistors whose resistance can be varied from a few milliohms to tens of kilo-ohms.

PIN diodes mainly have two states: forward bias and reverse bias. When the PIN diode is forward biased, holes and electrons are injected into the I-region [13]. These charges stay alive for an average time which is called carrier lifetime, τ . Thus, an average charge Q is stored in the I-region which lowers the resistance. On the other hand, when the PIN diode is at reverse bias condition, no charge is stored in the I-region. In this condition the PIN diode behaves as a capacitor in parallel with a high resistance. The reverse bias state is also called zero bias state.

The PIN diodes are specified with the following parameters:

C_T : total capacitance at reverse bias

R_p : parallel resistance at reverse bias

V_r : maximum allowed reverse bias voltage

R_s : series resistance when forward biased

τ : carrier lifetime

θ_{av} : average thermal resistance

P_D : maximum average power dissipation

W : intrinsic region width

It is possible to obtain the same R_s and C_t values with PIN diodes of different geometries. However, the performance will differ at high power levels. As the width of the I-region gets thicker, the breakdown voltage gets higher, the diode will have better distortion characteristics and the diode can handle high power levels. On the other hand, switching speed gets worse.

At frequencies below the transit time frequency of the I-region, the PIN diode behaves like a PN junction semiconductor diode [13]. The low frequency operation of a PIN diode primarily depends on its carrier lifetime and intrinsic region width.

2.1.1 Forward Biased PIN Diode

At forward bias, the PIN diode behaves like a small resistor with a series inductance as in Figure 2.1.

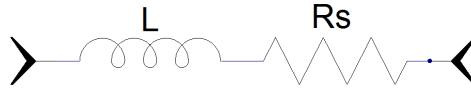


Figure 2.1: Forward Bias Lumped Element Model

When a DC current passes through the PIN diode, the holes and electrons are injected into the I-region and an amount of charge is stored here [14]. This stored charge is related to the forward bias current I_f and the carrier lifetime τ as:

$$Q = \tau I_f \text{ coulombs} \quad (2-1)$$

The series resistance of the PIN diode is inversely proportional to Q

$$R_s = \frac{W^2}{(\mu_n + \mu_p)Q} \text{ ohms} \quad (2-2)$$

where μ_n and μ_p are the electron and hole mobilities, respectively. This equation is valid for frequencies higher than the transit time frequency.

$$f > \frac{1300}{W^2} \quad (2-3)$$

where f is in MHz and W is in μm .

The series resistance of the PIN diode is generally limited by the parasitic resistance of the package in commercially available PIN diodes.

In a high power application, the PIN diode must be forward biased such that the stored charge Q is much greater than the incremental stored charge added or removed by the high RF current [13]. Thus, the inequality below must be satisfied.

$$Q \gg \frac{I_{RF}}{2\pi f} \quad \text{ohms} \quad (2-4)$$

2.1.2 Reverse Biased PIN Diode

At reverse bias, the PIN diode behaves like a capacitance in parallel with a high resistor. Also a small inductance might be added in series to this parallel structure as seen in Figure 2.2.

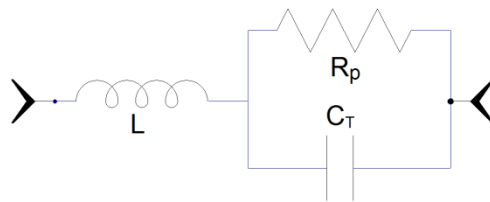


Figure 2.2: Reverse Bias Lumped Element Model

When the PIN diode is in reverse or zero bias condition, the carriers are depleted from the I-region, allowing the diode to behave as a high impedance device. The

capacitance of the reverse biased PIN diode can be simply calculated as the parallel plate capacitance.

$$C = \frac{\epsilon A}{W} \quad F \quad (2-5)$$

where ϵ is the dielectric constant of silicon, A is the area of diode junction. This equation is valid at frequencies above the relaxation frequency of the I-region.

$$f > \frac{1}{2\pi\rho\epsilon} \quad Hz \quad (2-6)$$

where ρ is the resistivity of the I-region. At frequencies lower than dielectric relaxation frequency, the PIN diode behaves as a varactor diode.

The value of parallel resistance R_p is usually higher than the reactance of C_T . The value of R_p increases as the applied reverse voltage is increased.

The applied reverse voltage should not be more than its voltage rating. In high power applications, the peak RF voltage should also be taken into account. In other words, the sum of applied reverse voltage and RF voltage should not exceed the breakdown voltage.

2.1.3 Power Handling and Thermal Issues

The PIN diode power handling is limited either by its breakdown voltage or its maximum power dissipation capability. Generally, the power handling limit is set by its power dissipation capability.

The dissipated power on a PIN diode should be carefully calculated, especially in a high power application. The allowed power dissipation on a PIN diode is

$$P_D = \frac{(T_j - T_a)}{\theta_{av}} \quad W \quad (2-7)$$

where T_j is the maximum junction temperature, T_a is the temperature of the ambient or the back plate and θ_{av} is the average thermal resistance. This equation can be used for CW applications. In pulsed applications, the approximation can be done by multiplying the equation by the duty factor. If the pulse width is less than the thermal time constant of the diode, the junction temperature reaches to a lower level than that found. The exact calculation can be done for short pulses.

Since the PIN diodes can control high power levels of RF with much lower levels of DC power, the dissipated DC power can be neglected in a high power application. In order to have a long operating life, it should be avoided to operate at temperatures close to maximum junction temperature.

It is also necessary to check if the power handling found by dissipated power satisfies the breakdown voltage specification of the PIN diode.

2.1.4 Switching Speed

Another important specification of PIN diode circuits is the switching speed. There are two switching speed characteristics; from forward to reverse bias, T_{FR} , and from reverse to forward bias, T_{RF} . T_{FR} depends primarily on carrier lifetime. The forward and initial reverse currents also take place in the equation.

$$T_{FR} = \tau \log_e \left(1 + \frac{I_F}{I_R} \right) \quad sec \quad (2-8)$$

This equation holds for small forward currents. However; the switching will be faster if the forward current level is saturating the I-region with holes and electrons.

On the other hand, T_{RF} primarily depends on I-region width. The reverse to forward bias switching does not occur as fast as forward to reverse bias switching. In other words, an instantaneous excursion of RF signal into the positive bias direction does not cause a reverse biased diode to go into conduction [13]. Thus, as the operation

frequency increases, necessary reverse bias voltage levels to handle high RF power levels decreases; i.e, reverse voltage does not have to be the same magnitude as peak RF voltage [14].

2.2 PIN Diode Switch Topologies

PIN diode switch performance is described with three main parameters; isolation, insertion loss and power handling. Isolation is a measure of how effectively the circuit is turned off. It is the difference between the output power when the switch is on and the output power when the switch is off. Insertion loss is the sum of resistive loss and mismatch loss when the switch is on. Power handling is also another parameter that PIN diode switches are evaluated. Although power handling depends mainly on the choice of PIN diode, circuit configuration and other circuit parameters should also be considered.

There are different types of switch topologies which have different advantages on these three switch performance parameters.

2.2.1 Series Switch

Series connected switches are commonly used for applications where low insertion loss over a wide frequency range is needed [13]. In this topology, the series connected PIN diode is conducting the RF signal when it is forward biased. When it is reverse biased, the switch is in isolation condition. The insertion loss primarily depends on the series resistance of the PIN diode. On the other hand, the maximum isolation depends on the off capacitance. High off capacitance may provide a leakage path for the RF signal. A sample series SPST switch is shown in Figure 2.3.

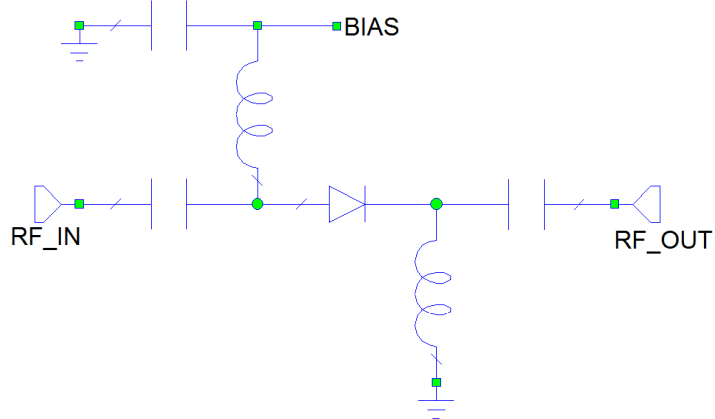


Figure 2.3: Series SPST PIN Diode Switch

For an SPST series switch the insertion loss, IL , can be calculated with;

$$IL = 20 \log \left[1 + \frac{R_s}{2Z_0} \right] \quad dB \quad (2-9)$$

For SPNT switches, the insertion loss is a little higher.

The isolation of an SPST series switch can be found by;

$$Isolation = 10 \log[1 + (4\pi f C Z_0)^{-2}] \quad dB \quad (2-10)$$

For multi-throw switches, the isolation is 6dB higher than that found above, due to the voltage reduction across the off diode [13].

The dissipated power on forward biased PIN diode in series configuration can be found by;

$$P_D = \frac{4R_s Z_0}{(2Z_0 + R_s)^2} P_{av} \quad W \quad (2-11)$$

For very small values of R_s , this equation can be approximated as;

$$P_D \approx \frac{R_s}{Z_0} P_{av} \quad W \quad (2-12)$$

For switches that are not perfectly matched, these power equations should be multiplied by $[2\sigma/(\sigma+1)]^2$ where σ is the voltage standing wave ratio VSWR.

The peak RF current in the series connected PIN diode is;

$$I_p = \sqrt{\frac{2P_{av}}{Z_0} \left(\frac{2\sigma}{\sigma + 1} \right)} \quad \text{amps} \quad (2-13)$$

Similarly, peak RF voltage can be found from;

$$V_p = \sqrt{2Z_0 P_{av}} \frac{2\sigma}{\sigma + 1} \quad V \text{ for SPNT} \quad (2-14)$$

A series single-pole-double-throw (SPDT) switch is shown in Figure 2.4.

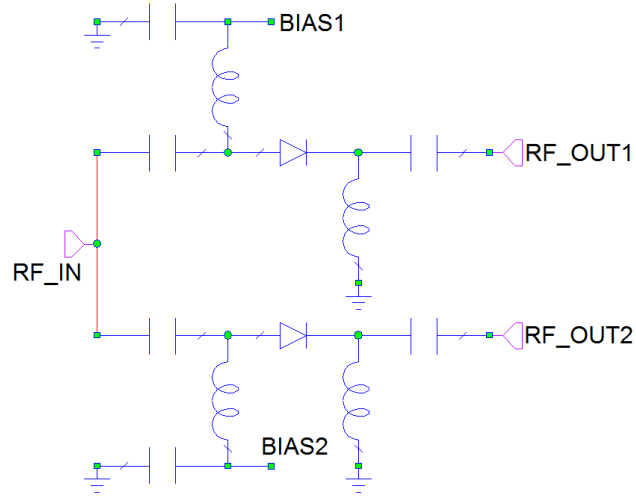


Figure 2.4: Series SPDT Switch

2.2.2 Shunt Switch

Shunt connected switches are commonly used in applications where high isolation over a wide frequency range is needed [13]. Since the PIN diode can be connected to a heat sink from one electrode, the shunt switch is capable of handling more RF power than the series switch.

In this topology, the switch is in isolation condition when the PIN diode is forward biased. When the diode is reverse biased, the switch is conducting the RF signal to the output. The insertion loss primarily depends on the diode's off capacitance. On

the other hand, isolation and power handling are functions of the series forward resistance. A sample shunt SPST switch is shown in Figure 2.5.

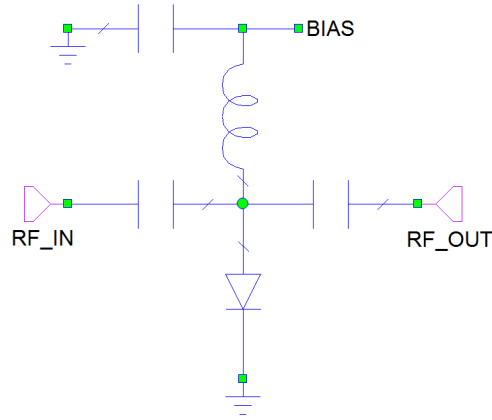


Figure 2.5: Shunt SPST PIN Diode Switch

For a shunt switch the insertion loss can be calculated with;

$$IL = 10 \log[1 + (\pi f C_T Z_0)^2] \quad dB \quad (2-15)$$

The insertion loss of shunt switch is less than that of series switch since there are no switching elements in series with the transmission line.

The isolation of an SPST shunt switch can be found by;

$$Isolation = 20 \log \left[1 + \frac{Z_0}{2R_s} \right] \quad dB \quad (2-16)$$

For multi-throw switches, the isolation is 6dB higher than that found above, due to the voltage reduction across the off diode [13]. Also, the quarter wavelength transformers introduced in multi-throw shunt switches enhance the isolation performance by approximately 3dB when compared to SPST shunt switches.

The dissipated power on forward biased PIN diode in shunt configuration can be found by;

$$P_D = \frac{4R_s Z_0}{(Z_0 + 2R_s)^2} P_{av} \quad W \quad (2-17)$$

where P_{av} is the available power from the source.

For very small values of R_s , this equation can be approximated as;

$$P_D \approx \frac{4R_s}{Z_0} P_{av} \quad W \quad (2-18)$$

The dissipated power on reverse biased PIN diode can be found by;

$$P_D = \frac{Z_0}{R_p} P_{av} \quad W \quad (2-19)$$

For switches that are not perfectly matched, these power equations should be multiplied by $[2\sigma/(\sigma+1)]^2$.

The peak RF current in the shunt connected PIN diode is;

$$I_p = \sqrt{\frac{2P_{av}}{Z_0}} \left(\frac{2\sigma}{\sigma+1} \right) \quad \text{amps} \quad (2-20)$$

Similarly, peak RF voltage can be found from;

$$V_p = \sqrt{2Z_0 P_{av}} \frac{2\sigma}{\sigma+1} \quad V \text{ for SPNT} \quad (2-21)$$

A shunt SPDT switch is shown in Figure 2.6.

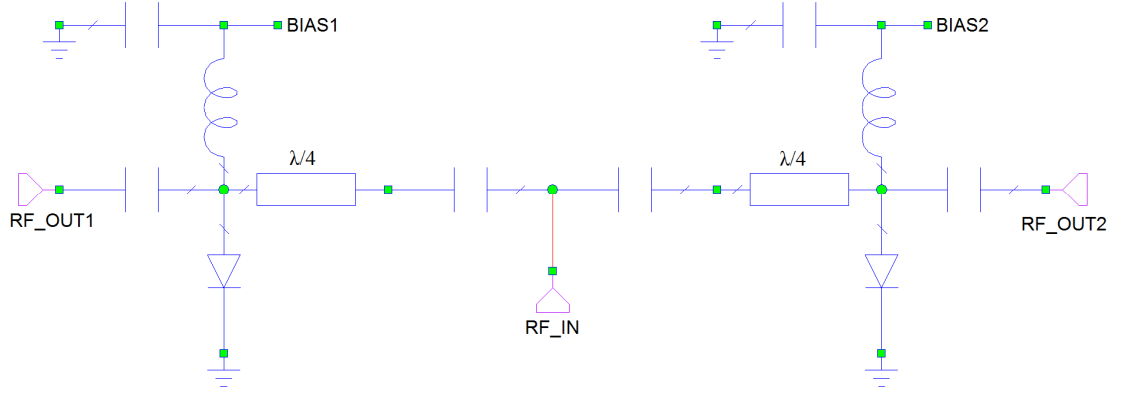


Figure 2.6: Shunt SPDT Switch

Such a tuned SPDT switch has limited bandwidth since it employs quarter-wavelength transformers. In order to obtain better isolation, more PIN diodes can be added in each arm with quarter-wavelength distance from each other. Such a structure may be thought to have higher insertion loss since it includes more switching elements, but lower insertion loss can be obtained due to resonant effect of the spaced diode capacitance.

2.2.3 Series-Shunt Switch

As the name implies, series-shunt switches are actually a combination of series switch and shunt switch. It consists of the advantages and disadvantages of both structures [13]. Broad band low insertion loss property of series switches is combined with broad band high isolation property of shunt switches, so the overall switch performance is improved. However; bias circuit gets more complex, thus the interaction of the bias circuit becomes important. Complex bias circuit usually makes the return loss worse.

In this topology, when the bias is positive, the series PIN diode is reverse biased providing high impedance and the shunt PIN diode is forward biased providing low impedance. In this situation the switch is in isolation condition. When the bias is negative, the switch is transferring the RF signal to the output. The insertion loss primarily depends on the forward resistance of the series diode and the off capacitance of the shunt diode. On the other hand, isolation depends on the forward

resistance of the shunt diode and the off capacitance of the series diode. Since it is difficult to heat sink the series diode, the power handling is not as good as all-shunt structure.

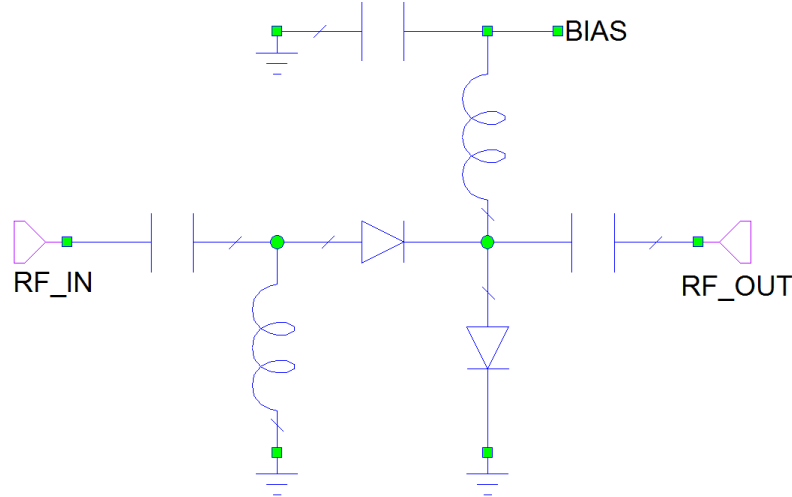


Figure 2.7: Series-Shunt SPST PIN Diode Switch

The insertion loss obtained with this structure is a little higher than series switch and shunt switch since there are more switching elements in each arm.

2.3 High Power PIN Diode Switching

The advantages and disadvantages of PIN diode switch topologies are given in Section 2.2 in this chapter. The performance of each topology is compared in this section considering the use in a high power application.

In a high power application, low insertion loss means less heating. The broadest bandwidth with low insertion loss can be obtained with series-shunt configuration. However; since this structure employs series switching elements, the insertion loss is not as low as that in all-shunt configuration.

Large values of VSWR imply that an appreciable amount of power reflects back to the source. As the power applied to the switch structure increase, the reflected power gets important. At high power levels, the reflected power may damage the RF source.

Series-shunt topology offers the widest band with low VSWR. However; the bias circuit complexity increases, causing interactions with the theoretical design. These interactions limit the wideband operation, and increase the VSWR. All-shunt configuration has about maximum 60% bandwidth due to the quarter-wavelength transmission lines. But their resonant structure offers very low VSWR within that narrow band.

When an application is high power, the most critical thing is to cope with high temperature. At high RF power levels, power handling of the elements used in the structures should be carefully considered. The designer should try to minimize the power dissipation, or try to cool the structure to prevent overheating. If there is no cooling in the system, the structure should be able to operate at high temperatures. Another option is to easily transfer the heat on the critical elements to a larger surface. Since it is easier to heat sink the shunt PIN diodes, all-shunt structure offers the best performance in high power applications.

2.3.1 PIN Diodes for High Power Applications

One of the most critical steps in high power RF switch design is the selection of the PIN diode. There are two failure mechanisms of PIN diodes in high power PIN diode switching. One of these mechanisms is valid for forward bias, and the other is valid for reverse bias.

In forward bias, the diode has a low resistance. The dissipated power on the forward biased PIN diode is the sum of the dissipated DC power and RF power. In low power applications, the dissipated RF power is negligible when compared to the DC power. On the other hand, DC power becomes negligible when compared to RF power in high power applications. According to the desired power handling, the appropriate PIN diode which safely handles the desired power should be chosen. Considering the analysis and formulation in Section 2.1 and 2.2, a PIN diode with high power handling capability should be chosen. PIN diodes with low series forward resistance and low thermal resistance are quite attractive for the designer. Considering the

operating temperature, these values of forward resistance and thermal resistance should satisfy the safe operation such that the diode does not burn due to high temperature.

When the PIN diode is reverse biased, there will be a high voltage swing on the diode. In the negative cycle of the RF signal, the applied reverse voltage and negative peak RF voltage should not exceed the breakdown voltage rating of the PIN diode. Otherwise, the diode will be damaged. Choosing the reverse voltage equal to the RF peak voltage requires that breakdown voltage be at least twice the RF peak voltage. A PIN diode with that much breakdown voltage is convenient, since there is a possible lower value of reverse bias voltage [15].

CHAPTER 3

HIGH POWER PIN DIODE SWITCH DESIGN FOR X-BAND

As explained in the previous chapters, power handling capability is determined by the voltage swing of the *OFF* device and maximum current limitation of the *ON* device [16]. In order to satisfy the high voltage swing, the PIN diode should have high breakdown voltage rating. On the other hand, PIN diodes which are able to handle high current levels have large junction area which means high off state capacitance. High off state capacitance means worse isolation. Keeping these in mind, the appropriate PIN diodes should be chosen.

3.1 PIN Diode Selection

The first step in the design is the selection of the PIN diode. As mentioned earlier, PIN diodes to be used in a high power application should have high power handling capability and high breakdown voltages. While choosing the PIN diodes, main properties considered were high breakdown voltage, low series resistance and low thermal resistance. Also, the capacitance of the PIN diode should not be large considering the operating frequencies. In order to experimentally observe the power handling capability, three PIN diodes of different characteristics are chosen. All three PIN diodes are products of Aeroflex Metelics. The electrical parameters of the chosen PIN diodes are summarized in Table 3.1.

Table 3.1: Electrical Parameters of Selected PIN Diodes

	V_r , V	C_T , pF	R_s , Ω	τ , ns	W , μm	Θ_{ic} , $^{\circ}\text{C/W}$
MPN7315	150	0.12	1.5	180	15	40
MPN7453A	300	0.15	1	700	60	20
MPN7453B	400	0.2	0.9	2500	60	20

3.2 Characterization of the PIN Diodes

The second step is the characterization of the PIN diodes. In order to obtain the lumped element equivalent circuits of the PIN diodes, each diode is measured using the probe station. The PIN diodes are mounted on a gold plated carrier as shunt elements between wideband test points designed in ASELSAN Inc. years ago. With this configuration all sample PIN diodes are measured under different bias conditions. Biasing is done with wideband bias tees, which are already included in the calibration. The data taken is in s2p format which describes the full two-port parameters of the structure. Figure 3.1 shows the measured structure. In this figure, the ports correspond to the probes. The rest of the setup is included in the calibration. The measured structure for sample characterization is shown in Figure 3.2.

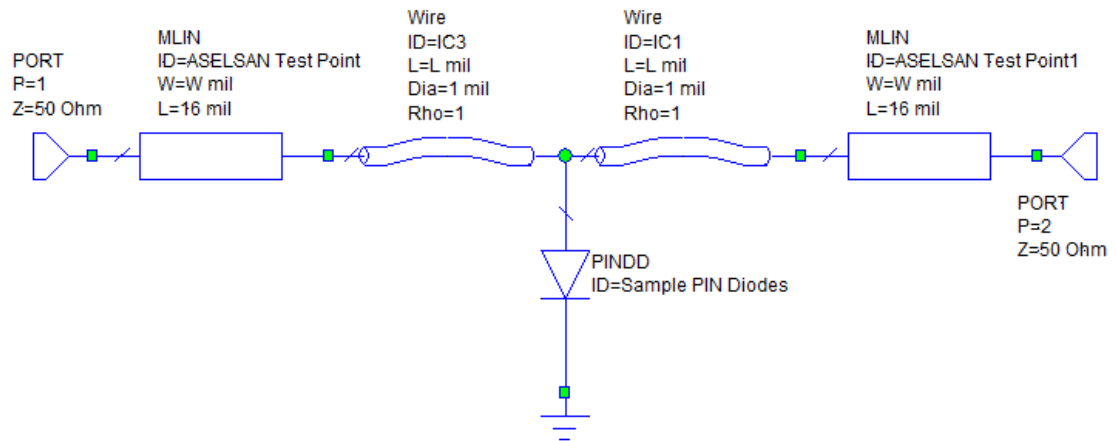


Figure 3.1: Measurement for PIN Diode Characterization

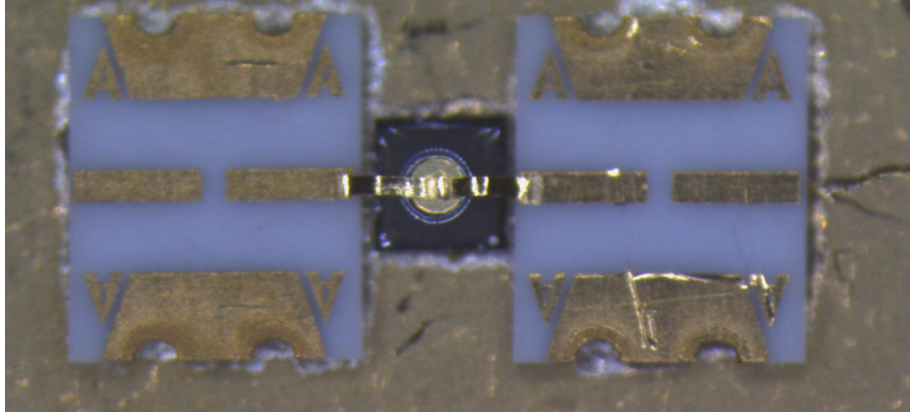


Figure 3.2: Measured Structure for Sample PIN Diode Characterization

The measured PIN diodes are analyzed. De-embedding the extra length brought by the ASELSAN test points, the characteristics of the PIN diode and the bond wires is obtained. Since the bond wires would take place in any design, there is no need to de-embed them. In order to obtain the lumped element equivalent circuits, the datasheets and measurements of the PIN diodes supplied by the manufacturer are used. The lumped element values are tweaked until the model/simulation results and the measurement results are in alignment to a reasonable extent. During the designs in this thesis, the measured data is used to simulate the PIN diode characteristics. The lumped element equivalents are used for double checking purposes.

3.3 Shunt SPDT Switch Design

As the name implies, shunt switches employ only shunt diodes as switching elements. When the PIN diode in one arm is reverse biased, that arm behaves like a low loss transmission line. Meanwhile, the impedance seen from the common junction to the other arm should be high enough to be isolated. This is obtained by forward biasing the PIN diode in that arm. The forward biased PIN diode acts as a short circuit. This low impedance is transformed to high impedance using a quarter-wavelength transmission line at the operating frequency. The use of quarter-wavelength transmission lines limits the bandwidth of the structure.

3.3.1 Shunt SPDT Switch Design Using MPN7315

As explained in Section 3.2, the sample shunt MPN7315 is measured under different reverse and forward bias conditions. ASELSAN test points are de-embedded from the s2p data obtained. Then, these measurements are imported to the simulation software AWR® for building an SPDT switch. The measurements are taken under small signal. The RF model of the PIN diode will slightly differ under high power, but same reverse and forward characteristics can be obtained by increasing the reverse voltage and forward current. Utilizing one PIN diode at each arm, the shunt switch configuration is optimized for X-Band and the circuit in Figure 3.3 is obtained.

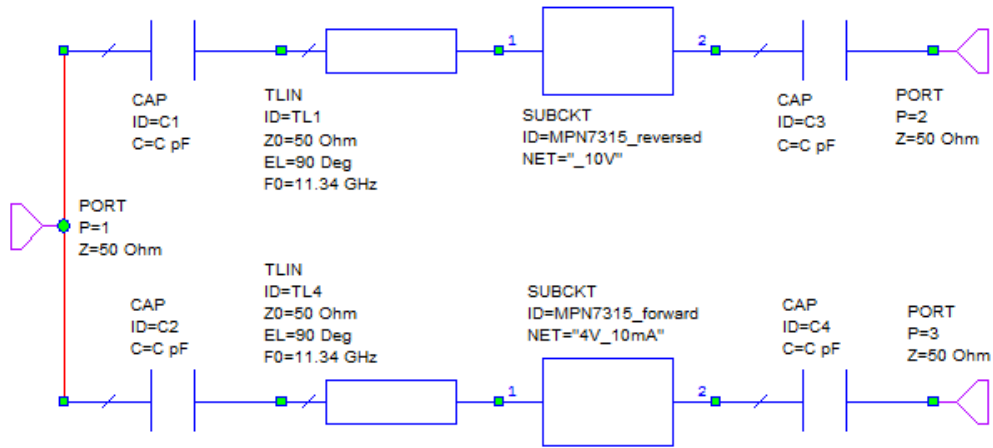


Figure 3.3: Shunt SPDT Switch Using MPN7315

The forward biased PIN diode acts like a short circuit. This short circuit is transformed to an open circuit using a quarter-wavelength transformer. For an ideal design, the length of this transformer should be $\lambda/4$ at the center of the frequency band, which is 10GHz for and X-band design. However, this length slightly differs in practice. The main reason for this slight difference is that the PIN diode is not an ideal short circuit when forward biased. The package capacitance and the reverse capacitance play an important role on the length of quarter-wavelength transmission line. Thus, shorter transmission lines are used while transforming a low impedance capacitive load to open circuit than transforming ideal short to open. In this case, the

optimized transmission line length is found to be quarter-wavelength at 11.34GHz instead of 10GHz.

The DC bias of both arms should be isolated from each other. DC block capacitors are used for this purpose. The value of the capacitor is chosen such that its reactance is smaller than 1 ohm at the lower edge of the frequency band. Also, considering the power handling of the available capacitors, 43pF is chosen, whose reactance is 0.46Ω at 8GHz. In the rest of this thesis, 43pF capacitors are used for DC blocking purpose.

$$X_c = \frac{1}{j2\pi fC} \quad \text{ohms} \quad (3-1)$$

The simulation of the structure in Figure 3.3 is done using the simulation software AWR[®]. The simulation results are shown in Figure 3.4. According to the results, the expected isolation is more than 35dB within X-Band. Better than 15dB of return loss is obtained, and the insertion loss is less than 0.5dB.

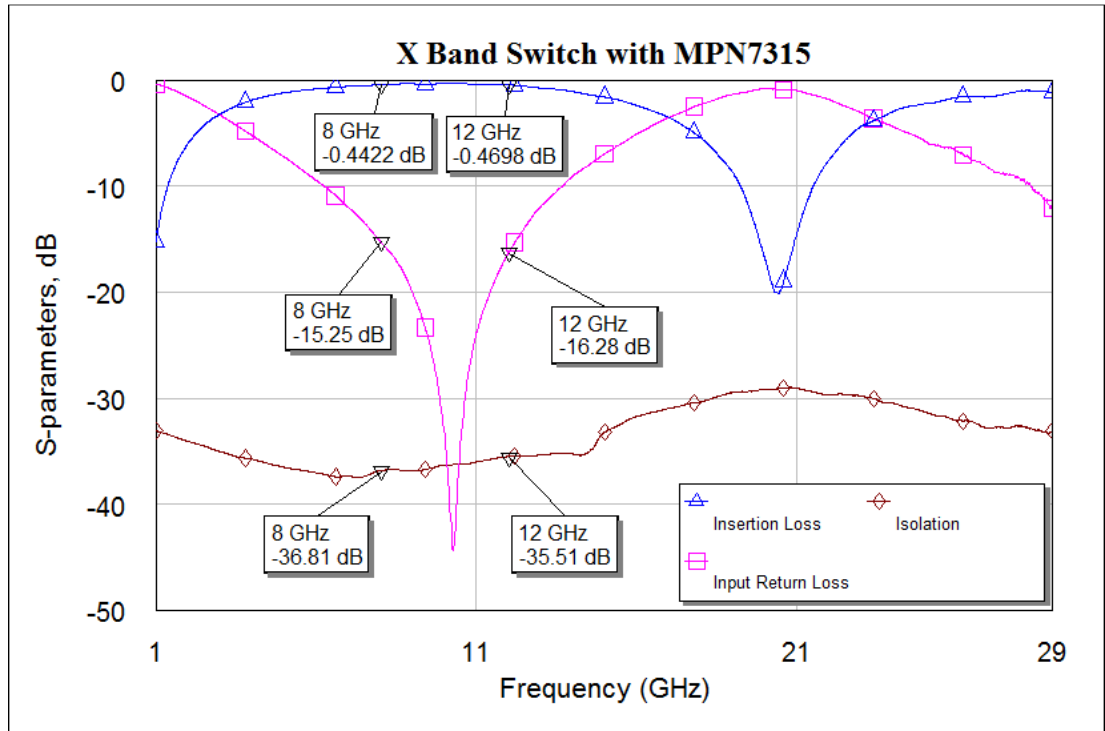


Figure 3.4: Simulation Result of X-Band Switch with MPN7315

In order to double check, the lumped element equivalent of the PIN diode is obtained. For better approximation, the datasheet and measured data obtained from

the diode supplier are used. Both reverse and forward biased shunt PIN diodes are matched with the samples measured as stated in Section 3.2.

The forward biased shunt equivalent of MPN7315 is obtained as in Figure 3.5.

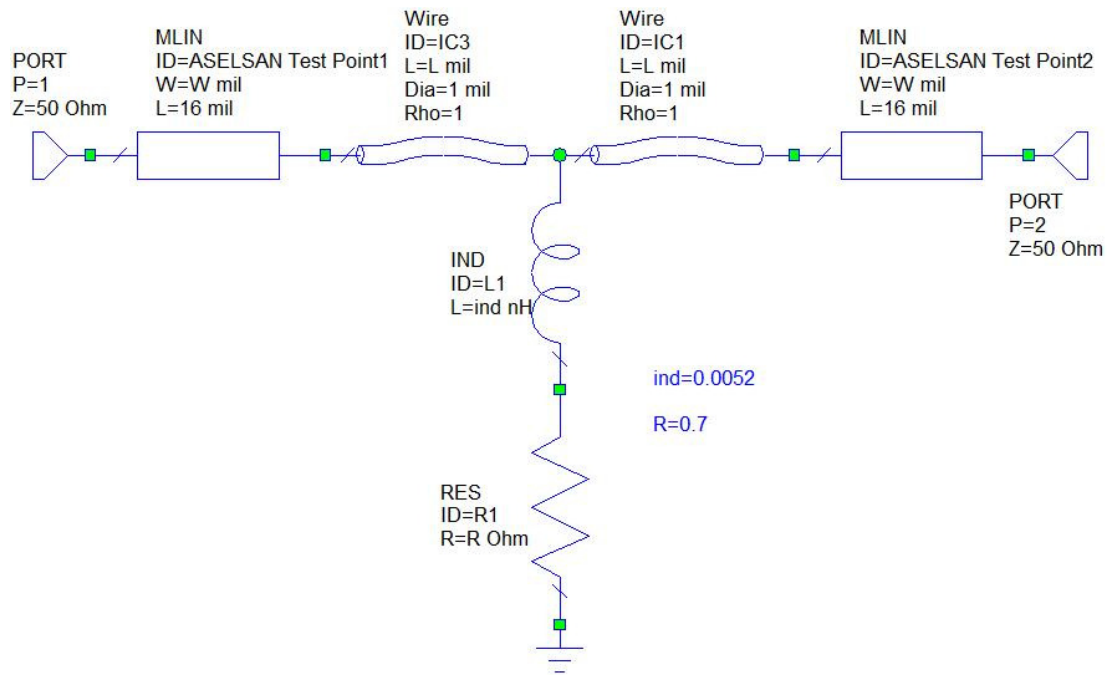


Figure 3.5: Lumped Equivalent Model of Forward Biased Shunt MPN7315

The approximate lumped equivalent forward bias model of MPN7315 is found to be a 5pH inductance in series with a $0.7\ \Omega$ resistance. With these values, the forward biased lumped equivalent approximately matched with MPN7315 at 48mA forward current as in Figure 3.6.

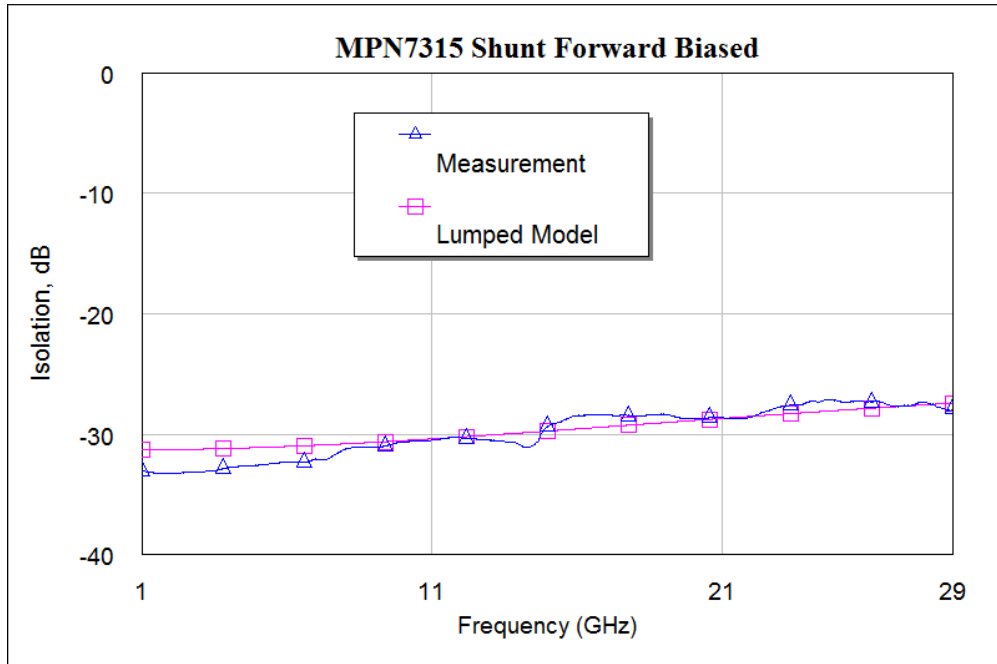


Figure 3.6: Lumped Equivalent Model Compared with Measured Shunt MPN7315 at 48mA Forward Current

Similarly, the reverse bias lumped equivalent is obtained as in Figure 3.7.

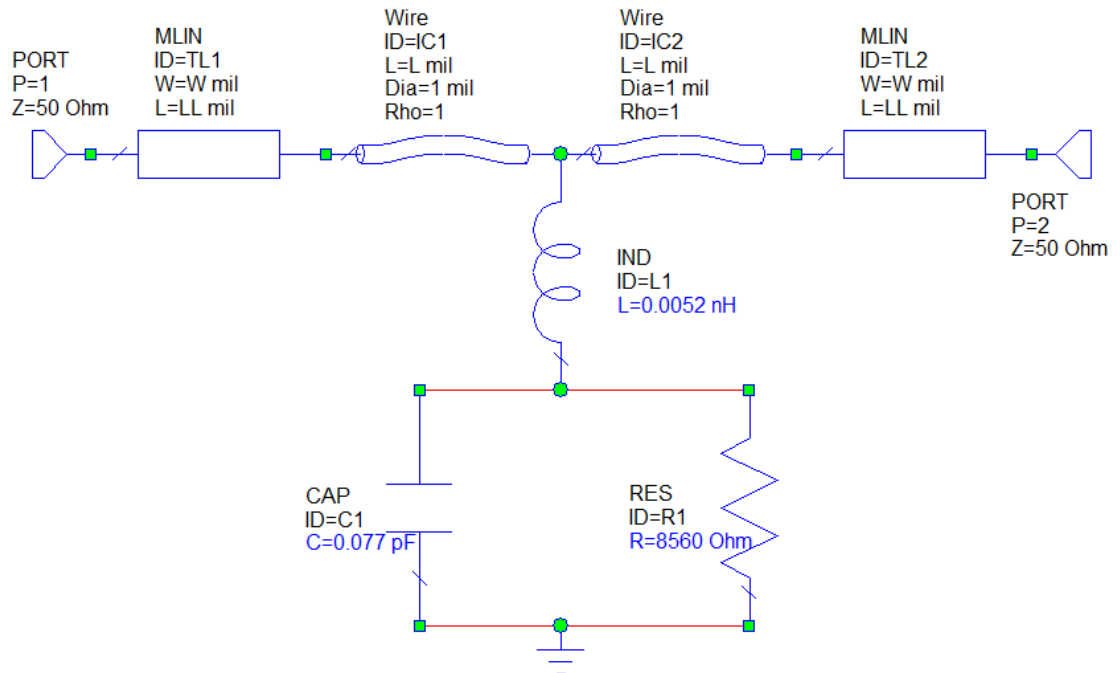


Figure 3.7: Lumped Equivalent Model of Reverse Biased Shunt MPN7315

The approximate lumped equivalent reverse bias model of MPN7315 is found to be a 5pH inductance in series with an 8.5k Ω resistance which has a parallel capacitance of 0.077pF. With these values, the reverse biased lumped equivalent approximately matched with MPN7315 at -10V reverse voltage as in Figure 3.8.

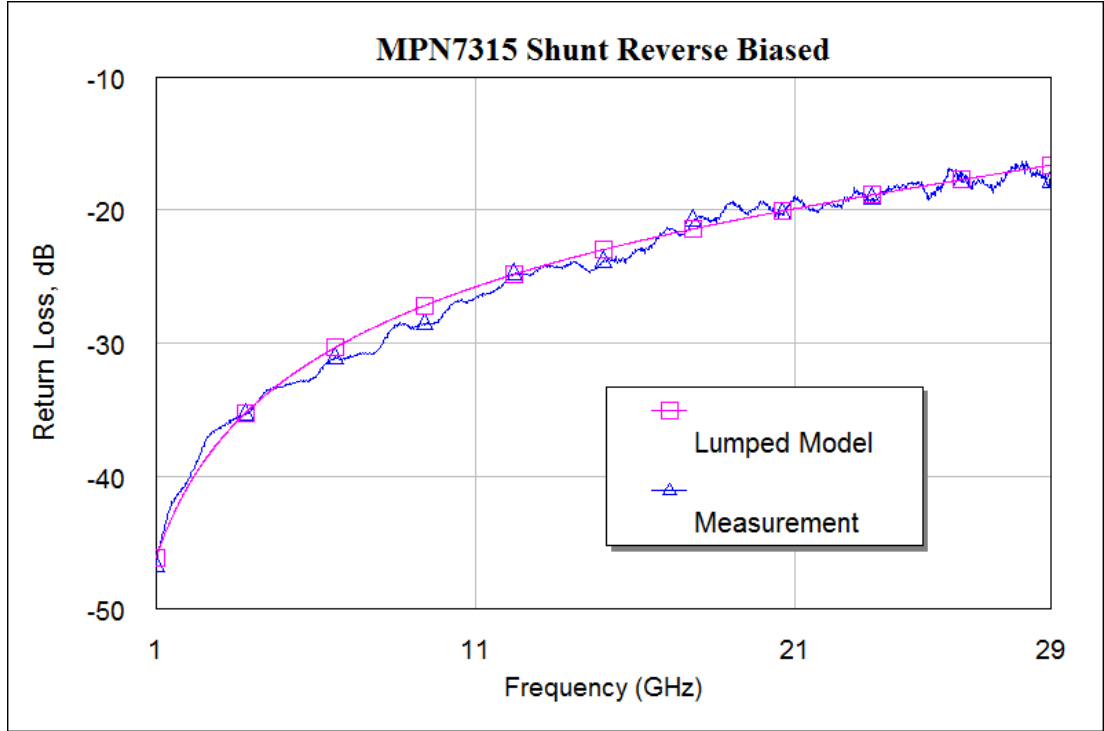


Figure 3.8: Lumped Equivalent Model Compared with Measured Shunt MPN7315 at -10V

Using the obtained reverse bias and forward bias lumped equivalent circuits, the switch designed using de-embedded sample measurement is verified. The simulation results of both designs are compared in Figure 3.9. As it can be seen from the graph, there is a slight difference between both designs. The lumped equivalent model's center frequency is about 300MHz above the center frequency of the one designed using the de-embedded measurements. This slight difference may be due to the use of perfect lumped elements while obtaining the equivalent model.

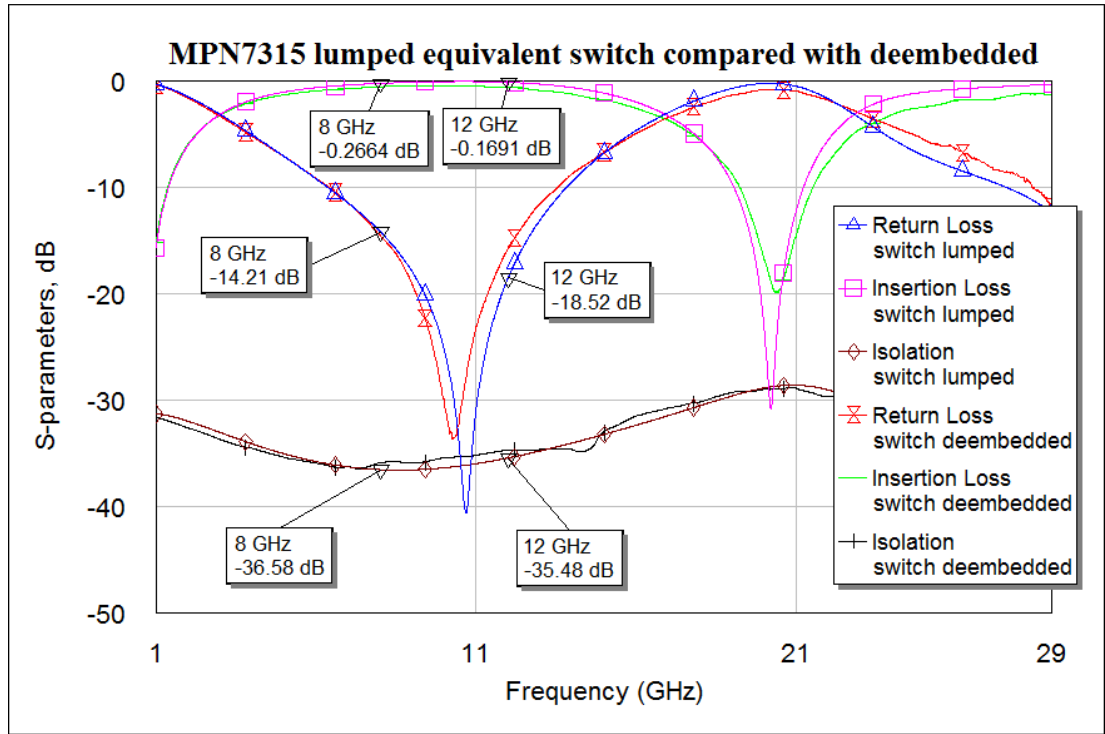


Figure 3.9: Lumped Equivalent Switch Compared with Switch Designed Using De-embedded Sample MPN7315 Measurements

Power handling capability of the designed structure can be evaluated using the equations given in Chapter 2. While calculating the power level, the first thing is to find the maximum allowable power dissipation on the diode. Since the ambient temperature of high power applications is generally high, the designs are made to ensure safe operation at 75°C ambient temperature. Given the maximum junction temperature 175°C and thermal resistance 40°C/W, Equation 2.7 gives the maximum dissipated power in the diode as 2.5W. However; in the datasheet of MPN7315, it is stated that maximum power dissipation is 0.5W. Using (2.18) with this value of P_D and 0.7Ω series resistance, the average RF power that the forward biased diode can handle is found to be 8.93W for a CW application, assuming unity VSWR. On the other hand the reverse biased PIN diode seems to handle 85W CW RF power when (2.19) is used. As expected, the power handling of the shunt structure is limited by the power handling of the *ON* device. Thus, it is concluded that the power handling of this structure is 8.93W CW. If the structure operates under pulsed RF with different duty cycles, the power handling increases and it can be found with a simple calculation.

3.3.2 Shunt SPDT Switch Design Using MPN7453A

Similar to Section 3.3.1, the sample shunt MPN7453A is measured under different reverse and forward bias conditions. Using these measurements an X-Band switch is designed. The lumped element equivalent circuits are obtained for double check. The optimized shunt switch with MPN7453A is shown in Figure 3.10.

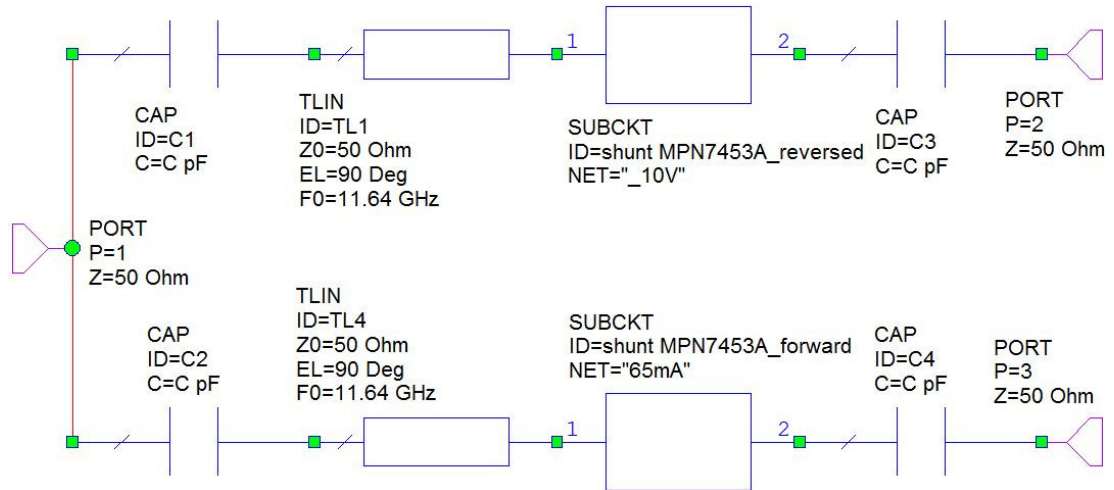


Figure 3.10: Shunt SPDT Switch Using MPN7453A

To transform the forward biased PIN diode to open circuit, transmission lines of quarter-wavelength are used. Having greater package and reverse capacitance than MPN7315, the used transmission lines have greater center frequency than the previous design.

The simulation result of the structure in Figure 3.10 is given in Figure 3.11. Simulation results show that insertion loss is less than 0.5dB. More than 15dB return loss is obtained and the isolation is more than 35dB covering X-Band frequencies.

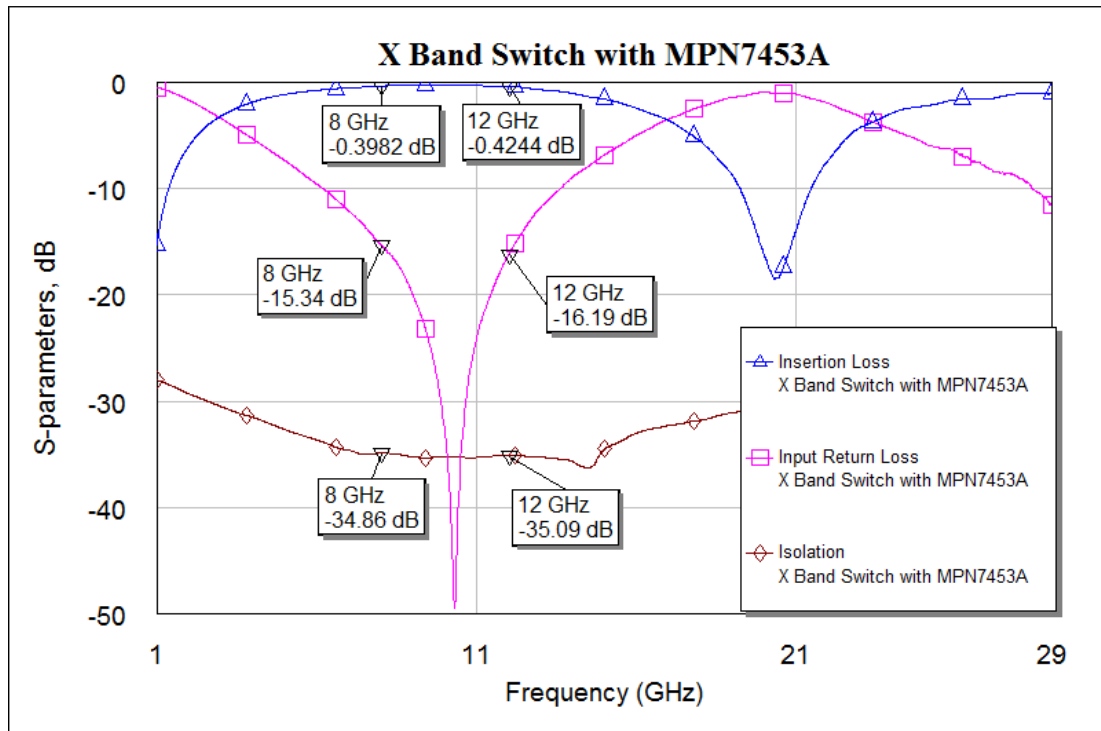


Figure 3.11: Simulation Result of X-Band Switch with MPN7453A

For double check, the forward biased shunt equivalent of MPN7453A is obtained as in Figure 3.12.

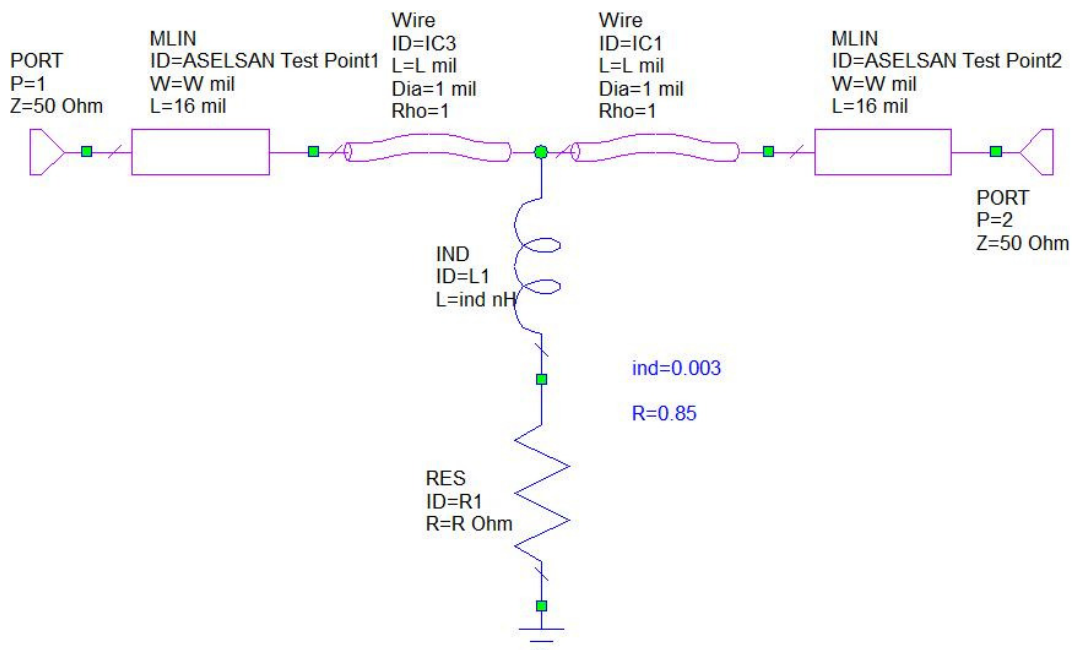


Figure 3.12: Lumped Equivalent Model of Forward Biased Shunt MPN7453A

Similar to previous design, lumped equivalent forward bias model of MPN7453A is found to be a 3pH inductance in series with a 0.85Ω resistance by matching the insertion characteristics as shown in Figure 3.13.

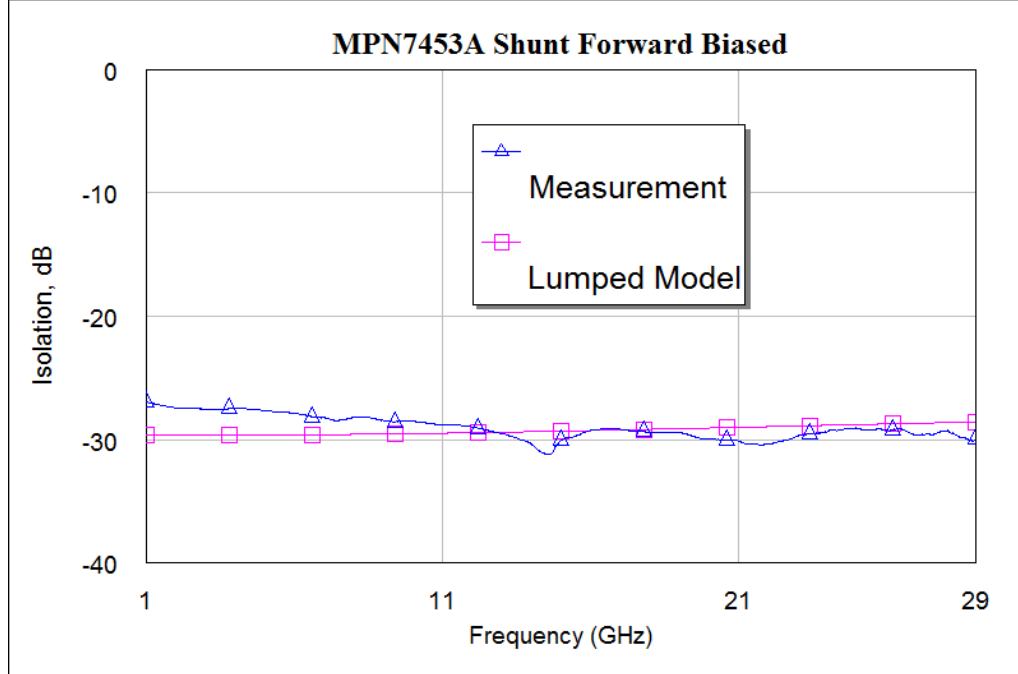


Figure 3.13: Lumped Equivalent Model Compared with Measured Shunt MPN7453A at 65mA Forward Current

Similarly, the reverse bias lumped equivalent is obtained as in Figure 3.14.

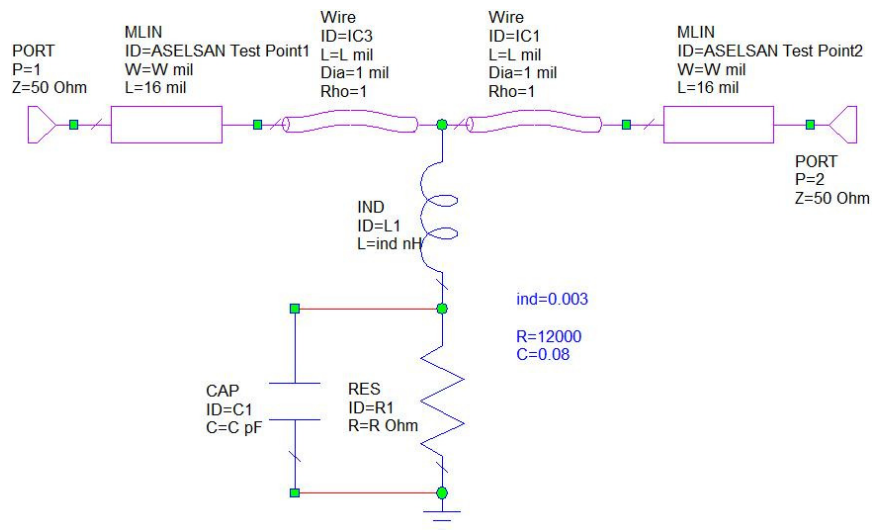


Figure 3.14: Lumped Equivalent Model of Reverse Biased Shunt MPN7453A

The reverse bias lumped equivalent model of MPN7453A is found to be a 3pH inductance in series with approximately 12k Ω resistance having 0.08pF parallel capacitance. Return losses of both measured and lumped equivalent model are shown in Figure 3.15.

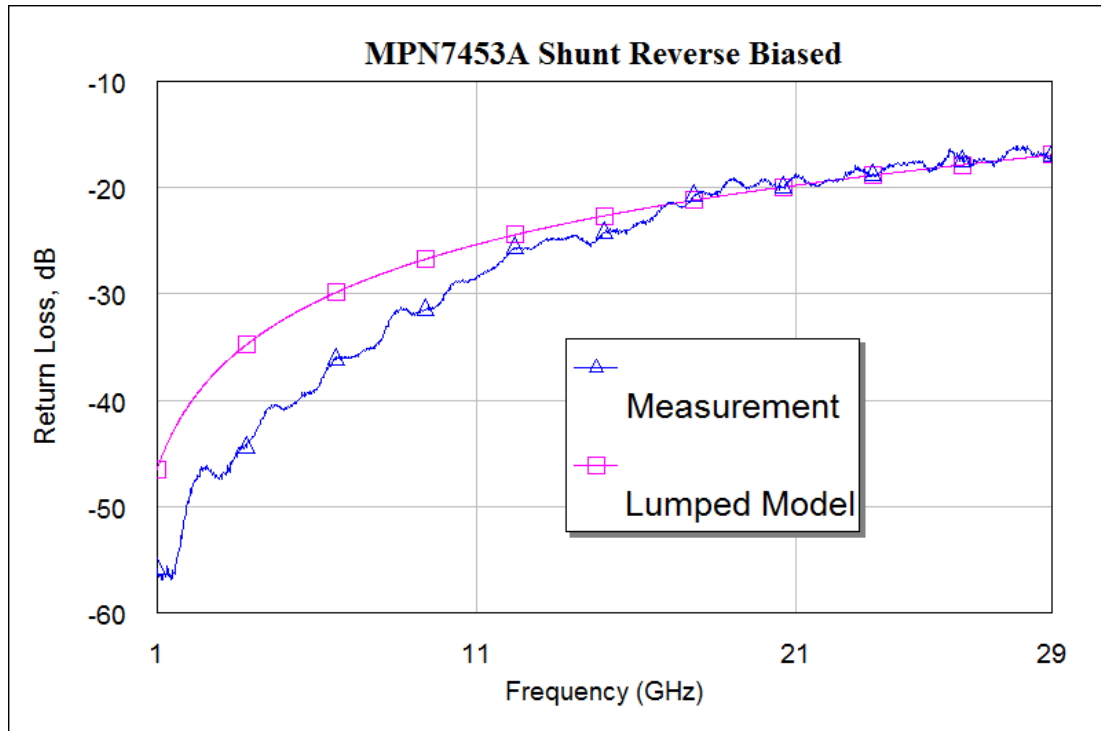


Figure 3.15: Lumped Equivalent Model Compared with Measured Shunt MPN7453A at -10V

Using the lumped equivalent models, the switch designed using de-embedded sample measurement is verified. The simulation results of both designs are compared in Figure 3.16.

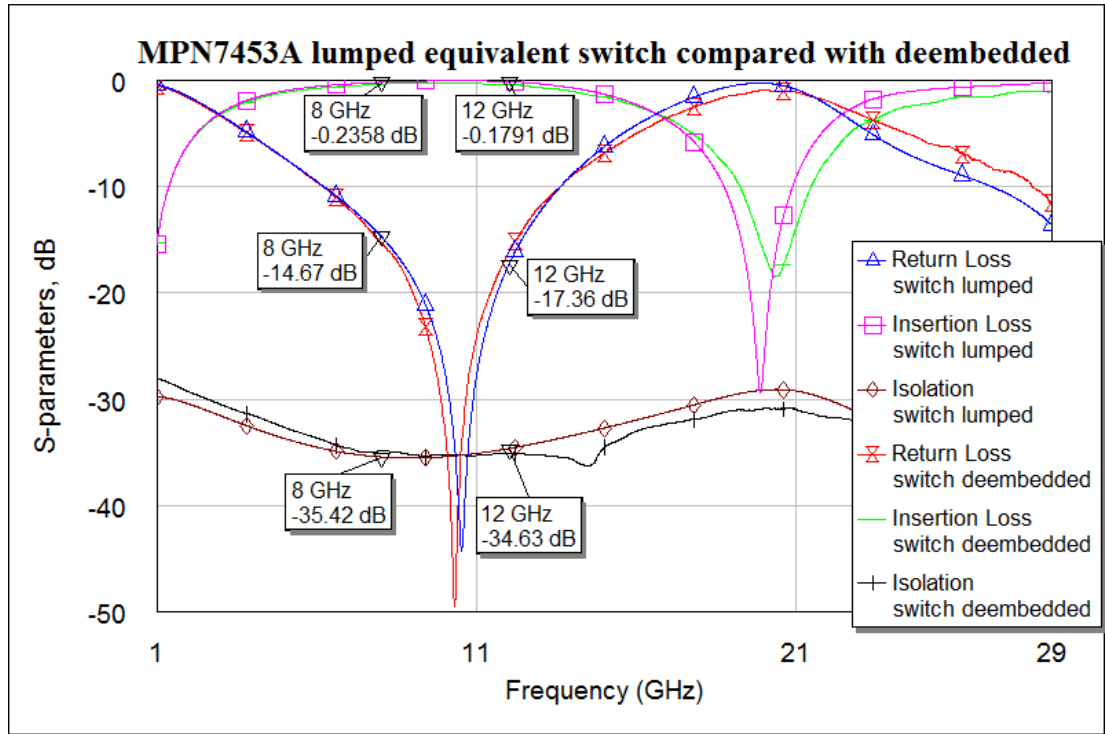


Figure 3.16: Lumped Equivalent Switch Compared with Switch Designed Using De-embedded Sample MPN7453A Measurements

Similar to that done in Section 3.3.1, power handling of the designed structure is evaluated using the equations given in Chapter 2. Having 20°C/W thermal resistance, (2.7) gives the maximum allowable dissipated power in the diode as 5W. Using (2.18) with this value of P_D and 0.85Ω series resistance, it is found that forward biased MPN7453A can handle 73.5W CW RF power. On the other hand the reverse biased PIN diode seems to handle 1.2kW CW RF power when (2.19) is used. Thus, it is concluded that the shunt switch with MPN7453A can handle 73.5W CW.

3.3.3 Shunt SPDT Switch Design Using MPN7453B

Similar to Sections 3.3.1 and 3.3.2, an X-Band switch is designed using the measured sample of shunt MPN7453B. The lumped element equivalent circuits are obtained for determining the power handling of the forward biased diode. High power X-Band switch utilizing MPN7453B as switching element is shown in Figure 3.17.

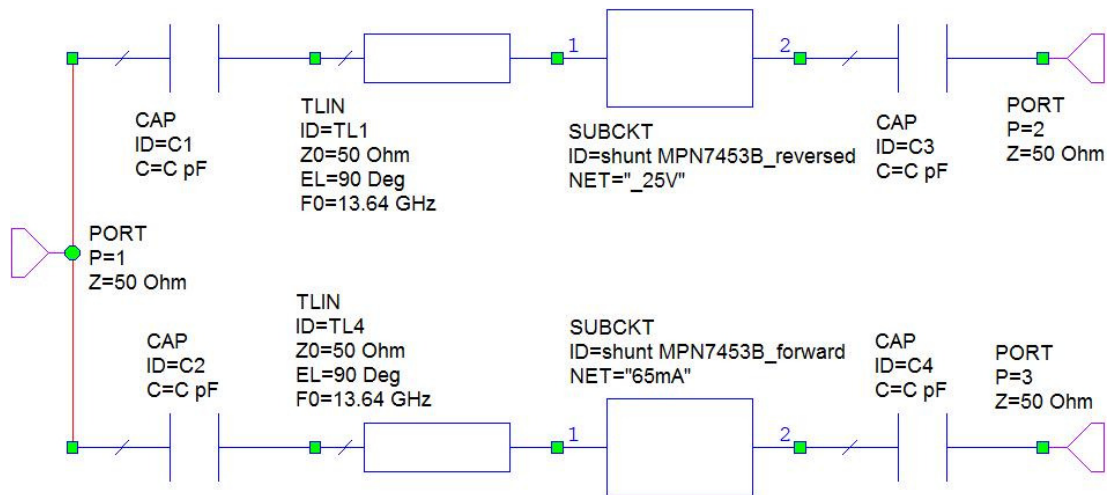


Figure 3.17: Shunt SPDT Switch Using MPN7453B

Quarter wavelength transmission lines used in this design have greater center frequency than previous designs since MPN7453B has greater reverse bias capacitance than both MPN7315 and MPN7453A. The optimized quarter wavelength transmission lines have center frequency at 13.64GHz. The simulation of the structure in Figure 3.17 is done and the results are given in Figure 3.18. According to the result, the expected isolation is more than 30dB within X-Band, more than 14dB of return loss is obtained, and the insertion loss is less than 0.5dB.

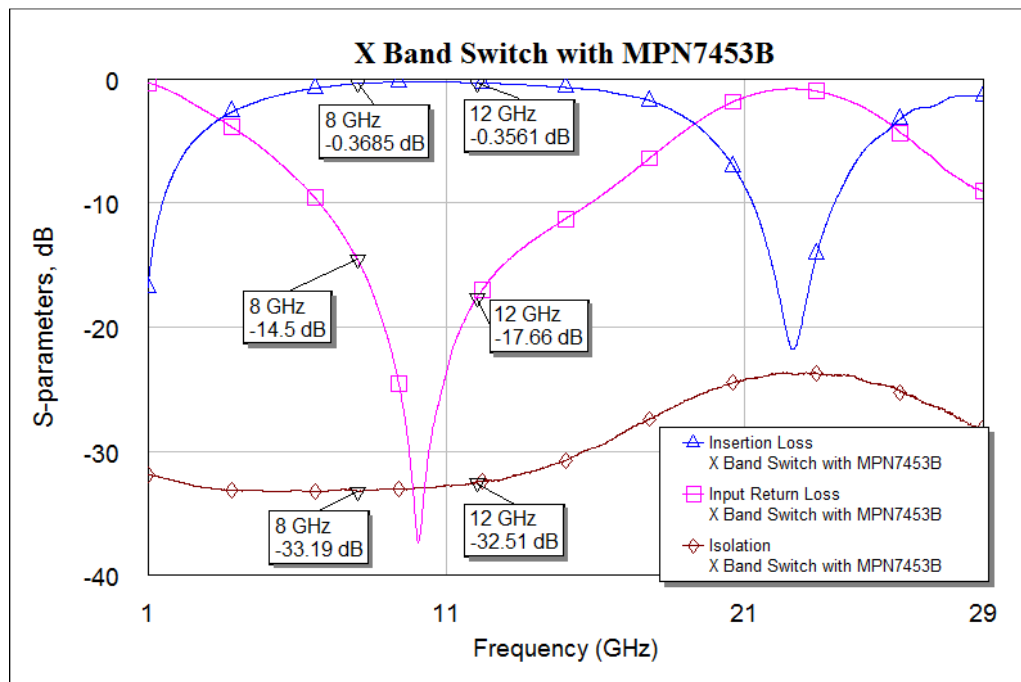


Figure 3.18: Simulation Result of X-Band Switch with MPN7453B

Lumped equivalent of forward biased shunt MPN7453B is obtained for determining the power dissipation. The related lumped equivalent is given in Figure 3.19.

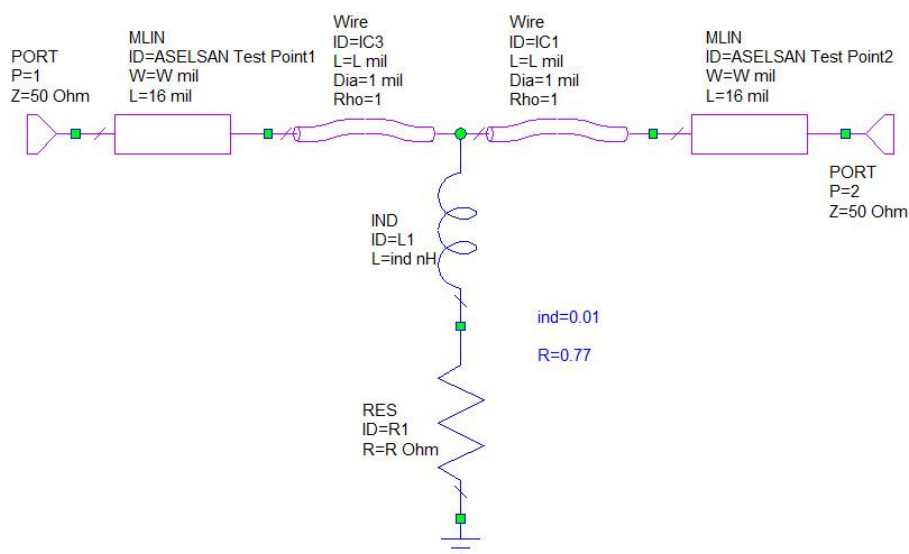


Figure 3.19: Lumped Equivalent Model of Forward Biased Shunt MPN7453B

The approximate forward state lumped equivalent model of MPN7453B is found to be a 0.77Ω resistance with 10pH series inductance. Similar to previous designs, insertion characteristics of measured sample is compared with lumped equivalent in Figure 3.20.

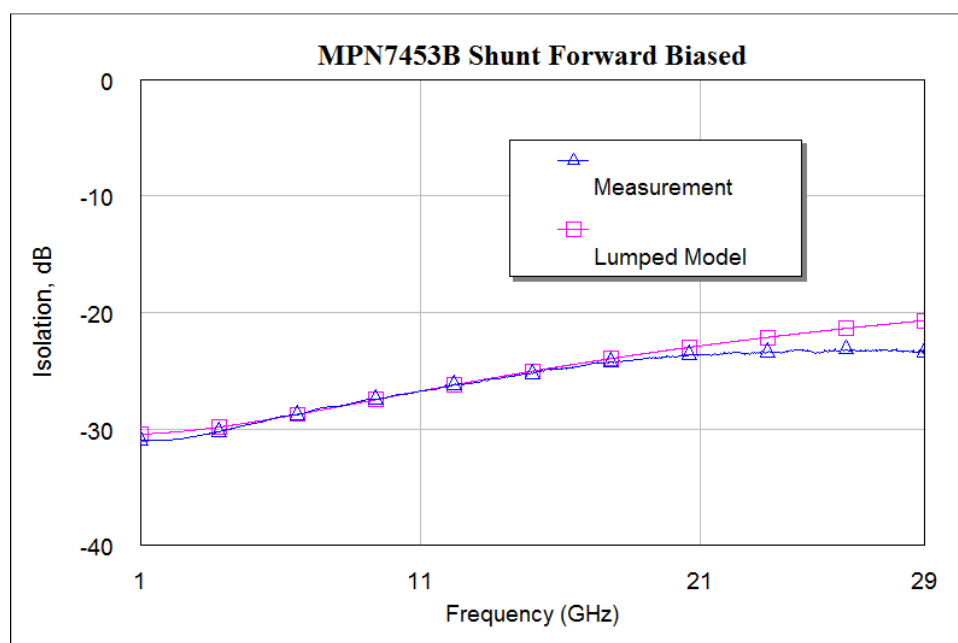


Figure 3.20: Forward State Lumped Equivalent Compared with Measured Shunt MPN7453B

Similarly, the reverse bias lumped equivalent is obtained and given in Figure 3.21.

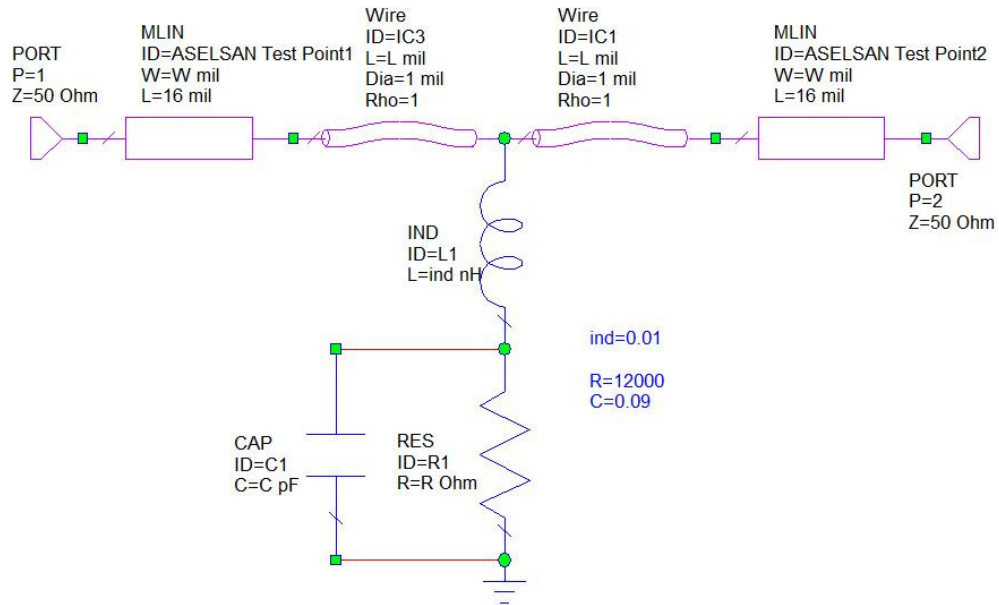


Figure 3.21: Lumped Equivalent Model of Reverse Biased Shunt MPN7453B

The reverse bias lumped equivalent model is found to be a 10pH inductance in series with a 9k Ω resistance which has a parallel capacitance of 0.09pF. With these values, the reverse biased lumped equivalent approximately matched with MPN7453B at -25V reverse voltage as in Figure 3.22. The values of reverse and forward bias lumped equivalent circuits may differ from that given by the manufacturer due to measurements taken under different conditions.

Simulation result of designed switch is compared with lumped equivalents included in Figure 3.23. As it can be seen from the graph, there is a slight difference between both designs, as in Sections 3.3.1 and 3.3.2. This slight difference may be due to the approximations made and the use of perfect lumped elements while obtaining the equivalent model.

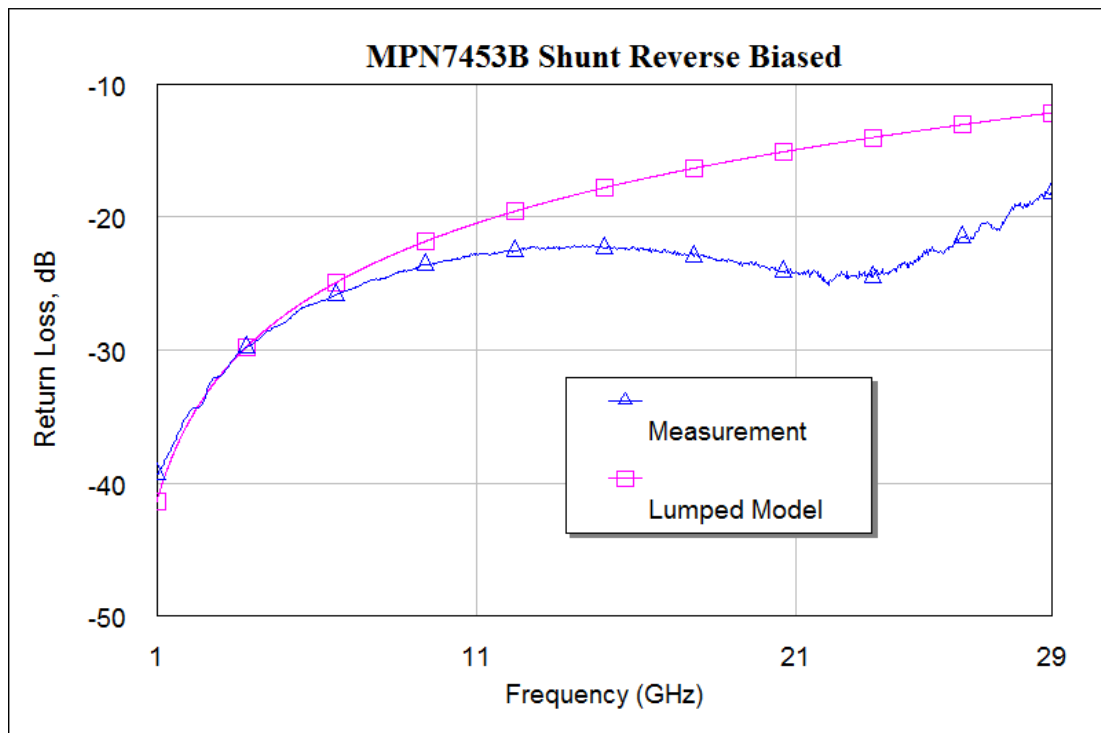


Figure 3.22: Lumped Equivalent Compared with Measured Shunt MPN7453B at -25V

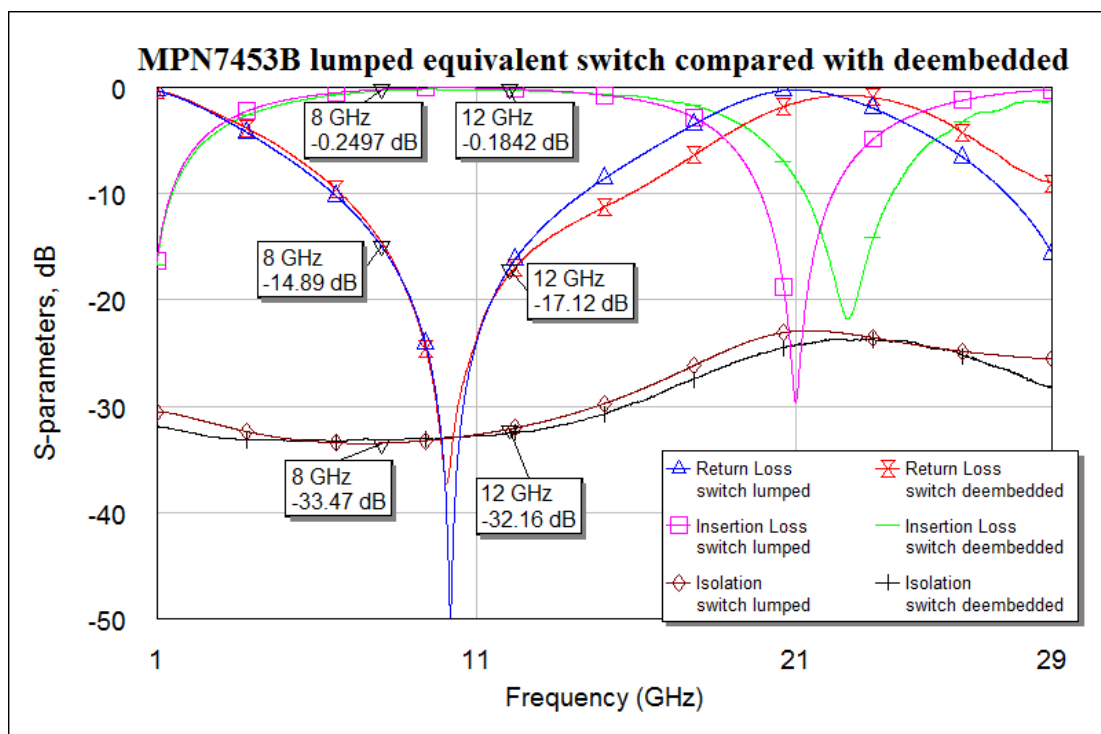


Figure 3.23: Lumped Equivalent Switch Compared with Switch Designed Using De-embedded Sample MPN7453B Measurements

Similar to that is done in Section 3.3.1 and 3.3.2, the power handling of the designed structure mainly depends on the maximum allowed power dissipation of the forward biased PIN diode. MPN7453B has the same thermal resistance as MPN7453A which is 20°C/W as given in the datasheet. Using this value and maximum junction temperature, the maximum allowable dissipated power in the diode is found to be as 5W. Having 0.77Ω forward bias resistance, the average RF power that the forward biased MPN7453B can handle is found to be 81.2W CW using (2.18). On the other hand the reverse biased PIN diode seems to handle 1.2kW CW RF power when (2.19) is used. Thus, the power handling is limited by the power dissipation of the forward biased PIN diode as expected.

As it can be seen, MPN7453A and MPN7453B have greater power handling capability than MPN7315 as they have wider I-region width. They also offer higher breakdown voltages. Having the same I-region width with MPN7453A but lower forward resistance, MPN7453B has higher power handling capability.

CHAPTER 4

FABRICATION AND MEASUREMENTS OF X-BAND HIGH POWER SWITCHES

In Chapter 3, the chosen PIN diodes were modeled and three switches were designed using these models. The expected performance of those designs was given, including the expected power handling. In this chapter, the details of fabrication of the designs in Chapter 3 are given. The fabricated designs are measured under small signal and large signal. The comparisons with expected performance are made. Alternative bias points are analyzed.

4.1 Dielectric Substrate Choice

As mentioned before, the most critical thing in a high power application is the thermal issues. Thermal problems can be observed in each component used in the high power circuit design. Each component's power dissipation should be carefully calculated and the component choice should be done accordingly. Dielectric substrate should also be chosen considering the thermal issues.

There are two main things to be considered while choosing the dielectric substrate. The RF peak voltage may breakdown the dielectric in high power applications. Thus, the dielectric material should have dielectric voltage breakdown higher than the applied peak RF voltage. For example, an incident power of 100W has peak RF voltage of 100V. The dielectric breakdown voltage ratings of dielectric materials used in microwave applications are generally much higher than this value. For instance, alumina has dielectric strength of 13.4MV/m, which is about 340V/mil. If

the substrate is ten mils thick, then the peak voltage allowed is 3400V, which is high enough for this application.

The other thing to pay attention is the thermal rise in dielectric material since the thermal conductivities of dielectrics are generally poor. For this purpose the dissipated power on the dielectric substrate should be decreased. The less the power dissipated, the less the temperature rise observed. The temperature rise occurs due to the losses on the PCB. As the losses on the PCB increase, the dissipated power increases. There are two main loss mechanisms on a microstrip transmission line; dielectric loss and conductor loss. The dielectric loss depends on the loss tangent δ of the dielectric material. A dielectric material with low loss tangent may work for this application. Among the two microstrip loss mechanisms, conductor loss is the one to pay more attention. Dielectric loss is much lower than the conductor loss, therefore it can be neglected and the main point is to decrease the conductor loss. For a fixed impedance microstrip transmission line, dielectric loss is almost constant for any substrate thickness [17]. However; conductor loss can be cut in half by doubling the line width which can be achieved by doubling the substrate thickness. Comparing two dielectrics of the same thickness, the same impedance can be realized with wider line using the dielectric material with lower dielectric constant. Also thicker substrate provides wider line for the same impedance, but there is an upper limit; depending on the operating frequency, as the thickness of the substrate increases beyond $(\lambda_{\text{guided}})/10$, waveguide modes start to dominate the microstrip.

Using the above information, a dielectric material with low dielectric constant can be chosen. Ten mils thick RO3003 which has relative dielectric constant of 3 is chosen. A transmission line with 50Ω impedance can be realized with 24 mils line width on the chosen substrate. RO5880 has lower dielectric constant but its thermal expansion characteristic is worse. Also RO3003 has high stability on dielectric constant over wide temperature range.

Surface roughness has important effect on conductor loss. Having the surface roughness on the order of skin depth increases the attenuation of transmission lines. The dielectric material with electro-deposited copper has worse roughness figures

but the adhesion with the substrate is better. On the other hand, rolled copper has lower roughness figures and it has lower loss when compared to electro-deposited copper plated dielectric material. Thus, RO3003 material with rolled copper option is selected in order to be able to realize low loss microstrip lines.

4.2 Fabrication of the High Power Switches

The designs described in Chapter 3 are fabricated and measured. The first step is the production of the PCB which includes the T-junction. This PCB includes quarter-wave transmission lines whose lengths were optimized in Chapter 3. Also right at the junction, the pads are separated from each other in order to attach the DC block capacitors. The T-junction PCB is manufactured in ASELSAN Inc. Since copper is oxidized and deformed within a short amount of time, the lines are gold plated. During gold plating process, nickel is added between copper and gold. If the gold plating is thinner than a few skin depths, a big portion of RF current will flow through nickel. This situation results in extra loss since nickel has worse conductivity than gold or copper. In order to avoid this, the plated gold should have thickness on the order of a few skin depths. This can be achieved by electroplated gold process. The gold plating is done accordingly in ASELSAN Inc. An alternative could be immersion silver/gold plating. In this process, the gold thickness is very thin, but having low loss silver between copper and gold does not increase the loss. Even lower insertion loss can be obtained since silver is less resistive than gold. However; this process has not proven yet on laminate substrates like RO3003. A sample of the produced T-junction PCB is shown in Figure 4.1.

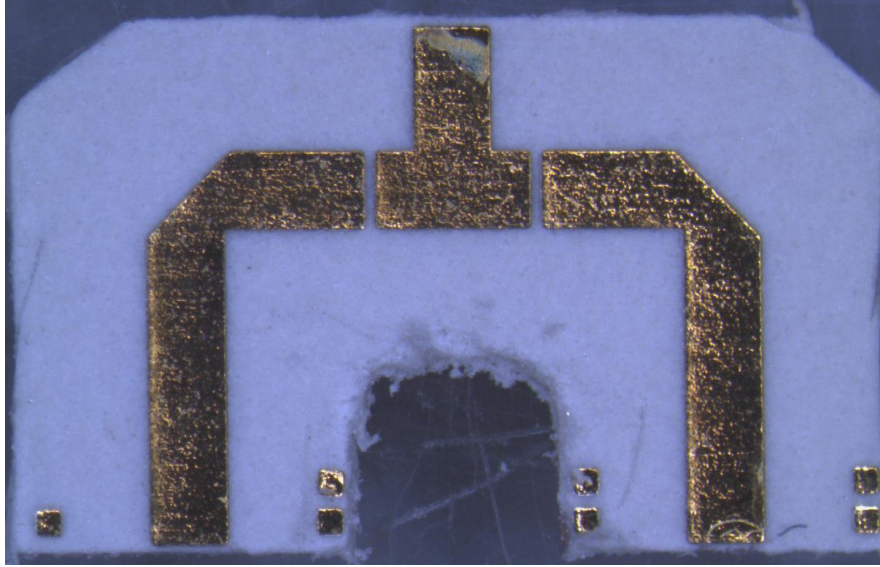


Figure 4.1: Sample T-junction

All the components used in the designs are attached on a gold plated carrier by epoxy. Since the power dissipation on the designed circuits is high, the gold plated carrier is made of CuW, which has low thermal resistivity. With this property of CuW, heat can be easily transferred to the surface where the circuit is mounted. CuW also has low thermal expansion coefficient which matches the TCE of silicon substrate. The most critical components are PIN diodes since most of the power is dissipated on them. While attaching the PIN diodes on the carrier, adhesives which have better thermal conductivities are used.

Biasing is done using 1 mil bond wire. 1 mil bond wire has high current handling capability depending on its length. Also its series resonant frequency is high enough so that it can be safely used as RF choke for X-Band applications. The biasing inductor should have high reactance in the operating frequency band so that RF does not leak to the biasing circuit. The bond wire is approximately 260 mils long, which makes about 6.5nH inductance. The reactance of this inductor at 8GHz is approximately 320 Ω . This 1 mil ribbon is connected between RF path and a 43pF capacitor which is used for DC filtering.

1 mil bond wire is also used for making the connections of the PIN diodes with the microstrip lines. For short wires the current handling is not a big problem, but PIN

diodes are bonded with maximum number of wires as the PIN diode pad allows. Ten mil ribbons are used for the rest of the connections. All assembling processes are performed in clean room facilities of ASELSAN Inc.

4.3 Small Signal S-Parameter Measurements

The designed switches are first measured under small signal in order to justify the frequency response of the designs. The measurements of all three switches designed using different PIN diodes and the related comments are given in this section.

The first design is the one employing MPN7315s. The picture of the assembled switch is given in Figure 4.2. A temperature sensor is attached very close to the PIN diode, in order to see the temperature increase in high power measurements.

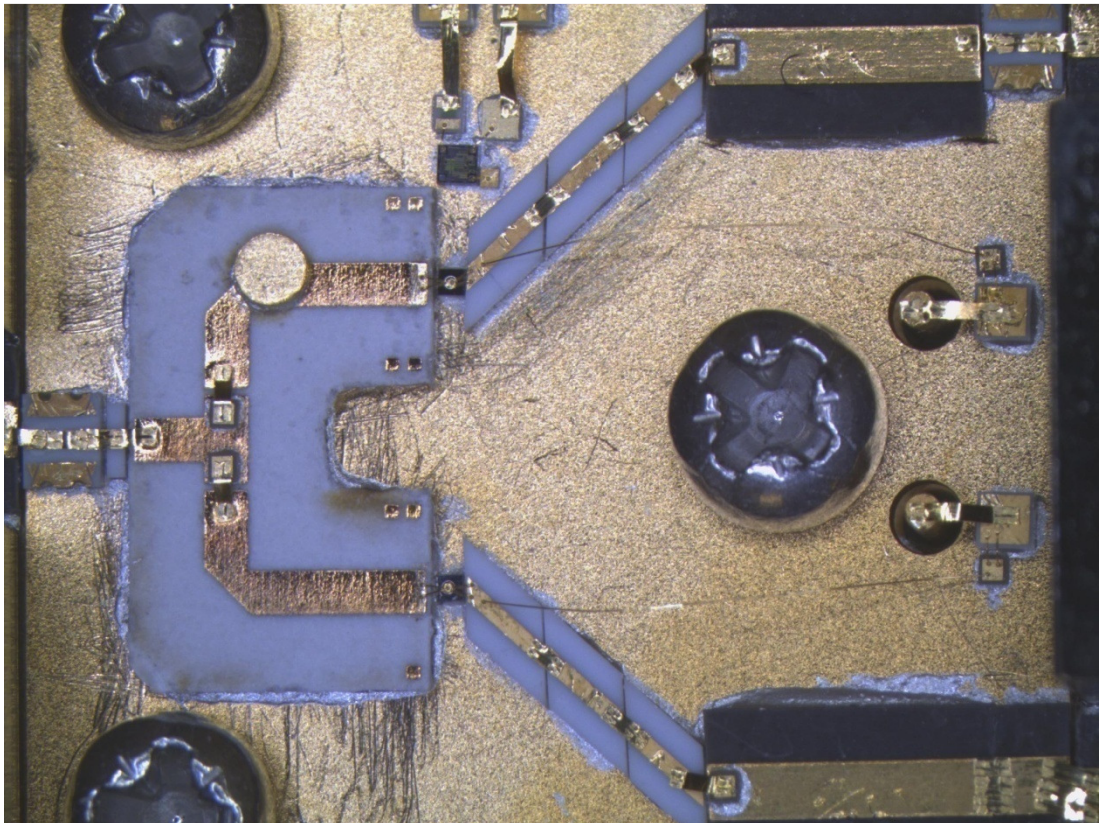


Figure 4.2: X-Band Switch with MPN7315

A gold disc is attached to a point where slightly better frequency response is obtained. The PIN diodes are biased with the voltage and current values used during the design. The exact forward current and reverse voltage under high power are determined using analysis and measurements given in the following sections.

The measured S-parameters of the SPDT switch employing MPN7315s as switching elements are shown in Figure 4.3. As can be seen from the figure, insertion loss is about 0.7dB, going up to 0.9dB at 12GHz. The switch is going to be implemented in the end product without the extra alumina and RO5880 microstrip lines. In other words, the measured insertion loss includes the loss of these extra transmission lines, thus the final product is expected to have less insertion loss. Also it should be noticed that the structure includes DC block capacitors at the output arms and the biasing circuit. Return loss is greater than 16dB within the band. The nominal isolation is 30dB. For a 10W switch, the isolated arm will see only 10mW RF power.

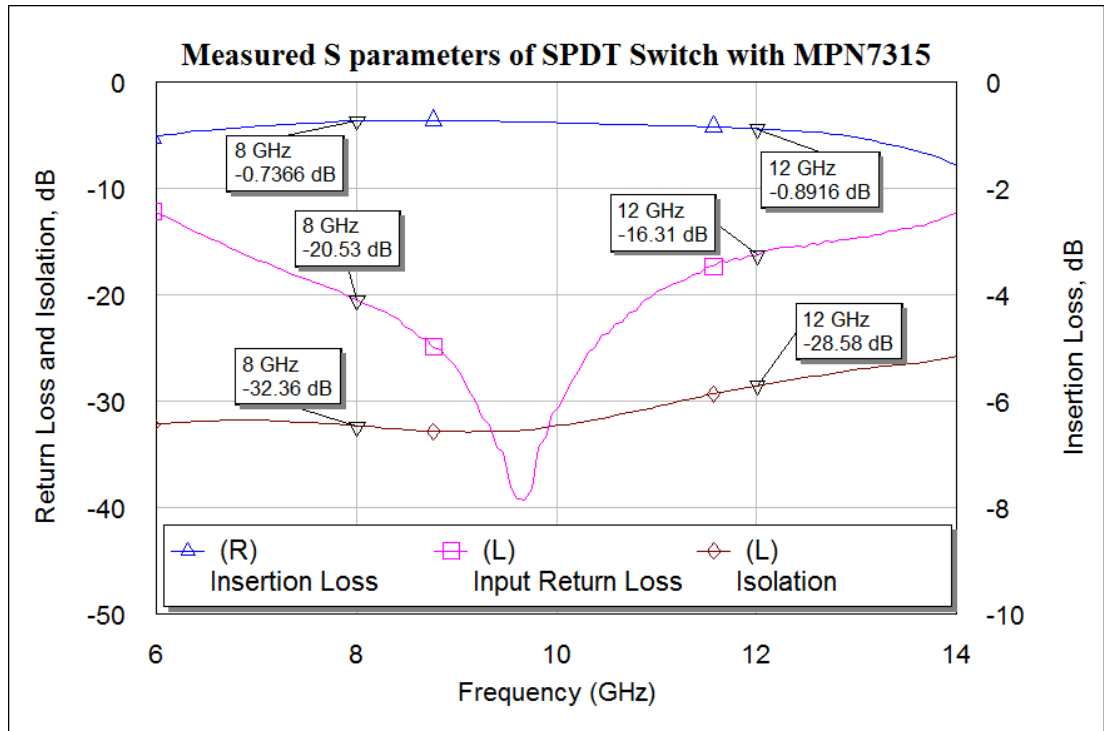


Figure 4.3: Measured S-parameters of SPDT Switch with MPN7315

The second measurement is conducted on the switch designed with MPN7453As. The assembled switch is shown in Figure 4.4.

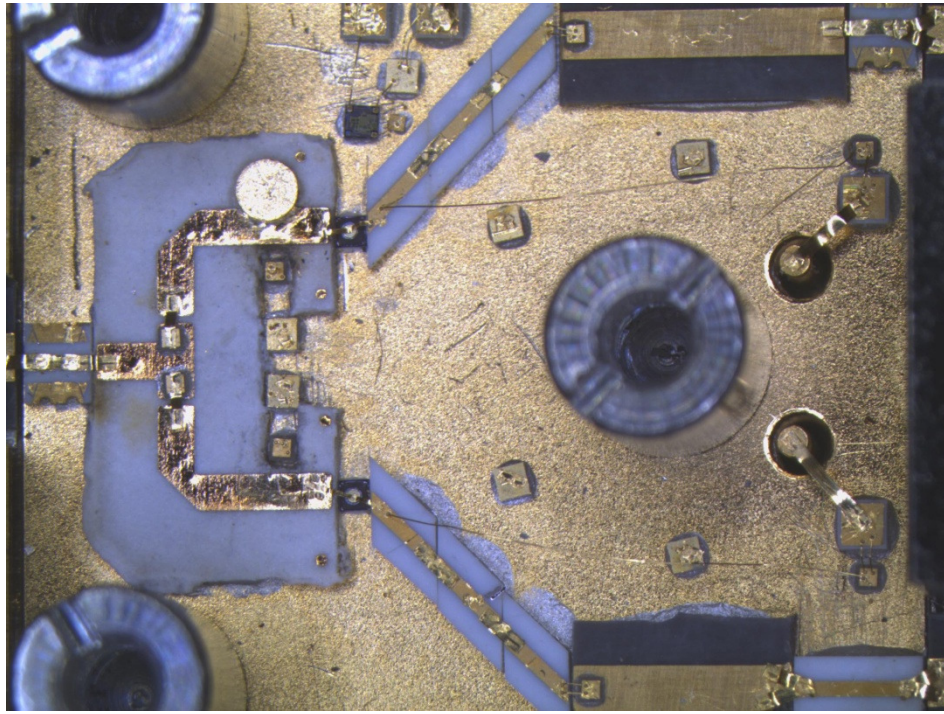


Figure 4.4: X-Band Switch with MPN7453A

Similar to previous designs, a temperature sensor is attached on the carrier in order to see the temperature change during further high power measurements. A gold disc is placed for slightly better frequency response. Also different biasing circuits are tried on this carrier. Using conical or air core inductor as RF choke has worse frequency response, especially when the insertion loss is considered. The frequency response of the SPDT switch employing MPN7453As as switching elements is shown in Figure 4.5.

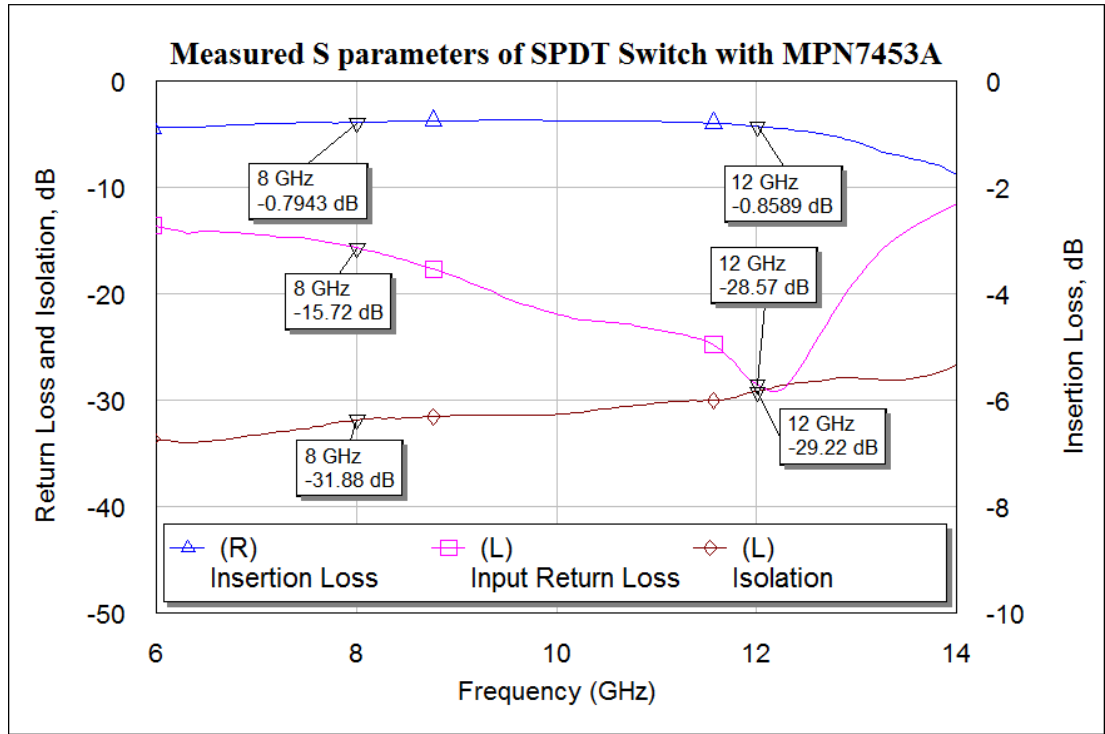


Figure 4.5: Measured S-parameters of SPDT Switch with MPN7453A

As it can be seen from Figure 4.5, insertion loss is about 0.8dB within the band. At 10GHz, insertion loss of 0.7dB is obtained. Return loss is better than 15dB within the band. It should be noted that return loss has the greatest value at the upper edge of the frequency band. A gold disc is attached for decreasing the loss at 12GHz. Thus, the location of the gold disc is chosen such that better return loss at 12GHz is provided. Isolation of the switch is approximately 30dB. The bias points are the same as given in Chapter 3. The exact bias points are chosen according to analysis given in next sections.

The final small signal S-parameters measurement is conducted on the SPDT switch utilizing MPN7453Bs. The picture of assembled switch is given in Figure 4.6.

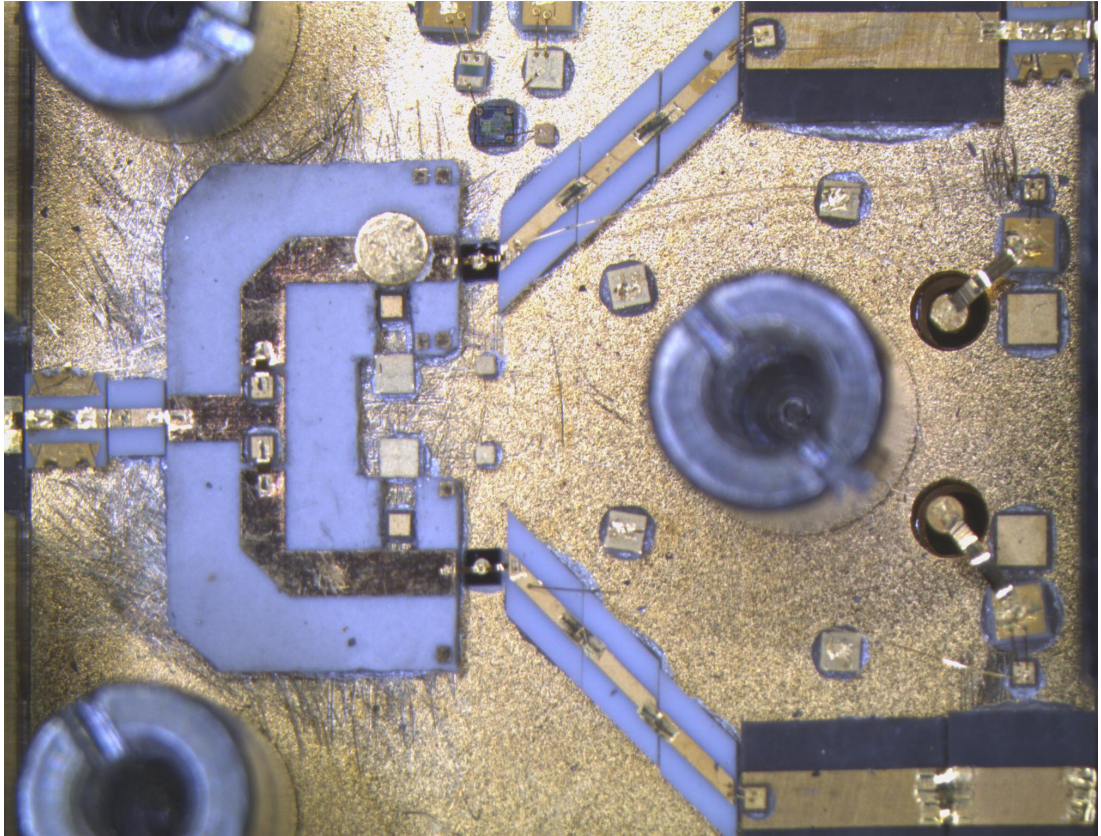


Figure 4.6: X-Band Switch with MPN7453B

Similar to the switch designed with MPN7453As, different biasing inductors are tried on this design. Capacitors with different values are inserted into the bias circuit for DC filtering in order to see the change in switching time. Also gold disc is used to obtain slightly better frequency response. The measured frequency response is given in Figure 4.7.

The obtained insertion loss is about 0.7dB, going up to 0.85dB at 12GHz. Return loss is better than 15dB covering all X-Band. More than 30dB isolation is obtained with this design.

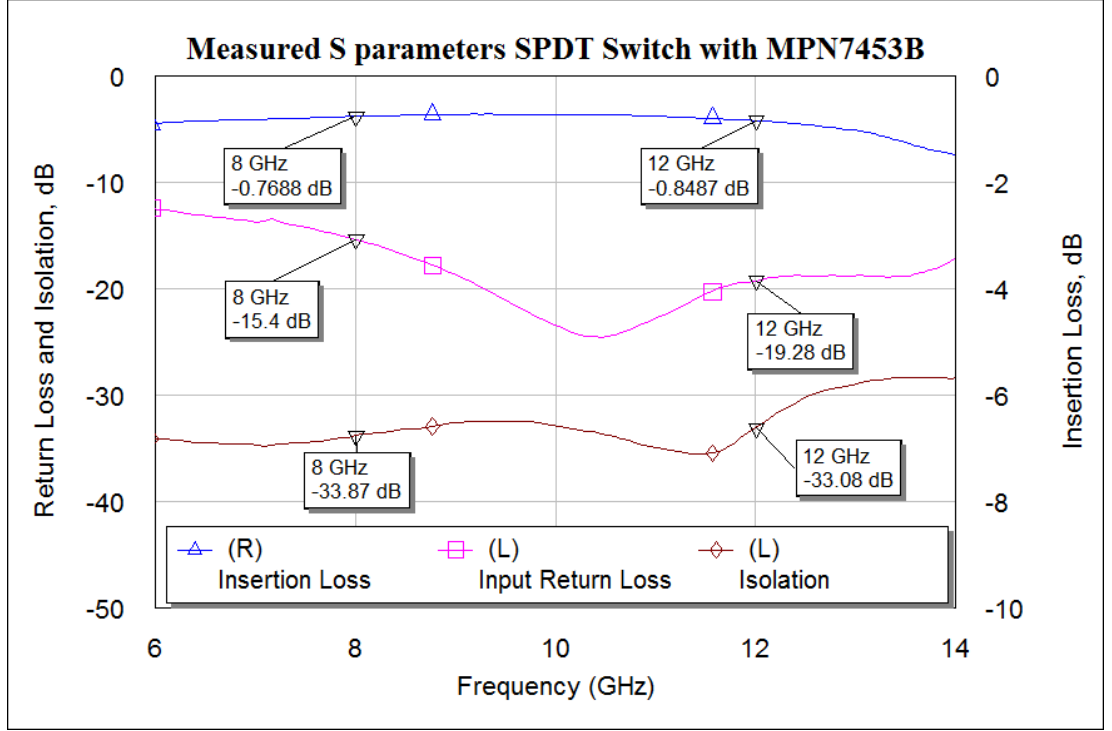


Figure 4.7: Measured S-parameters of SPDT Switch with MPN7453B

Considering the isolation and insertion loss values, all three designs have similar frequency response since the PIN diodes have similar OFF capacitance and ON resistance values. As analyzed earlier, their power handling abilities differ due to their power dissipation capabilities and breakdown characteristics.

4.4 Establishing the Minimum Reverse Bias

In high power switch applications, not only the microwave circuit is critical but also the other parts like biasing circuit and control circuit are important.

There are two states that the PIN diode operates during switching. Those are forward bias and reverse bias. The forward bias current is chosen such that the forward series resistance is at an appropriate value. Also, the stored charge Q should be much greater than the incremental stored charge added or removed by the high RF current [13] so that the required distortion characteristics are met. On the other hand, in reverse bias state the instantaneous voltage across the PIN diode should never exceed

its breakdown voltage and the diode should not go into forward conduction during the positive portion of the RF signal. This requires that the applied reverse voltage should be at least equal to the RF peak voltage, thus the breakdown voltage should be at least twice the peak RF voltage. In a switch application with 100W power handling, the peak RF voltage is 100V. Reverse biasing the PIN diode with 100V is usually difficult, since such great voltages are often not available in the system and it is expensive to implement such a control circuit. However; since the PIN diodes have slow reverse to forward bias switching speeds, they require lower reverse bias voltages. Usually required reverse bias levels are chosen after several trials but Caverly and Hiller made an analysis on selecting the appropriate reverse bias voltage [15]. Their analysis is presented in this section in detail. Related measurements on sample PIN diodes are conducted and comparison with analysis is done.

Since the PIN diodes do not have the same instantaneous turn-on time as the ideal rectifier diodes, the RF should be positive for a finite amount of time to make the PIN diode conduct. Due to this property, required reverse voltage levels are much less than the peak RF voltage swings. In the presence of an RF signal, a DC voltage is developed on the PIN diode. This voltage is called the self-generated DC voltage. Caverly and Hiller showed with experiments [18] that applying a reverse voltage similar to the self-generated DC voltage significantly prevents forward conduction in the diode. Using this relation, an expression for the self generated DC voltage of a PIN diode is derived [15] and this value is chosen to be the minimum reverse bias voltage for the high power application.

The analysis is based on the existence of both displacement and conduction currents [19]. Assuming equal hole-electron drift velocities, v , and equal hole-electron densities, n , the total current density is

$$J(t) = \epsilon dE/dt + 2nqv \quad (4-1)$$

where ϵ is the permittivity, E is the electric field and q is the elemental electronic charge. Assuming a uniform flux density D through the diode cross section A gives

$$\oint DdA = \int \rho dV = DA = Q = A\epsilon E \quad (4-2)$$

with total I-region charge density ρ and sum of DC and RF components of I-region stored charge Q . Combining equations 4-1 and 4-2 results in a total charge density

$$J(t) = (1/A) dQ/dt + 2nqv \quad (4-3)$$

Thus, the PIN diode has a total current of

$$I = dQ/dt + Q/T \quad (4-4)$$

where T is the I-region transit time and defined by $W/2v$ [19]. Assuming a time variation of the form $e^{j\omega t}$ for the RF component, this equation may be written as

$$I = I_{RF} + I_{DC} = Q_{RF}(1 + j\omega t)/T + Q_{DC}/T \quad (4-5)$$

The resistance of the PIN diode can be calculated using the I-region stored charge, electron-hole mobilities μ , and I-region width W [20]. Assuming equal hole and electron mobility for simplicity, RF and DC voltages can be calculated.

$$V_{RF} = \left(\frac{W^2}{2\mu Q_{RF}} \right) I_{RF} = \left(\frac{W^2}{2\mu} \right) \frac{1 + j\omega T}{T} \quad (4-6)$$

$$V_{DC} = \left(\frac{W^2}{2\mu Q_{DC}} \right) I_{DC} = \left(\frac{W^2}{2\mu T} \right) \quad (4-7)$$

Using equations 4-6, 4-7 and the definition for the transit time, the ratio of the DC and RF voltages can be defined as

$$\left| \frac{V_{DC}}{V_{RF}} \right| = \frac{1}{\sqrt{1 + (\pi f W / v)^2}} \quad (4-8)$$

The carrier drift velocity is actually a function of electric field which increases approximately linear as the electric field increases. However, this is valid only for relatively low electric fields. For high values of the field, the drift velocity is limited to a value called saturation velocity, v_{sat} [21]. An approximation for the drift velocity dependence on electric field including saturation velocity is [22]

$$v(E) = \frac{2\mu E}{\left[1 + \sqrt{1 + \left(\frac{2\mu E}{v_{sat}} \right)^2} \right]} \quad (4-9)$$

In order to obtain the carrier drift velocity in a pulsed power application, the rms value of the electric field should be found. Approximating the electric field across the I-region as $E = V_{RF}/W$, the rms value for a pulsed application with duty cycle D is given by

$$E = \frac{V_{RF}\sqrt{D}}{W} \sqrt{\left[\frac{1}{\pi^2} + \frac{1}{8}\right]} \quad (4-10)$$

Substituting equation 4-10 into 4-9 and 4-9 into 4-8, the self generated DC voltage under a pulsed RF signal with peak voltage V_{RF} can be found by

$$|V_{DC}| = \frac{|V_{RF}|}{\sqrt{1 + \left[\pi f W^2 / 0.95 \mu V_{RF} \sqrt{D} \left[1 + \sqrt{1 + [0.95 \mu V_{RF} \sqrt{D} / W v_{sat}]^2} \right]^2 \right]}} \quad (4-11)$$

Assuming a carrier mobility of $0.15 \text{ cm}^2/\text{V-s}$ and saturation velocity of approximately 10^7 cm/s for electrons in silicon at 290K, equation 4-11 becomes

$$|V_{DC}| = \frac{|V_{RF}|}{\sqrt{1 + \left[0.0142 f W^2 / V_{RF} \sqrt{D} \left[1 + \sqrt{1 + [0.056 V_{RF} \sqrt{D} / W]^2} \right]^2 \right]}} \quad (4-12)$$

where f is in MHz and W is in mils. If the RF voltage is low enough such that drift velocity is not saturated, the self generated voltage can be simplified as

$$|V_{DC}| = \frac{|V_{RF}|}{\sqrt{1 + [0.0285 f W^2 / V_{RF} \sqrt{D}]^2}} \quad (4-13)$$

On the other hand, at large values RF where the drift velocity saturation occurs, the developed DC voltage approaches

$$|V_{DC}| = \frac{|V_{RF}|}{\sqrt{1 + [\pi f W / v_{sat}]^2}} \quad (4-14)$$

4.5 Self Generated DC Voltage Measurements

Based on the theory explained in Section 4.4, the self generated DC voltages of the sample PIN diodes are measured under different power levels and different duty cycles.

The measurements are conducted on the shunt sample PIN diodes with different I-region widths under zero applied bias open circuit condition. In order to better approximate an open circuit, 153M Ω resistor is inserted between voltmeter and the measurement point. Since the voltmeter used has 17M Ω internal resistance, the voltage read is approximately 10% of the diode's self generated DC voltage. The measurement setup is shown in Figure 4.8.

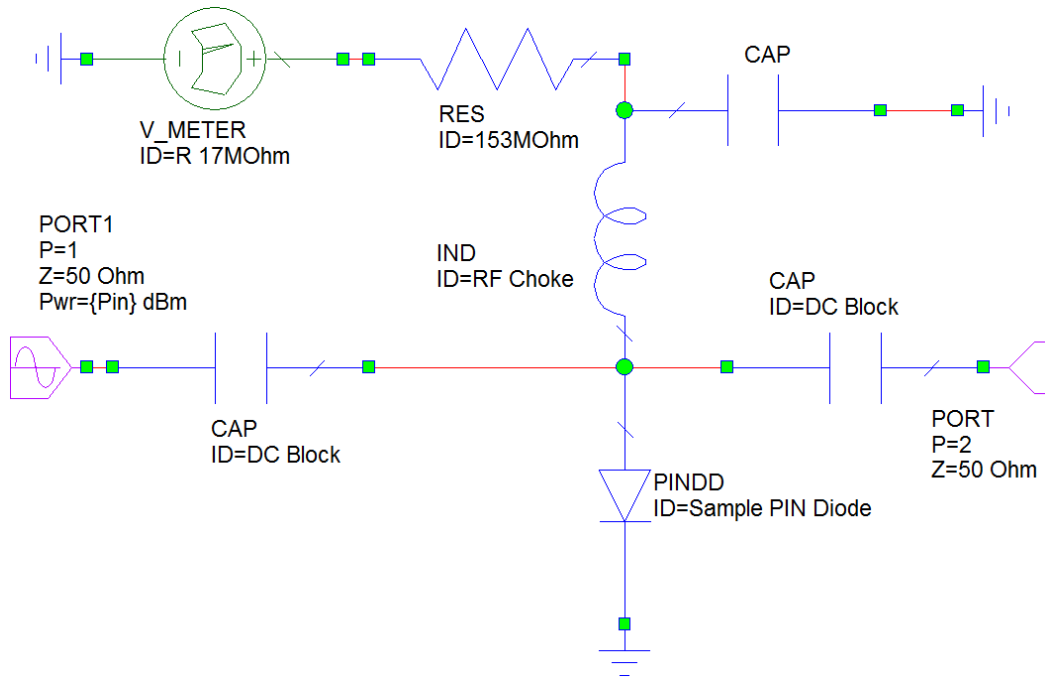


Figure 4.8: Self Generated DC Voltage Measurement Setup

Using the setup shown in Figure 4.8, all sample shunt PIN diodes' self generated voltages are measured. The PIN diode with part number MPN7315 is measured up to 27W CW at 10GHz. The measured self generated voltage under zero bias open circuit condition is given in Figure 4.9 and compared with calculations of the previous section.

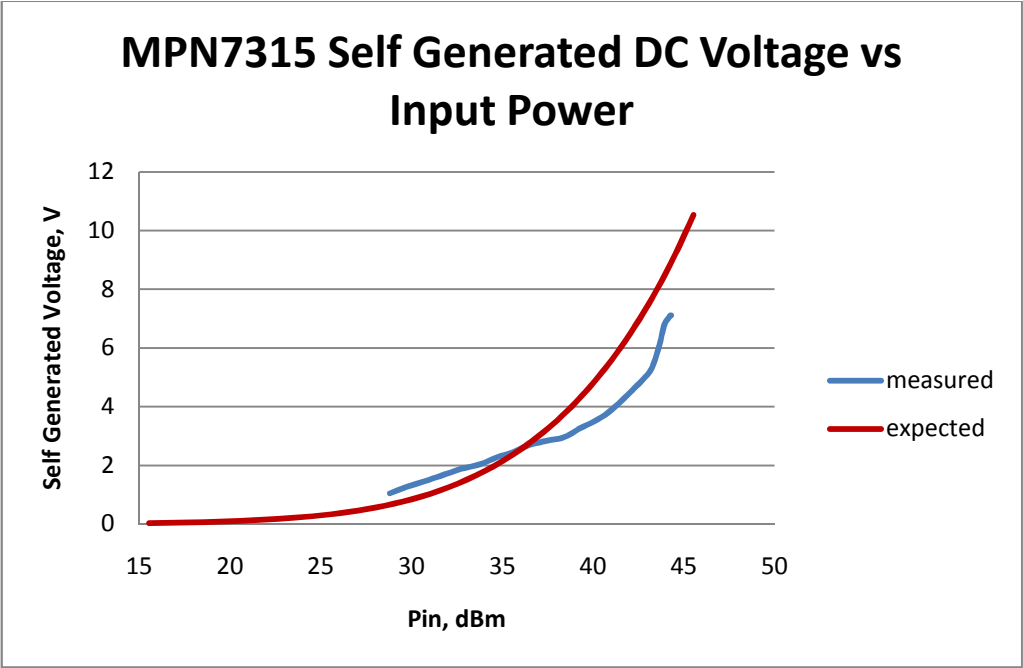


Figure 4.9: MPN7315 Measured Self Generated DC Voltage vs Expected

Similarly, sample PIN diode with part number MPN7453A is measured up to 51.7W with 5% duty cycle at 10GHz. The measured self generated DC voltage is compared with expected values in Figure 4.10.

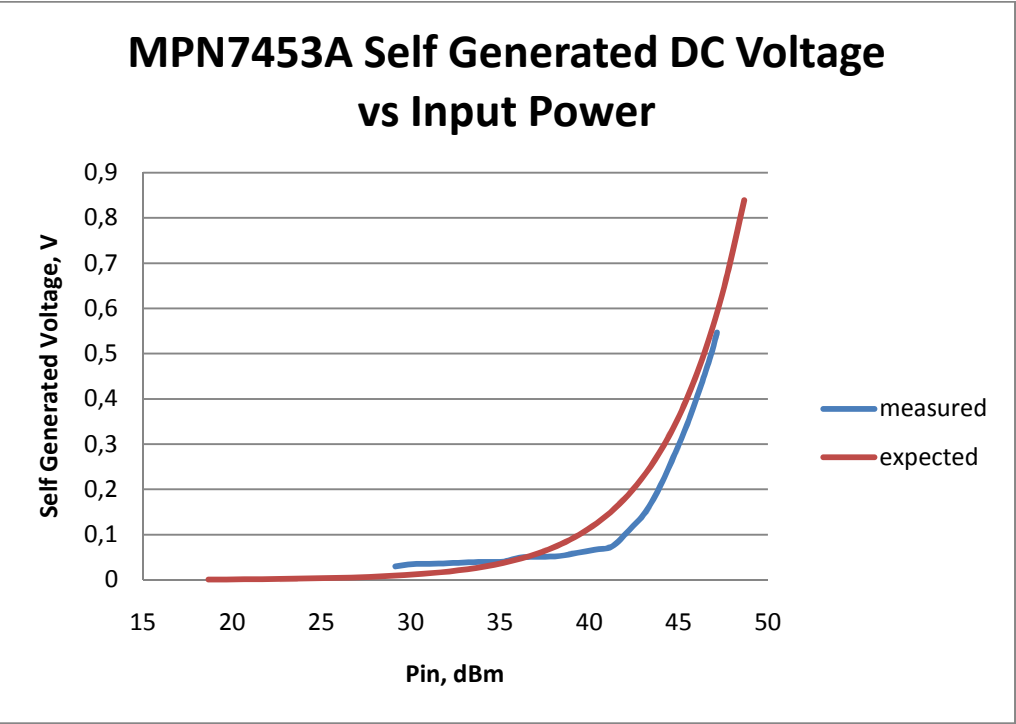


Figure 4.10: MPN7453A Measured Self Generated DC Voltage vs Expected

Since MPN7453A and MPN7453B have similar I-region widths, their self generated voltages under same power levels are similar. Thus, the measured self generated voltage of MPN7453B is given and compared with expected values in Figure 4.11 for up to 45.7W CW at 10GHz.

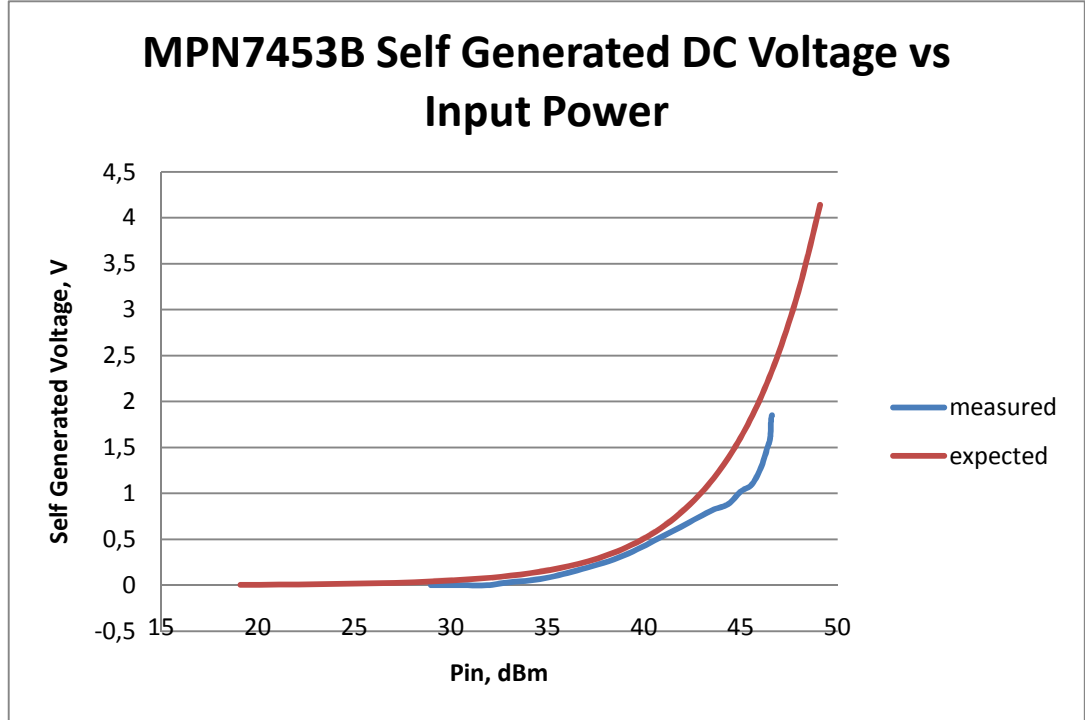


Figure 4.11: MPN7453B Measured Self Generated DC Voltage vs Expected

During the measurements, it is justified that decreasing the frequency increases the self generated voltage as expected from the derivation in Section 4.4. Similarly, the comparisons given show great consistence between measured voltages and expected voltages, for all sample PIN diodes. Also, having narrower I-region width than the others, MPN7315 generates greater voltage under similar power levels as expected.

The expected power handling of the designed switches were given in Chapter 3. The measured and expected self generated voltages at these power levels are summarized in Table 4.1.

Table 4.1: Expected and Measured Self Generated DC Voltages Under Expected Power Handlings

Part Number	CW Power, W	Self Generated DC Voltage, V	
		Expected	Measured
MPN7315	9	4,47	3,31
MPN7453A	73,5	3,74	3,55
MPN7453B	81,2	4,14	3,84

4.6 High Power Measurements

The designed switches with different power handlings are measured at high power levels. Temperature rise under expected power handling, power handling at high temperature and harmonics with respect to the applied reverse voltage are the three main performances considered in this section. High power RF with different duty cycles at X-Band is supplied by a solid state power amplifier. In order not to damage the peak power analyzer and the spectrum analyzer, high power attenuators with enough attenuation are used at the output of the switch. The measurement setup is shown in Figure 4.12.

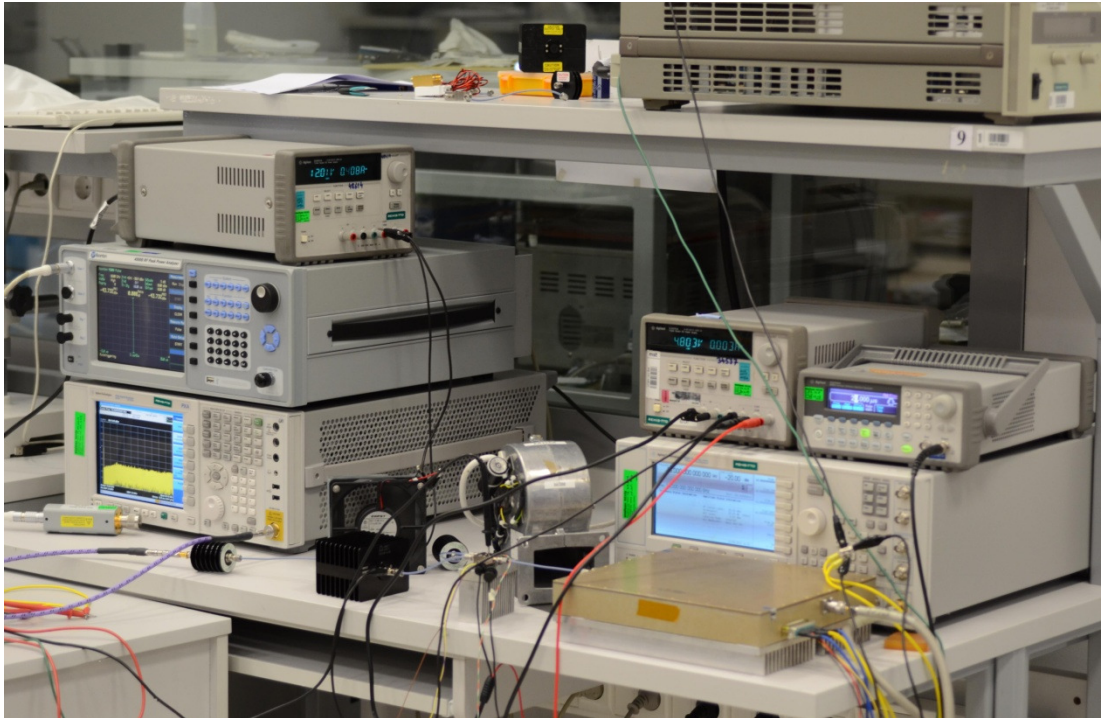


Figure 4.12: High Power Measurement Setup

The carriers on which the microwave components of the switches are attached are screwed into a mechanical case for high power measurements. Since the flatness of the carriers is not perfect, the heat is not perfectly transferred to the case. Thus, indium foil is inserted between the case and the carrier for better heat transfer. The case with the carrier screwed inside is shown in Figure 4.13.

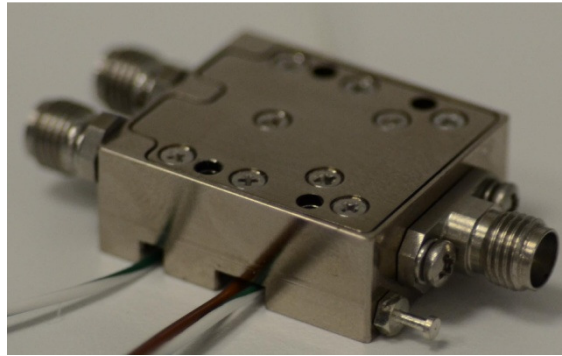


Figure 4.13: Constructed Switch Module

For better heat sinking the switch module is screwed to a finned heat-sink. Similarly, a thermal interface material is used between the case and heat-sink. The switch attached on the heat-sink is shown in Figure 4.14. The part in this figure is used during all measurements at high power levels.

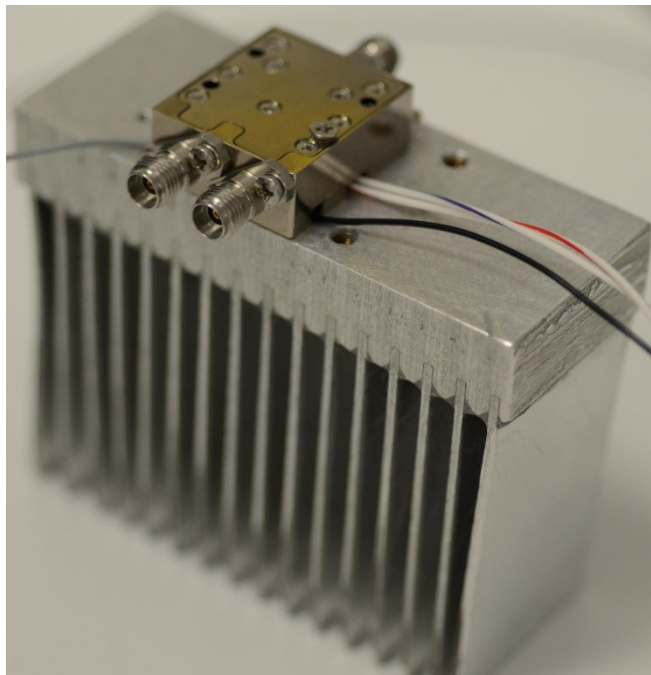


Figure 4.14: Switch Module Attached on the Heat-Sink

The power amplifier and the high power attenuators are cooled using fans. The switches are also cooled using fans during measurements in which temperature change is not desired to be observed.

All three switches are measured under their expected power handling levels. According to the calculations in Chapter 3, expected power handlings and power dissipations are summarized in Table 4.2.

Table 4.2: Expected Power Handlings and Power Dissipations

Part Number	Expected CW Power, W	Total Power Dissipation on PIN Diodes, W
MPN7315	9	0,56
MPN7453A	73,5	5,3
MPN7453B	81,2	5,4

The switches with different PIN diodes are measured in the form of the structure shown in Figure 4.14. No active cooling is used while observing the temperature rise on the carrier. The temperature rise of each carrier at their expected power handlings within twenty minutes of operation is given in Figure 4.15.

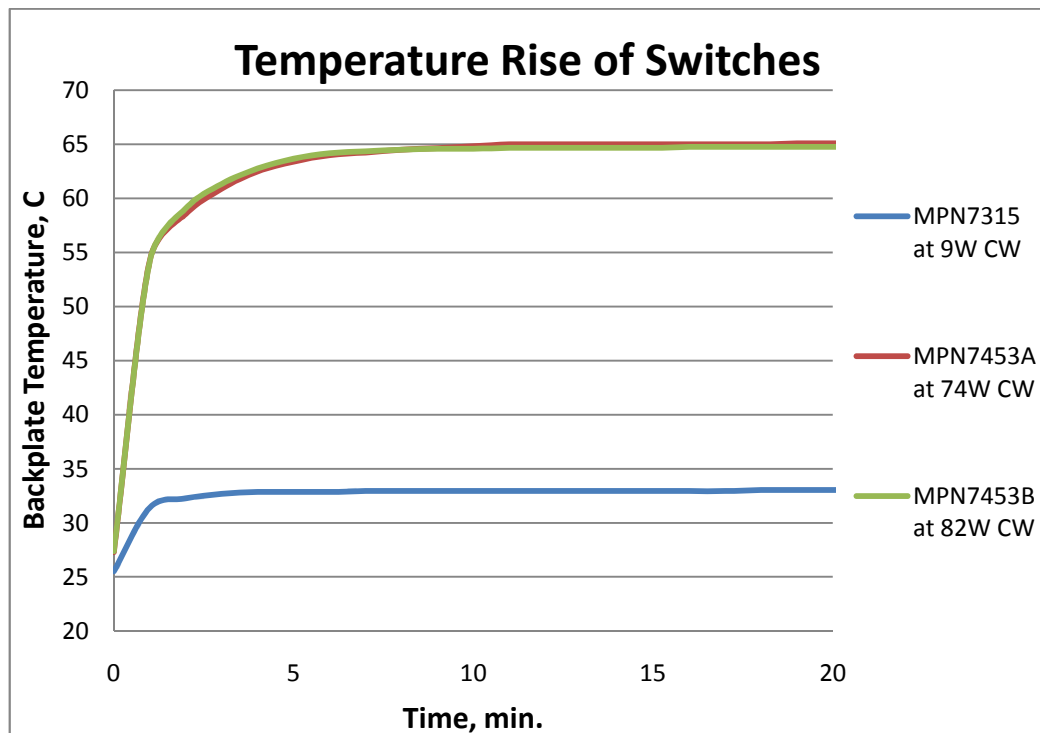


Figure 4.15: Temperature Rise of Carriers at Their Expected Power Handlings

Having very low power dissipation, temperature rise of the switch with MPN7315 is about 7°C . Since the switches with MPN7453A and MPN7453B have much more power dissipation, their temperature raised about 37°C . Having the same amount of temperature rise, it can be seen that they dissipate same power at different incident power levels. This also justifies that MPN7453A has higher forward resistance than MPN7453B.

The calculations related to power handling were done in Chapter 3 assuming 75°C backplate temperature. The temperature rise given in Figure 4.15 shows that the switches can handle the expected power level at 65°C . With further measurements, power handlings of all switches at 75°C are justified. In other words, three switches with CW power handlings of 9W, 73.5W and 81.2W are successfully designed. During the measurements, the minimum reverse bias obtained in Section 4.5 is used and no compression is observed.

The peak pulsed power handlings are measured in another setup shown in Figure 4.16. A TWTA is used in this setup to supply the desired power level. Necessary precautions are taken in order not to damage the peak power analyzer.

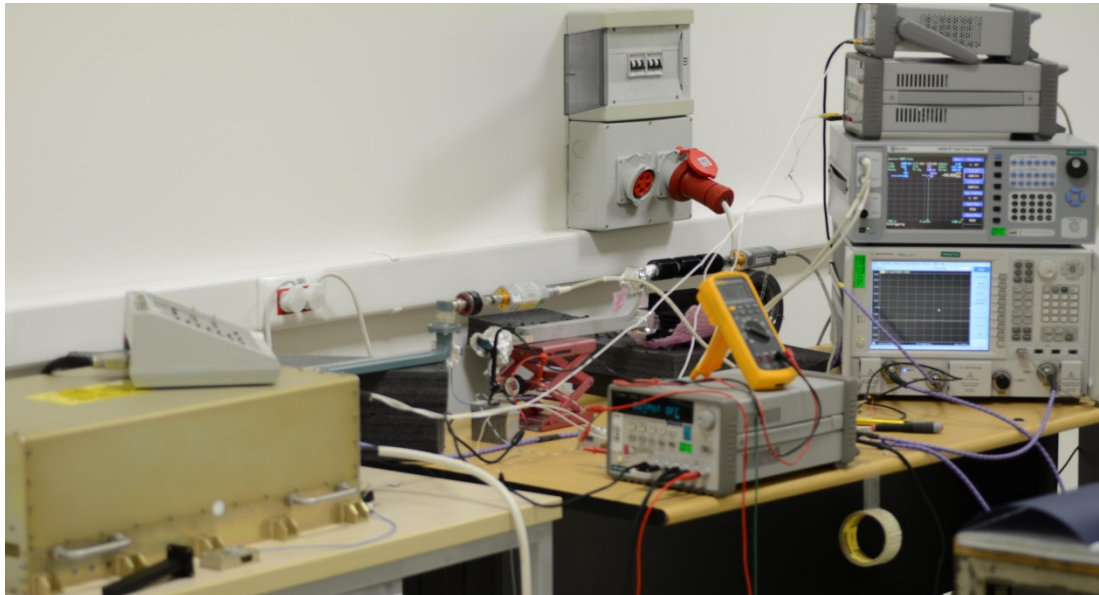


Figure 4.16: Setup for Measurements of Peak Pulsed Power

The peak pulsed power measurements are done at 1% duty cycle with $5\mu\text{s}$ pulse width. Since the pulse width is much less than the thermal time constant and the duty cycle is small, the switches are expected to handle as much power as their breakdown voltages allow. Applying only -15V as reverse voltage, the designed switches could handle the RF powers given in Table 4.3. The switch with MPN7315 could also handle 80W peak power at 10% duty cycle with $20\mu\text{s}$ pulse width.

Table 4.3: Breakdown Voltages and Peak Pulsed Power Handlings of the Switches

Part Number	Breakdown Voltage, V	Peak Pulsed Power Handling, W
MPN7315	150	120
MPN7453A	300	750
MPN7453B	400	1200

4.7 Second Harmonic and IP3 Measurements

Nonlinear components like switches generate distortion. The distortion components may affect the overall system performance. Thus, the nonlinear characteristics should be known. Although very high order distortion components are generated, the most significant ones are second and third order components since the higher order components have lower coefficients. Related to the distortion characteristics, second harmonics and third-order intercept points of three switches are measured with respect to the applied reverse voltage.

The 9W switch with MPN7315 has output third order intercept point of 48dBm when it is 0V of reverse bias is applied to the PIN diode in the *ON* arm. As the applied reverse voltage is increased, IP3 increases. About 57dBm output IP3 is obtained when the PIN diode is reverse biased at -25V. The related measurement is shown in Figure 4.17.

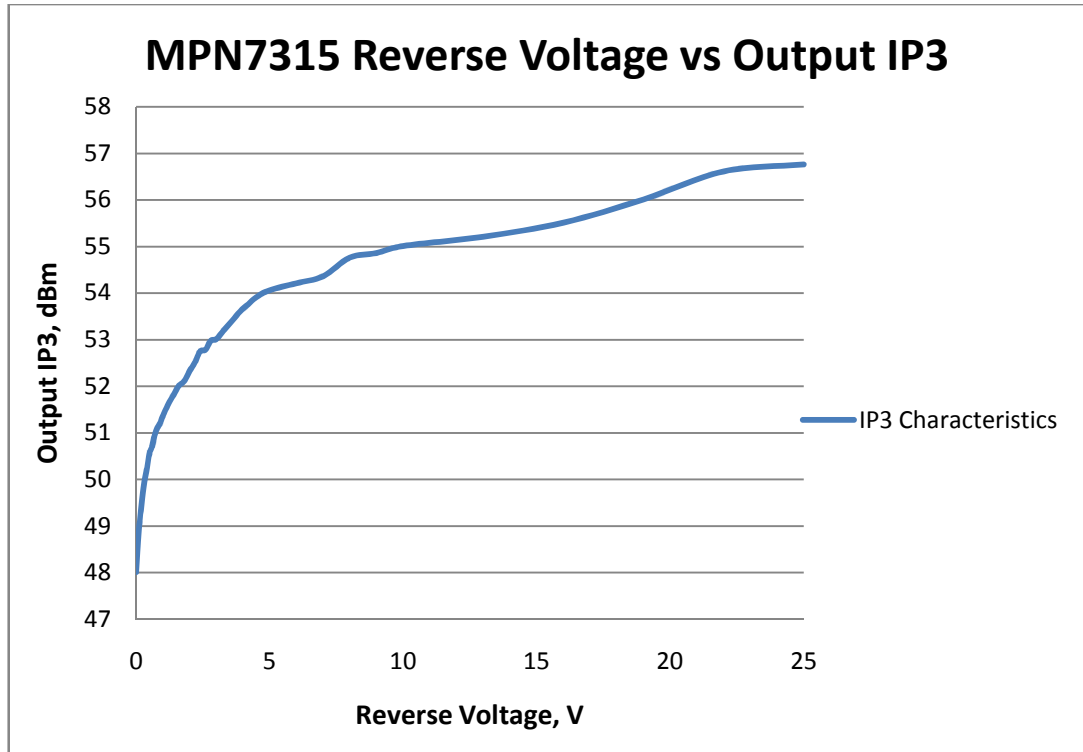


Figure 4.17: Reverse Voltage vs Output IP3 of Switch with MPN7315

PIN diodes with wider I-region width have better distortion characteristics [23]. Employing MPN7453A and MPN7453B which have wider I-region widths, the 73W and 81W switches have higher output IP3. Even when 0V is applied as reverse voltage, these switches have output IP3 greater than 58dBm.

Similarly, second harmonic of 9W switch with respect to reverse voltage is measured and shown in Figure 4.18. The second harmonic is about 60dB suppressed when -4V of reverse bias voltage is applied. The loss under the same condition is also measured and shown in Figure 4.19. It should be noticed from both figures that applying a reverse voltage same as the self generated DC voltage measured in Section 4.5 significantly increases the harmonic suppression and decreases the loss.

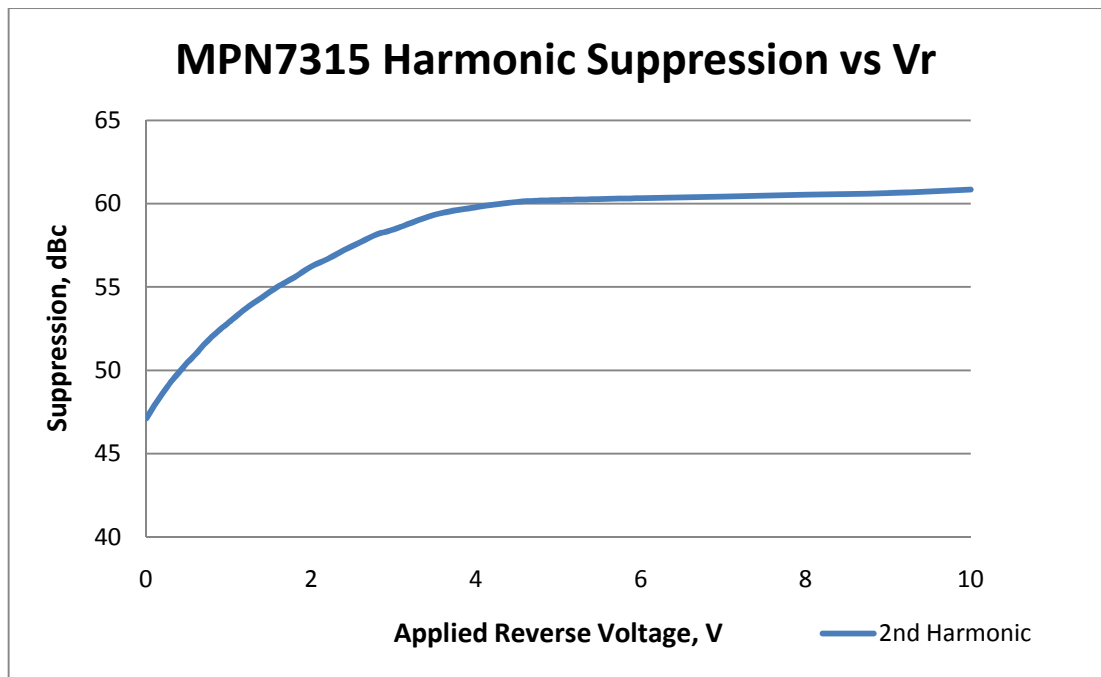


Figure 4.18: Reverse Voltage vs Second Harmonic of Switch with MPN7315

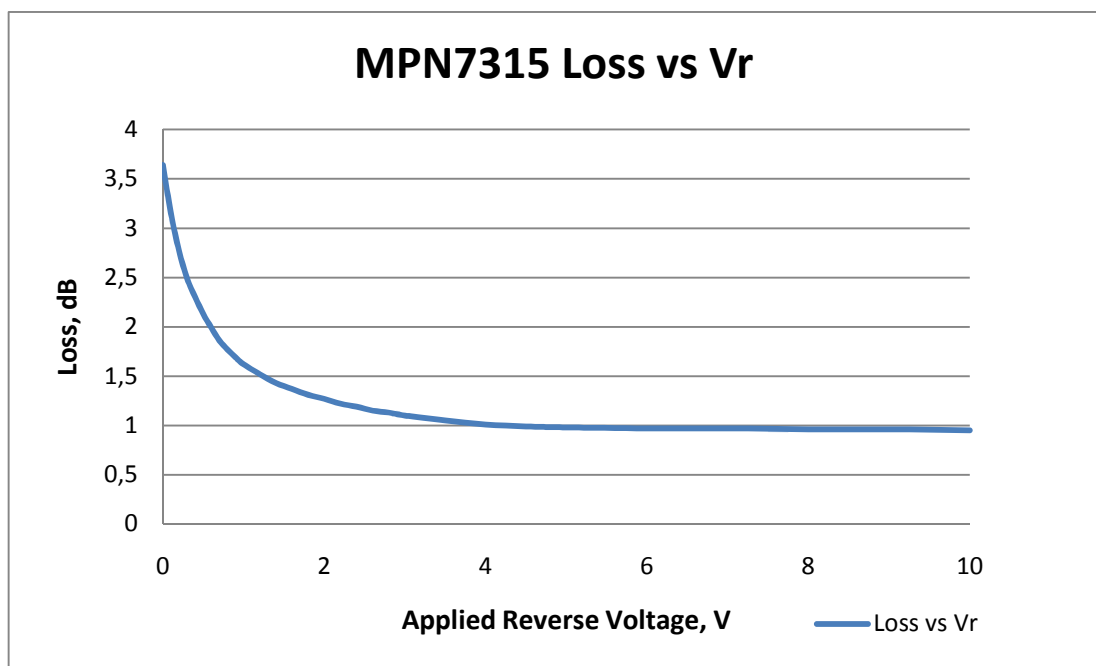


Figure 4.19: Reverse Voltage vs Loss of Switch with MPN7315

Similar measurements are conducted on the higher power switches. The second harmonic suppression of the switch with MPN7453B is shown in Figure 4.20. Second harmonic 65dBc below fundamental component is obtained by applying the reverse voltage same as the self generated voltage found in Section 4.5.

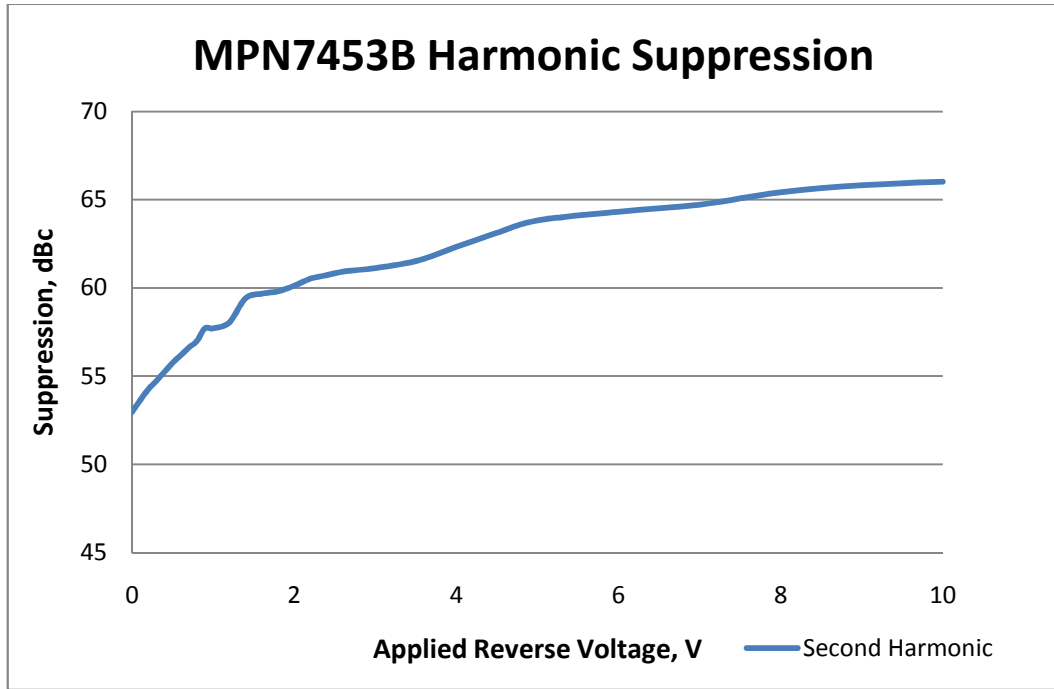


Figure 4.20: Reverse Voltage vs Second Harmonic of Switch with MPN7453B

The switch with MPN7453A has similar distortion characteristics as the one with MPN7453B, thus the related graphics are not given.

In this section, the measurements of generated reverse bias distortions of the designed high power switches are given. There is no forward biased PIN diode in the *ON* arm. The forward biased PIN diode is placed in the *OFF* arm and the contribution of this diode to the distortion is negligible. For this reason the distortion generated by the forward biased diodes are not analyzed.

The summary of the distortion measurements is given in Table 4.4. The given values are the measurements with PIN diodes reverse biased at their self generated voltages.

Table 4.4: IP3 and Second Harmonic Suppression of the High Power Switches

Part Number	IP3, dBm	Second Harmonic Suppression, dBc
MPN7315	54	60
MPN7453A	>58	63
MPN7453B	>58	64

4.8 Summary of Results and Comparison with Simulations

In this section, the general performance of the designed switches is evaluated and compared with simulations. The basic performance criteria are high power handling, low insertion loss and good isolation. The harmonic characteristics are evaluated and switching speed is shortly discussed.

The designs of all three switches were based on the selection of the PIN diodes for the particular applications. Resonating out the shunt capacitance of these PIN diodes at X-Band, good matching with low insertion loss and high isolation is obtained. The measured S-parameters are quite consistent with the simulations. The comparisons are given in Figure 4.21, Figure 4.22 and Figure 4.23. Small differences are due to the biasing circuit interference which is not included in given simulations. Small shifts in the return loss response are also negligible since the return loss is better than 15dB within the frequency band.

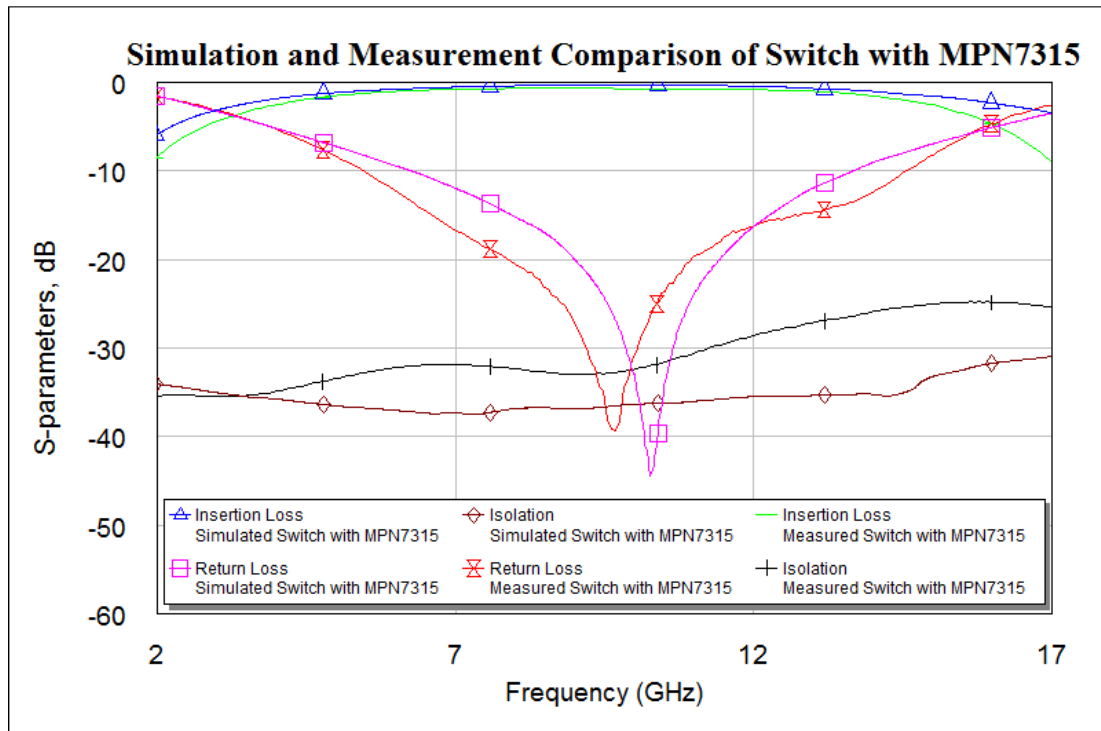


Figure 4.21: Simulation and Measurement Comparison of Switch with MPN7315

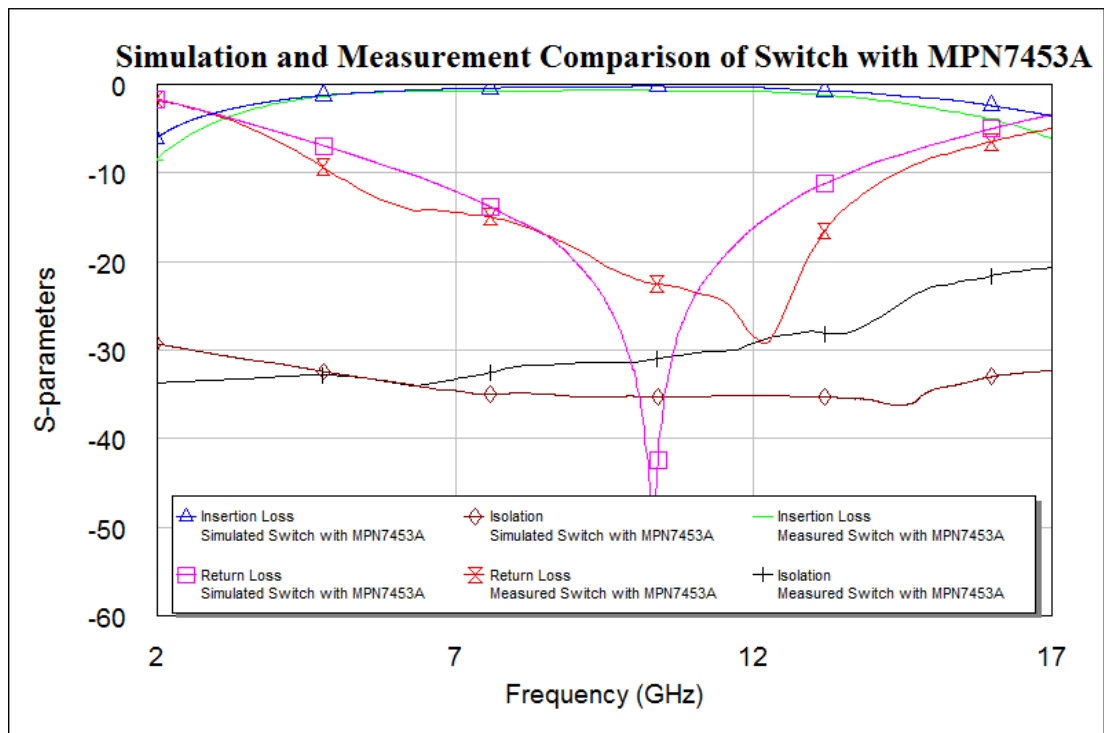


Figure 4.22: Simulation and Measurement Comparison of Switch with MPN7453A

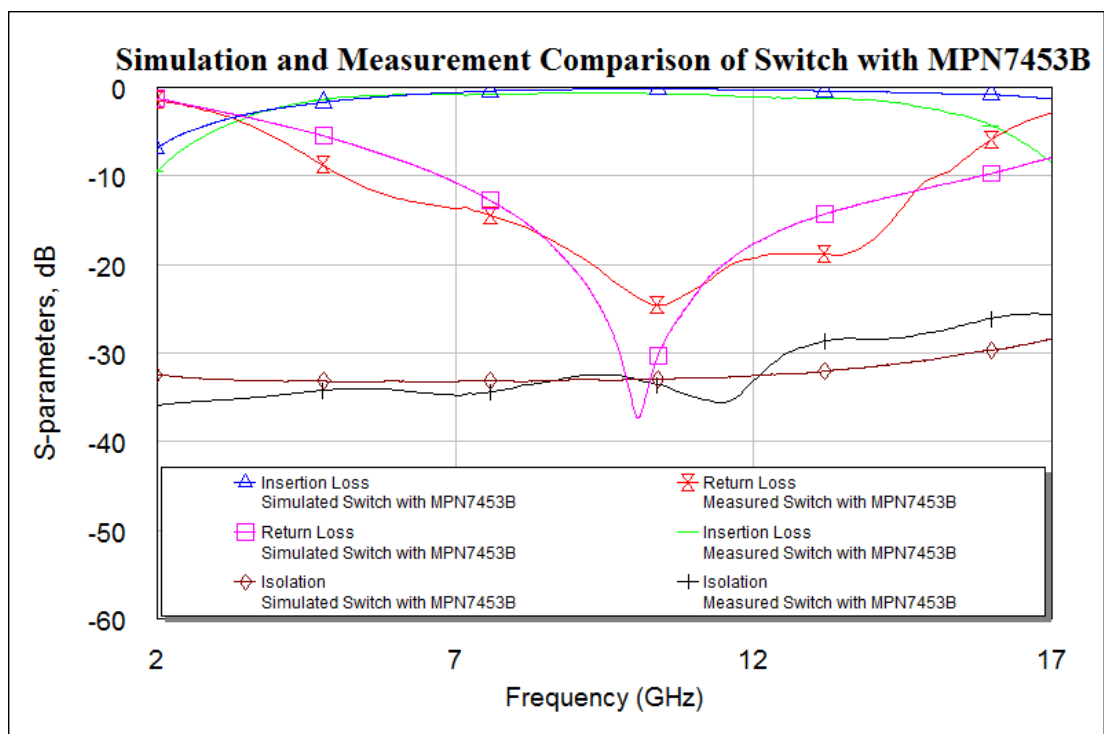


Figure 4.23: Simulation and Measurement Comparison of Switch with MPN7453B

The expected power handlings of the switches were calculated in Chapter 3. The high power measurements given in Section 4.6 have shown that the switches could safely handle the expected power levels.

The switching speeds of the designed switches show great difference. The difference is mainly due to the differences in the carrier lifetimes of the PIN diodes. Having carrier lifetimes of 150ns, 700ns and 2500ns, the 9W, 70W and 80W switches have 70ns, 450ns and 1.1us switching speeds, respectively. PIN diodes have slow reverse to forward bias recovery time than forward to reverse bias. Based on this statement, slightly faster switching speed is observed for forward to reverse bias transition.

The harmonic characteristics of the switches can be considered to be perfect. All three switches have more than 60dBc second harmonic suppressions and higher than 54dBm output IP3. With these measurements, there is no need to measure the third harmonic and IP2. It is known that the second order intermodulation products are 6dB higher than the second harmonics. Similarly, third order harmonics are 9.54dB lower than the third order intermodulation products.

The temperature of the switches increased under high power since significant amount of power is dissipated in the structure. The effects of temperature rise on S-parameters are observed. Since the loss of the lines and components increases with temperature insertion loss also increases, as expected. The isolation mainly depends on the mismatch of the isolated arm. The resistive loss can be negligible with respect to the mismatch loss in the isolated arm. The change in mismatch with temperature can be counted as negligible, especially when the level is around 30dB. On the other hand, similar resistive loss as the other arm is observed. Thus, it is concluded that temperature did not have significant effects on isolation in this design.

The general performance of all three switches is given in Table 4.5.

Table 4.5: Summary of General Performance of Switches at X-Band

Part Number	MPN7315	MPN7453A	MPN7453B
Insertion Loss, dB	< 0.9	< 0.85	< 0.85
Return Loss, dB	> 16	> 15	>15
Isolation, dB	> 28	> 29	> 33
CW Power Handling, W	9	70	80
Peak 1% Pulsed Power Handling, W	120	750	1200
IP3, dBm	54	> 58	> 58
2nd Harmonic Suppression, dBc	60	63	64
Switching Speed, ns	70	450	1100

One superior advantage of solid state switches is their small size. They can be realized in very small dimensions when compared to their ferrite or electromechanical counterparts. The carriers on which the switches are assembled are 7mm x 5mm. There are extra microstrip lines in order to have enough length between two connectors. If these lines were not used, the approximate dimensions of the switch would be 3.5mm x 4mm.

The overall losses of the switches were given in Table 4.5. In addition to the main switching part, the given measurement includes the losses of extra lines mentioned, DC block capacitors and biasing circuit. The loss of each component loss is measured separately. The extra microstrip lines have 0.11dB loss. Also each 43pF DC block capacitor used here has 0.1dB loss at 10GHz. The interference of the bias circuit is negligible at X-Band. The designed switches have 0.7dB insertion loss at 10GHz. So, it is concluded that the main switching part including PIN diodes and lines having length of $\lambda/4$ has only 0.4dB loss.

CHAPTER 5

CRITICAL DESIGN RULES FOR HIGH POWER SWITCH APPLICATIONS

In high power applications, the most critical thing is to cope with the thermal issues. The most often observed situation in a high power setup is the failure of a component due to high temperature. Thus, power dissipation at each component used and as a result temperature rise should be carefully analyzed in such high power applications. Similarly, power handling of each component should be limited to its maximum capability.

In this chapter, the failure mechanisms of components used in a high power switch are analyzed. Related simulations are given. Samples of failed components are shown. Accordingly, a matching method used in low power switches is investigated and it is shown that this method is not applicable in a high power switch application. A method for increasing the power handling is given with related simulations and measurements.

5.1 PIN Diode Failure

As mentioned in Section 2.3.1, there are two PIN diode failure mechanisms. The forward biased PIN diode may be damaged due to excessive power dissipation. On the other hand, reverse biased PIN diode may get damaged if the instantaneous voltage across the diode exceeds its breakdown voltage. Being the most critical element in a high power switch, the PIN diode should be chosen with great care.

During the design, the power dissipated on the forward biased PIN diode should be carefully analyzed. The dissipated power should not exceed its maximum. For less power dissipation, a diode with lower forward resistance should be chosen. Also, the diode should be able to handle large amount of current. These two properties require large diode cross section area. However; a PIN diode with large cross section area has higher capacitance, which may provide a leakage path for the RF signal when the diode is reverse biased. In addition, larger capacitance is more difficult to resonate out. That is the main limiting factor in realizing wideband high power PIN diode switches.

If the incident power is increased such that more power than PIN diode's maximum power dissipation is dissipated, the diode will obviously be damaged. A sample picture of a PIN diode switch on which excess incident power is applied is shown in Figure 5.1.

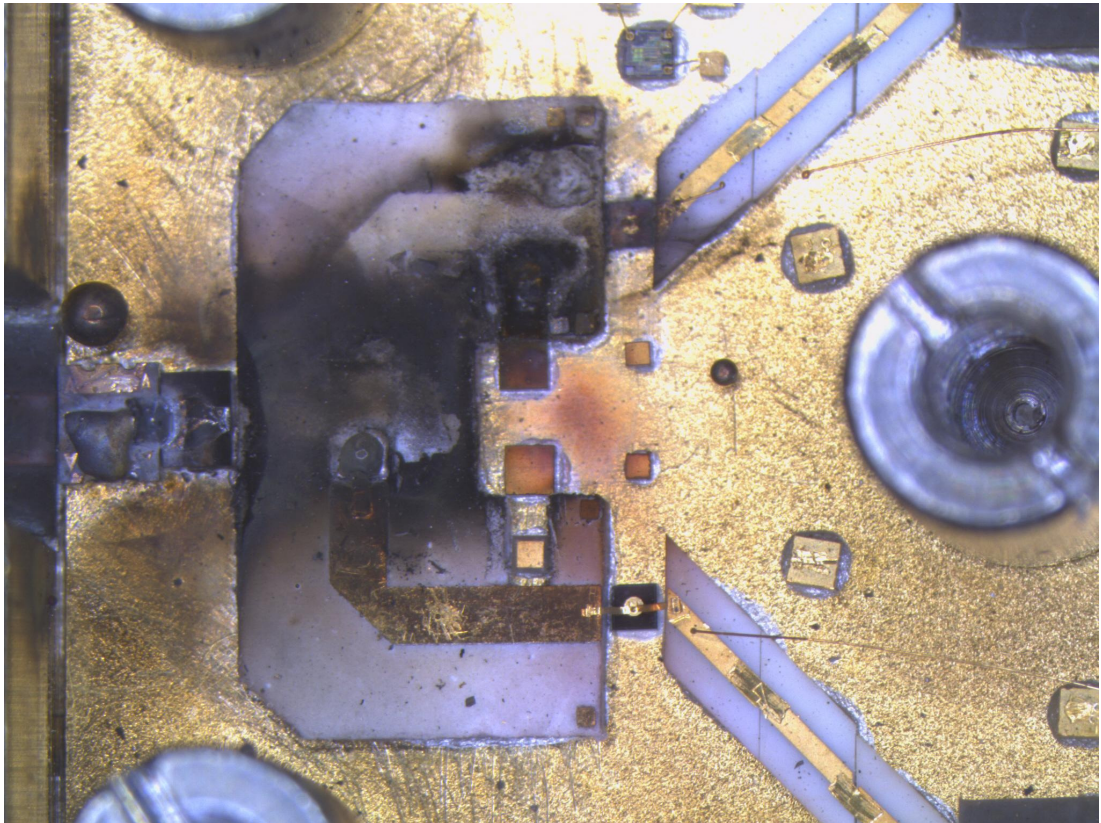


Figure 5.1: Excess Incident Power Applied on a PIN Diode Switch

The other power limitation on a PIN diode switch is the breakdown voltage rating of the PIN diode. The maximum voltage across the diode's electrodes is observed when it is reverse biased. During the negative cycle of the RF signal, magnitude of the voltage across the electrodes is the sum of reverse voltage and peak RF voltage. This total value should not exceed the breakdown rating. A sample picture of MPN7453B after -430V of total voltage applied is shown in Figure 5.2.

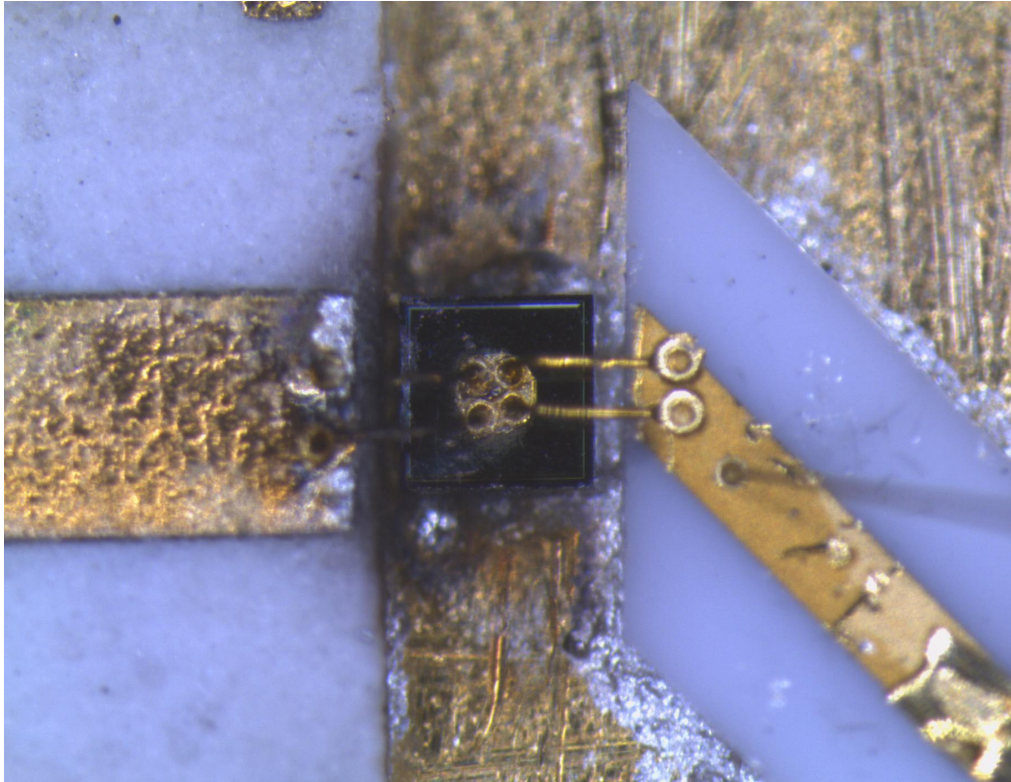


Figure 5.2: Excess Instantaneous Voltage Applied on a PIN Diode

The applied voltage on the PIN diodes used in a high power application should not exceed its breakdown voltage rating. Similarly, the dissipated power on the diode should not exceed its maximum value. Thus, the PIN diodes should be chosen considering their breakdown and power dissipation characteristics for the application.

5.2 Failure of RF Choke Inductor

As mentioned earlier, any component used in a high power application should be carefully chosen. As the RF choke inductor carries only the bias current one may claim that it is one of the safest components. However; this is not the fact.

In high power PIN diode switches, the reverse voltage applied does not have to have the same magnitude as the RF peak voltage. As explained in sections 4.4 and 4.5, there is a possible lower value for the reverse voltage. However; this situation requires an RF choke inductor with higher current handling. Similar is valid for the RF choke inductor used for forward biased PIN diode. In applications where there is a budget on power drawn from the source, the PIN diodes should be biased with less amount of power. Since PIN diodes are current controlled devices, the required current for turning the diode on should be drawn in any case. Decreasing the power can be succeeded by decreasing the voltage from which the current is drawn. In addition, although controlling the switch with high voltages increases the switching speed of the PIN diodes, switching high voltages at control circuit is slow. Thus, it is better to switch voltages as low as possible. This requires the choice of a resistor with smaller value at the output of control circuit. It was stated earlier that lowest insertion loss was obtained with the use of 1 mil bond wire as RF choke inductor. Obtained 7-8nH inductance has approximately 440-500 Ω reactance at 10GHz. Mounting a small resistance after this inductance results in a low impedance for the biasing line. Thus, RF current through the bias line becomes significant, which requires components with high current handling at the biasing lines.

The switches designed in this study are biased at +5V/-5V at 20mA for 9W switch and 40mA for higher power switches. Thus, the resistors used for controlling the PIN diode current are 200 Ω and 100 Ω respectively. Related circuit for the simulation is shown in Figure 5.3. Also, the simulation result of the current through the RF choke inductor is shown in Figure 5.4 for both forward biasing and reverse biasing arms of 9W switch. Note that if the biasing line was perfect open and the applied voltages had the same magnitude as RF peak, then the current through the reverse biasing line

would be zero and current through the forward biasing arm would be only the forward DC current. However; current through the forward biasing line is a sine wave having 60mA peak to peak with 80mA average although the PIN diode is biased at only 20mA. This simply shows the requirement of RF choke inductors with higher current handlings.

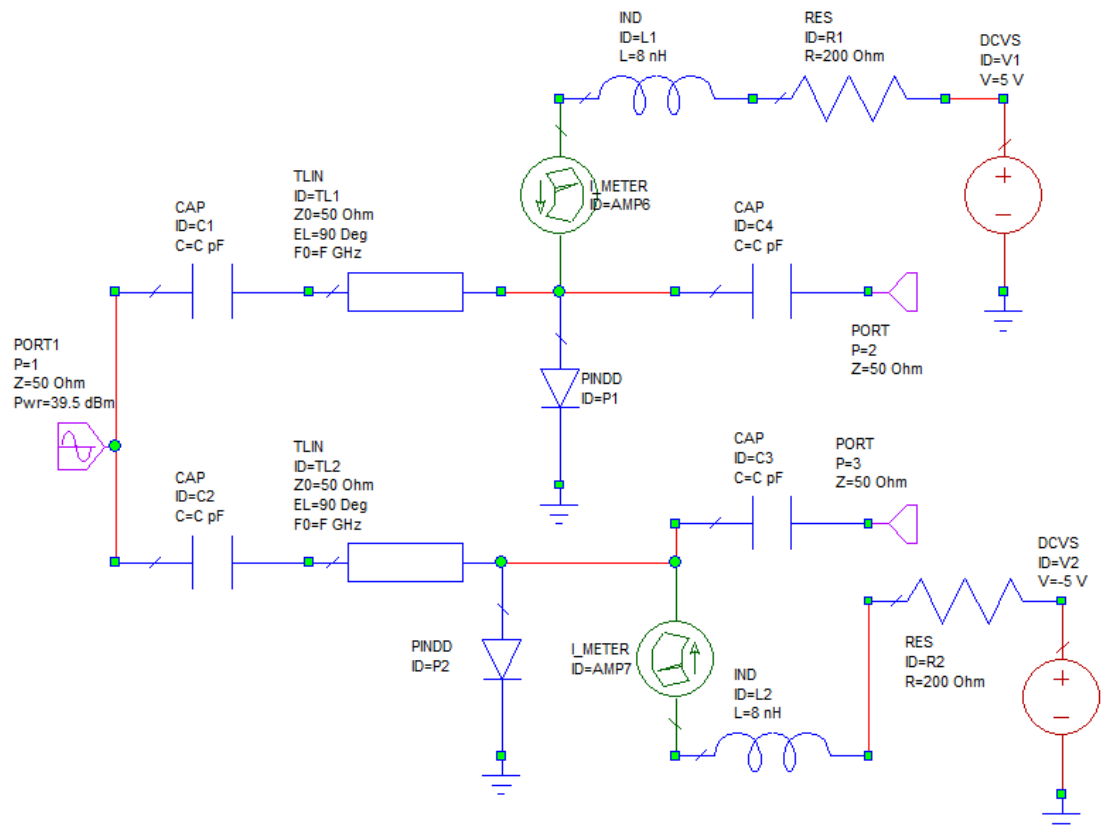


Figure 5.3: Simulation of Currents Through Biasing Arms at 9W Switch

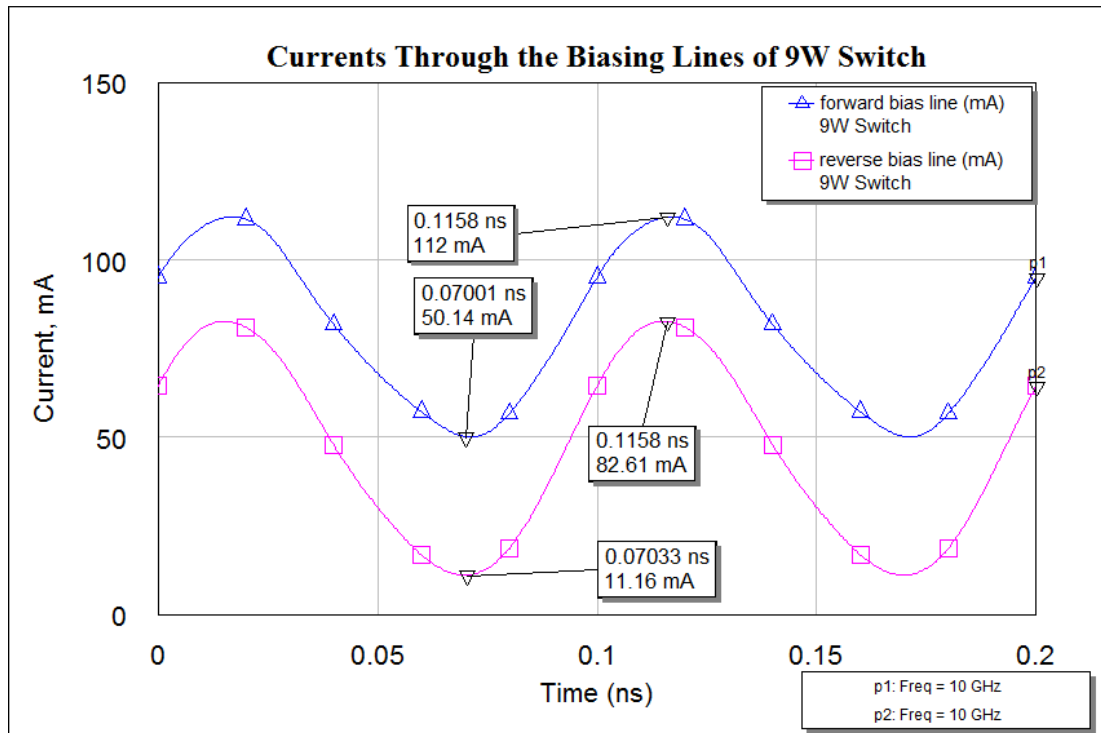


Figure 5.4: Currents Through Biasing Arms at 9W Switch

The currents through the other switches are also simulated. Since the other two high power switches have similar power handlings, the simulation results of 80W switch is shown in Figure 5.5. Similar to previous simulation result, the current through the forward biasing arm is much higher than the diode current, which is 40mA in this case.

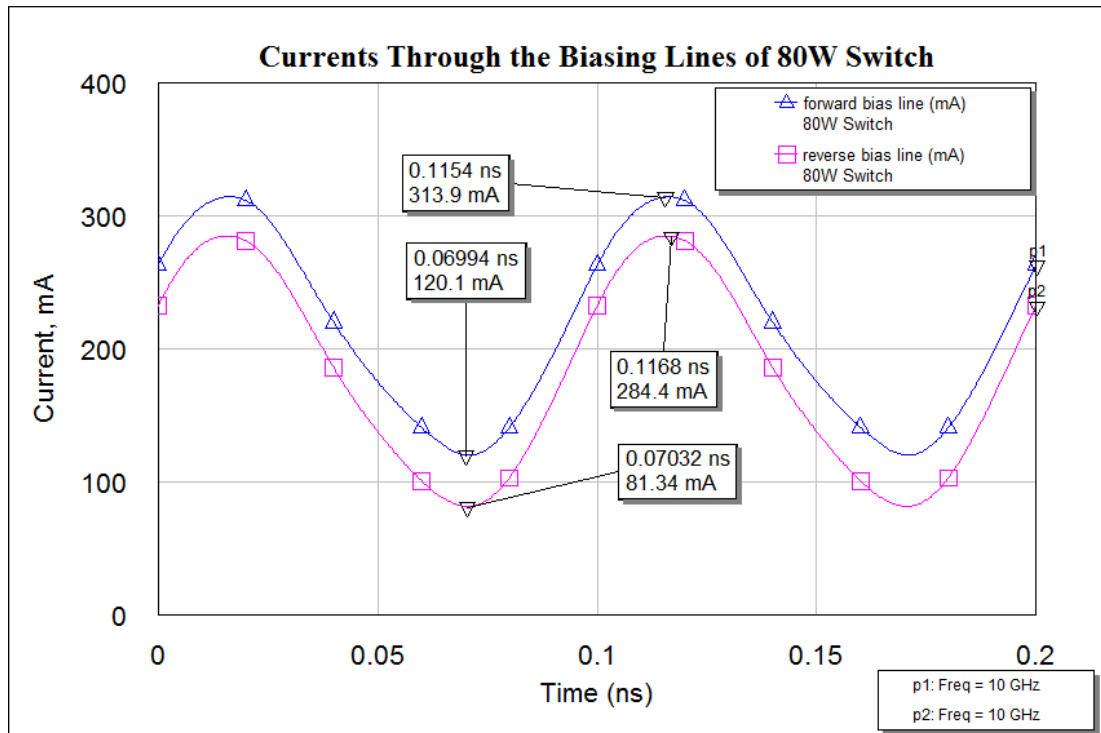


Figure 5.5: Currents Through Biasing Arms at 80W Switch

The current handling of the RF choke inductor becomes important in a high power switch application, although it is one of the safest components in low power applications. The main purpose in this study is obtaining high power handling while keeping low insertion loss. Also, high power switching in this study should be done with quite low voltages. These two properties in this study require RF choke inductors with high current handlings. A 10nH inductor with 100mA DC current handling was tried during the high power measurements. It was observed that 100mA current handling is not enough for this application. The inductor burned and the insulator around the wire disappeared, making the inductor useless. The picture of the related RF choke inductor after high current passed through it is shown in Figure 5.6. The 1 mil bond wire used in this study as RF choke has approximately 500mA current handling.

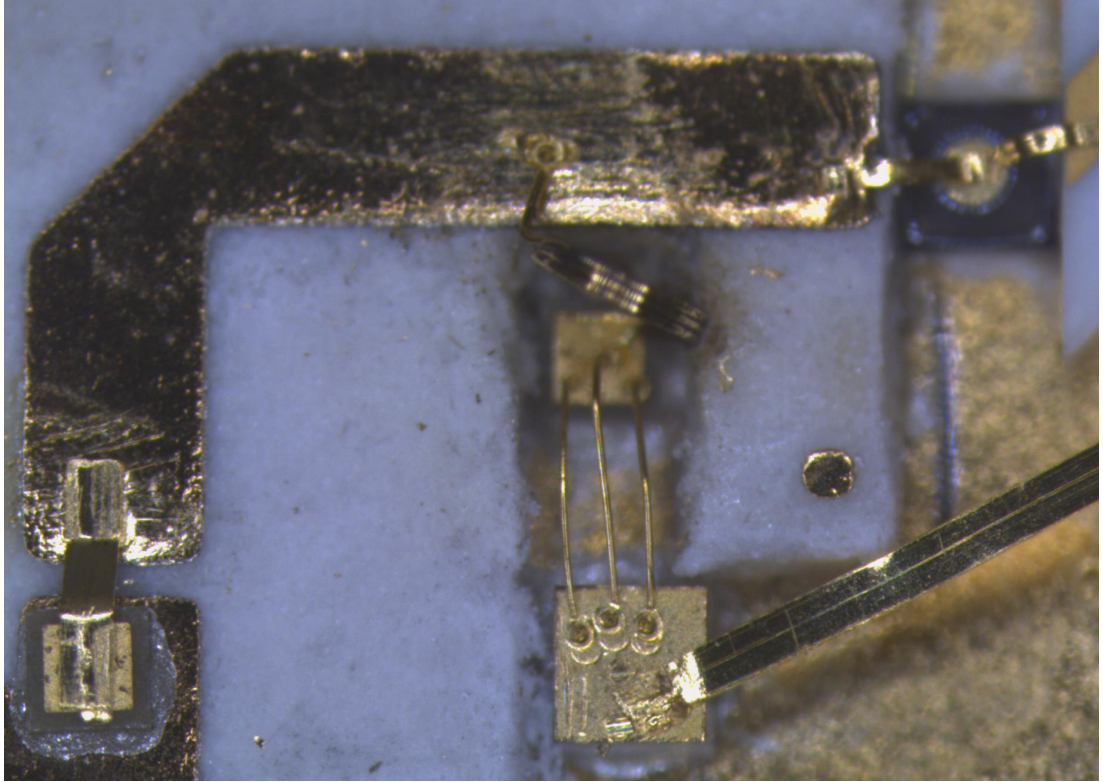


Figure 5.6: RF Choke Inductor after High Current Passed Through It

5.3 Increasing the Power Handling

There are two limiting factors on power handling in a switch. Those are the breakdown voltage and the power dissipation capability of the PIN diodes. Usually, the breakdown voltage is high enough that it does not limit the power handling. Then, the power dissipation capability gets more important, as it is the case in this thesis work.

In a high power shunt switch, depending on the ratio between forward resistance and reverse resistance, power dissipation on the forward biased PIN diode is generally much higher than the power dissipation on the reverse biased PIN diode. Thus, the limiting factor for power handling is the power dissipated on forward biased PIN diode. So, decreasing the power dissipation on the forward biased PIN diode increases the power handling of the switch.

It is expected to halve the RF current on the forward biased PIN diode by connecting two shunt PIN diodes at the same node. This method is generally used in high power MMIC switches, since those PIN diodes do not have high power handling capabilities. Thus, the RF current through the forward biased diode decreases by half and RF power dissipated on the diode becomes 1/4 of the initial value. This means that power handling of the switch is now four times greater than the previous power handling, provided that reverse biased PIN diodes are still safe. In this case, with approximately same amount of total power dissipation, the switch is expected to handle twice the power it handles with one PIN diode at each arm.

In such a circuit with regular shunt switch topology, the matching gets worse since the total shunt capacitance of the PIN diodes are doubled. Simulation result of s-parameters of a regular shunt switch with two MPN7315s at each arm is shown in Figure 5.7. Note that return loss gets worse. The results might be acceptable but better frequency response can be obtained by tweaking the matching networks.

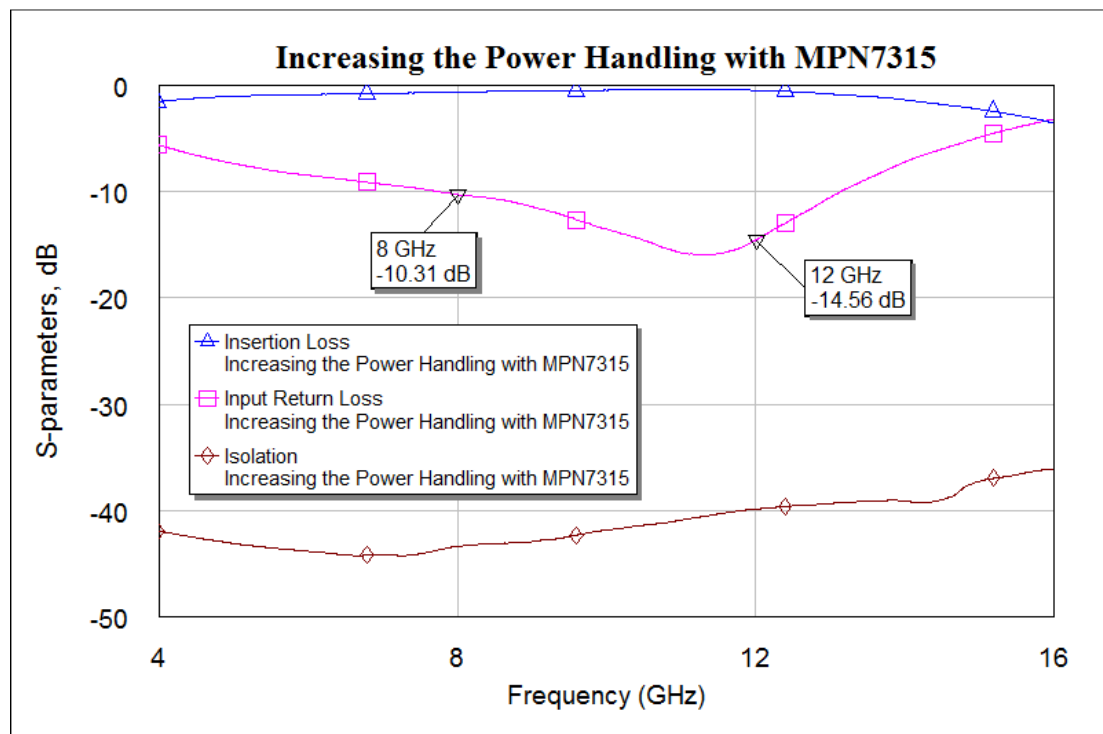


Figure 5.7: S-parameters of a Regular Shunt Switch with two MPN7315s at Each Arm

One of the matching methods includes some different transformations. The isolated arm is transformed to the common junction as a pure reactive load so that no real power is transferred to this arm. At the same time, the other should be transformed to the common junction as a pure real load, so that all real power is transferred to this arm during conduction state. For maximum power transfer the input port should be transferred to the impedance that is the complex conjugate of the impedance seen from the junction, in other words the parallel combination of both arms. Although great small signal performance can be obtained, such a switch actually is not a high power switch. Employing low impedance transmission line between common junction and forward biased PIN diodes leads to higher RF currents on the PIN diodes. In addition, the isolated arm is transformed to ideally a pure reactive load, in other words there is a resonant structure. Such a resonant structure also leads to higher currents. So in conclusion, such a design results in higher total power dissipation in the structure making it a low power switch, although the small signal s-parameters are good.

There is another matching method which is much simpler. High shunt capacitance can be resonated out by a series capacitance. This method employs DC block capacitors with low capacitance values. Figure 5.8 shows the impedances seen from the junction towards the isolated arm and the *ON* arm in the regular shunt switch. Note that the impedance of the *ON* arm is approximately $j21.4\Omega$ away from 50Ω . This reactance can be resonated out by inserting a series capacitance of 0.7pF , which has $-j22\Omega$ reactance at 10GHz . The impedances of both arms seen from the junction are given in Figure 5.9. Note that since the isolated arm has very high impedance, the inserted reactance did not have significant effect on the impedance of this arm.

There are two DC block capacitors used at each arm, one at the junction and the other at the output ports. The critical matching is done at the junction. So, using 0.7pF at the junction and 43pF at the output ports, the switch with higher power handling is designed as in Figure 5.10.

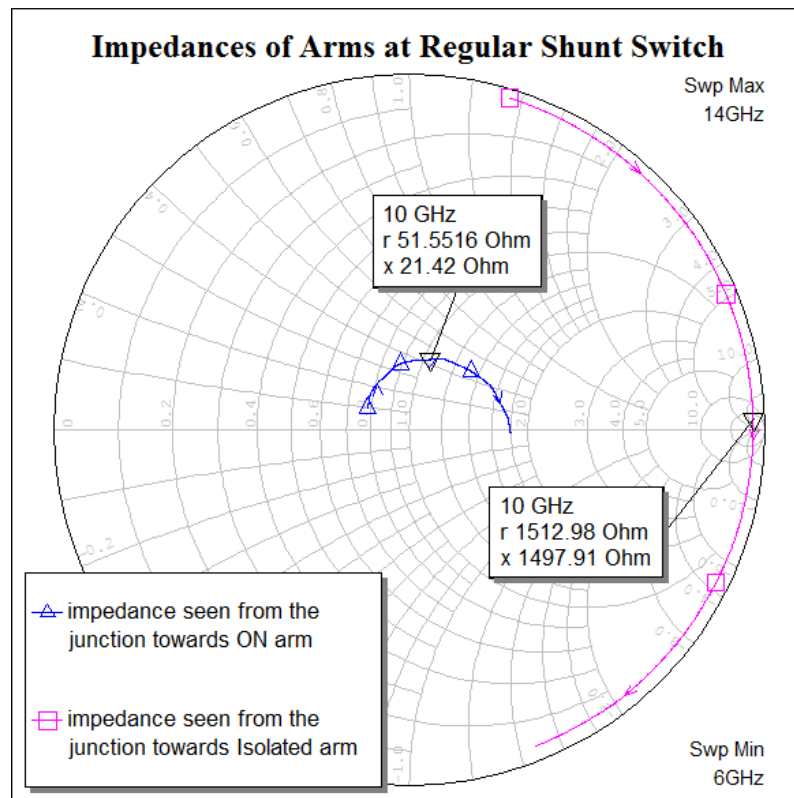


Figure 5.8: Impedances of Arms at Regular Shunt Switch

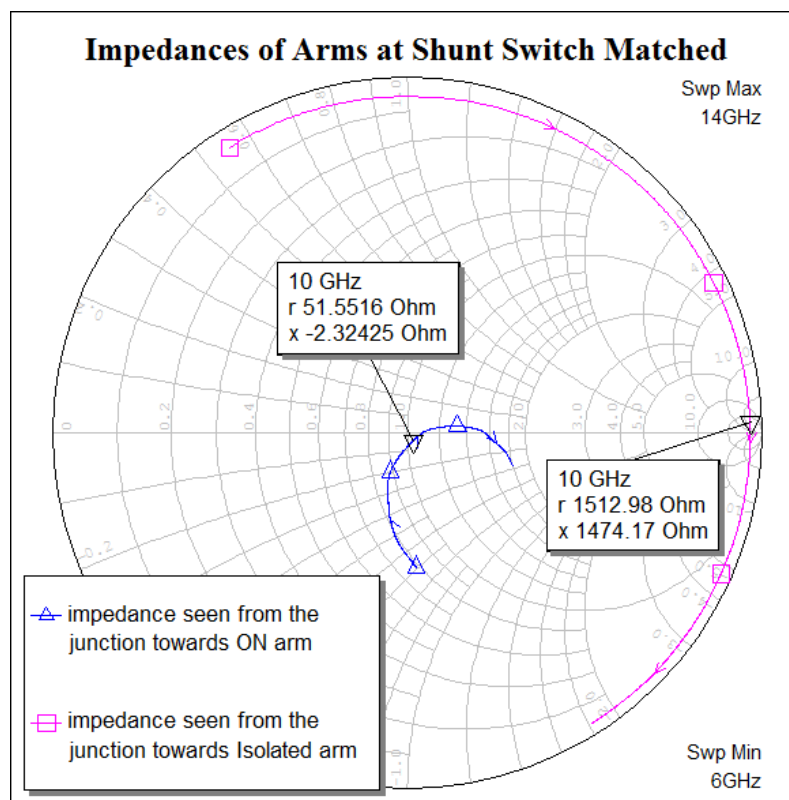


Figure 5.9: Impedances of Arms at Shunt Switch Matched with Small DC Block Capacitors

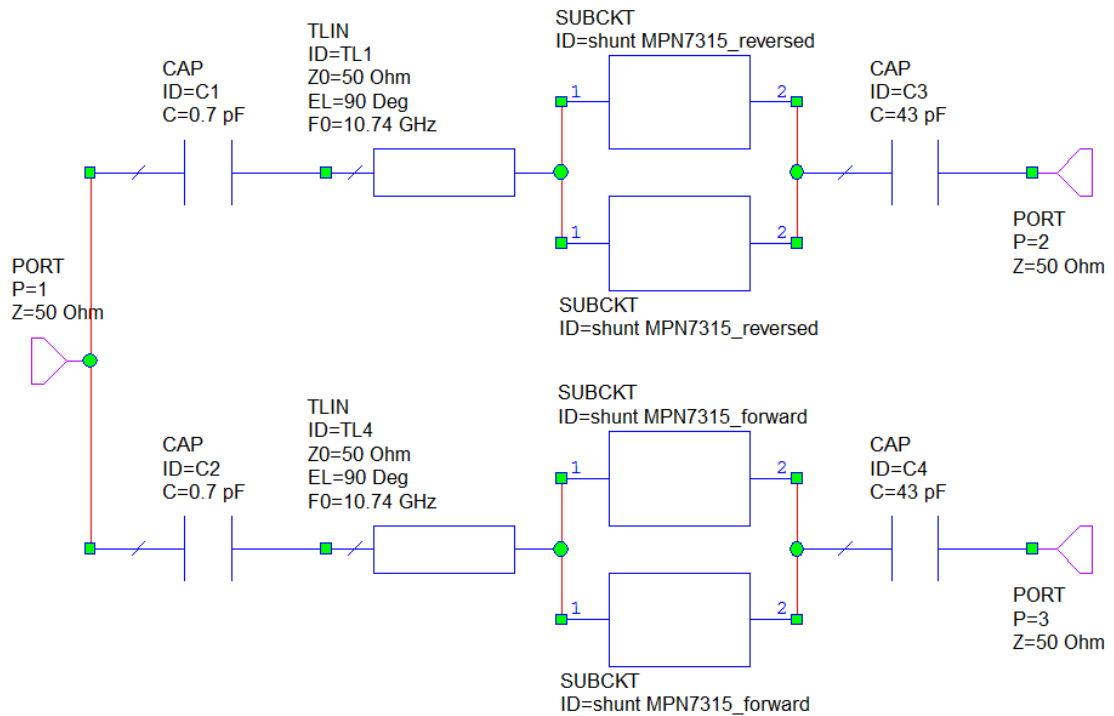


Figure 5.10: Higher Power Switch Designed Using Two MPN7315s at Each Arm

The simulated small signal s-parameters are given in Figure 5.11. As it can be seen, PIN diodes having high shunt capacitances can be matched.

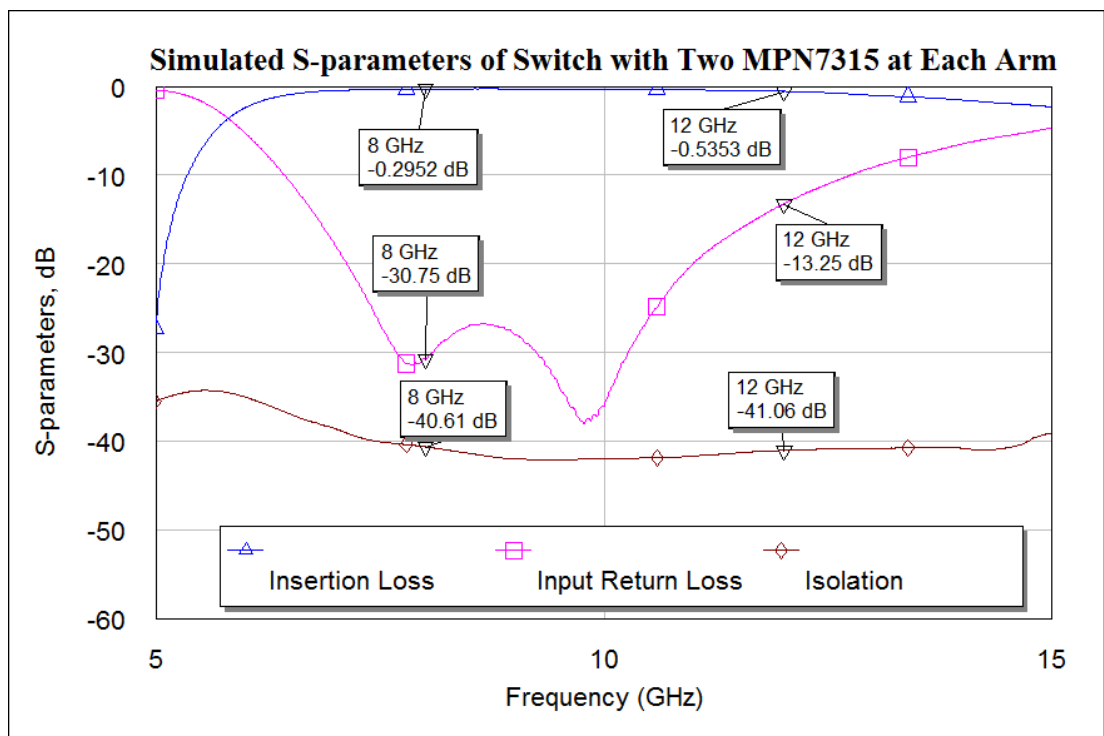


Figure 5.11: Simulated Small Signal S-parameters of the Switch in Figure 5.10

The main purpose of this design is to decrease the power dissipation on the forward biased PIN diode by decreasing its RF current by half. The currents of both regular switch and this type of switch are shown in Figure 5.12 for the same amount of power. In this figure, all PIN diodes are biased at 100mA DC current and 24dBm RF is applied to the switches, in order to show that RF current is cut in half.

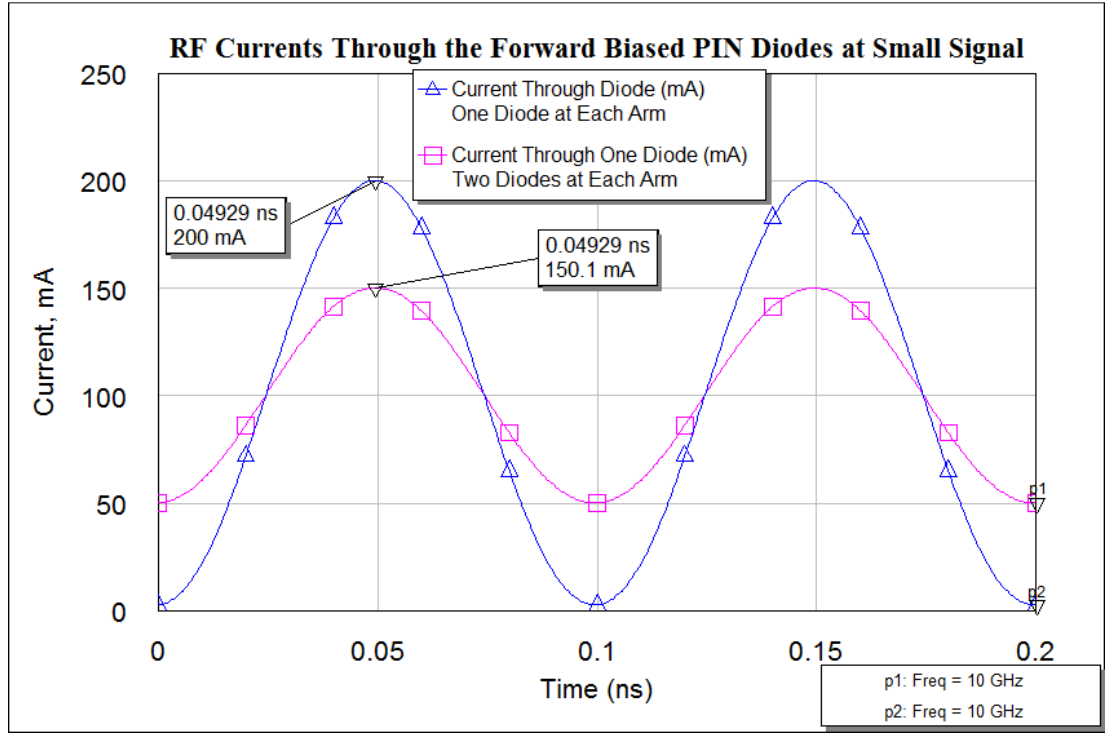


Figure 5.12: Currents Through the Forward Biased PIN Diodes at Small Signal

The designed switch with higher power handling is assembled on the same type of carrier as the previous designs. Similar measurements are conducted. The small signal s-parameters of this design are given in Figure 5.13. Note from the figure that the insertion loss is less than 1dB with little degradation at 12GHz. Since the matching is done for X-Band frequencies, return loss is also at considerable levels. Having two PIN diodes at the same node decreases the forward state resistance by half, which results in a better open circuit at the junction. Thus, the isolation is better than regular shunt switch with one diode at each arm.

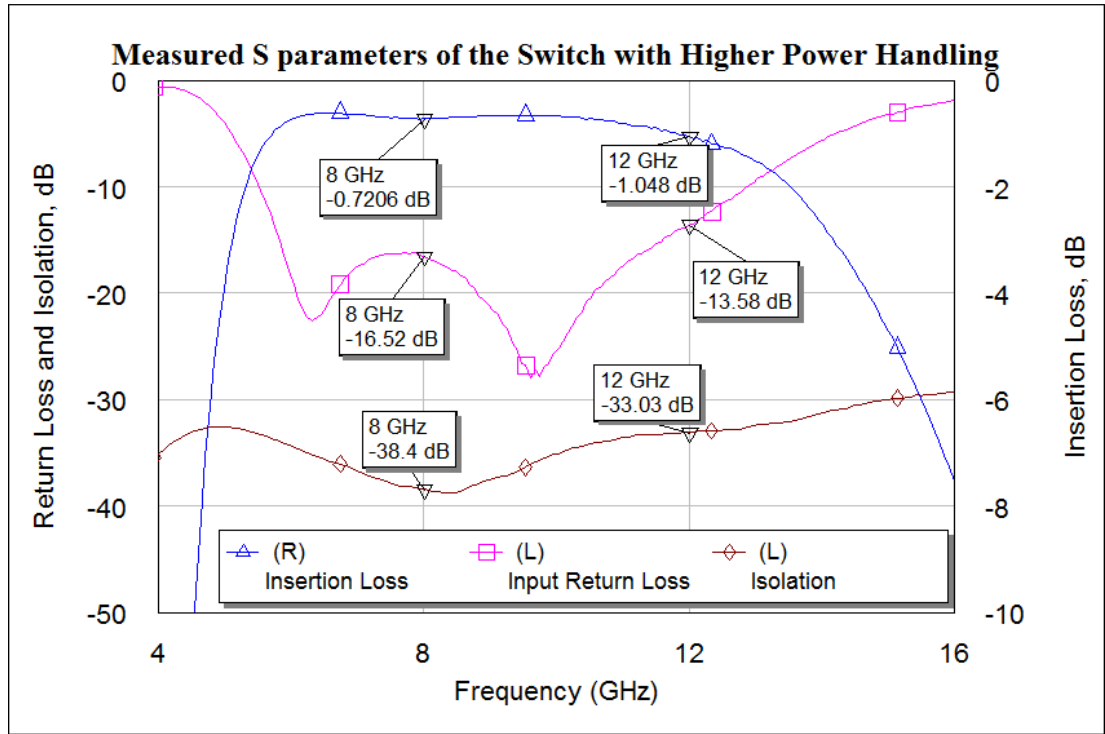


Figure 5.13: Measured S-parameters of the Switch with Higher Power Handling

Temperature rise of regular shunt switch with 9W CW power handling was shown in Figure 4.15 and it was stated that temperature rise at 9W incident power was 7°C. This higher power switch is expected to have approximately same temperature rise at 18W CW incident power. Measurements have shown that under similar environmental conditions, this switch has 9°C temperature rise when twice the power is applied. Small difference of 2°C is due to the neglected power dissipation on the additional reverse biased PIN diode and the increased power dissipation on the other components like microstrip lines.

Using the PIN diodes at stocks, approximately twice the power handling can be obtained with such a design while keeping the temperature rise similar. Note that power dissipation of each forward biased PIN diode is now 1/4 of that in previous design for the same incident power. Since the main failure mechanism is the power dissipation of the forward biased PIN diode, four times greater power handling can be obtained in applications where cooling is not problem. In an urgent need of a switch with 320W CW power handling for a measurement setup, the switch designed

with MPN7453B with 80W CW power handling can be upgraded, provided that the switch is heat sunk well.

5.4 Increasing the Power Handling and Isolation while Keeping DC Current Consumption Low

Method for increasing the power handling by decreasing power dissipation on critical components is introduced in Section 5.3. It was also mentioned in Section 2.2.2 that isolation of a shunt PIN diode switch can be increased by inserting additional shunt PIN diodes with quarter wavelength transmission lines between each other. A shunt SPDT switch with increased isolation is shown in Figure 5.14 with biasing circuits excluded.

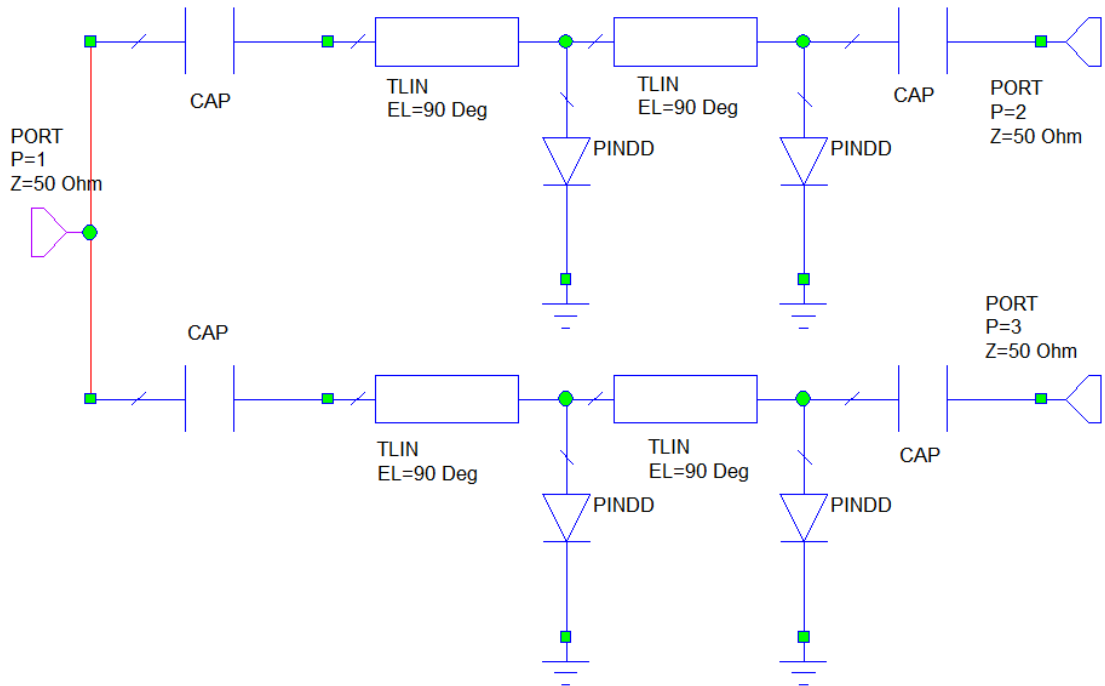


Figure 5.14: Shunt SPDT Switch with Increased Isolation

More than 60dB isolation can be obtained with the switch in Figure 5.14 while one diode provides approximately 30dB isolation as shown in Figure 5.15.

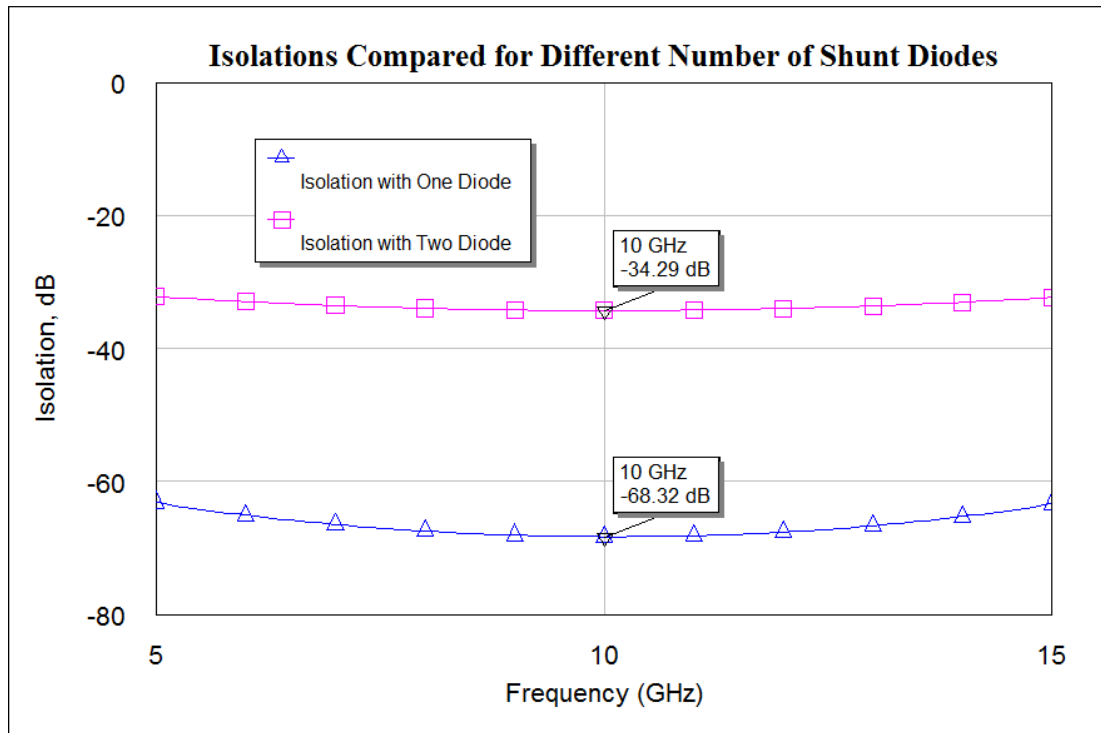


Figure 5.15: Isolations Compared for Different Number of Shunt Diodes

Using the method for increasing the power handling, in other words connecting two PIN diodes at each node, a switch with high isolation and high power handling can be obtained. However; this requires four PIN diodes at each arm. During the isolation state, forward biasing all the diodes in one arm requires four times the DC current that one diode requires. This situation significantly increases the DC power consumption. Remember that DC power consumption is the main disadvantage of PIN diode switches over FET switches.

Design approach given in this section represents such a high power switch with high isolation while keeping the DC power consumption low. In this approach all PIN diodes are placed such that their directions are the same. Applying the DC voltage from one side, one can provide that same DC current passes through all PIN diodes. With such an orientation four PIN diodes can be forward biased with only the current level that one PIN diode requires. However; this orientation requires that quarter wavelength transmission lines realized with coupled lines. In addition, the PIN diodes with quarter wavelength distance between each other should be isolated by an RF choke for better isolation. Each PIN diode should be placed between the RF line

and RF ground. RF ground at one electrode is provided by a shunt capacitor with high capacitance. The overall circuit is shown in Figure 5.16.

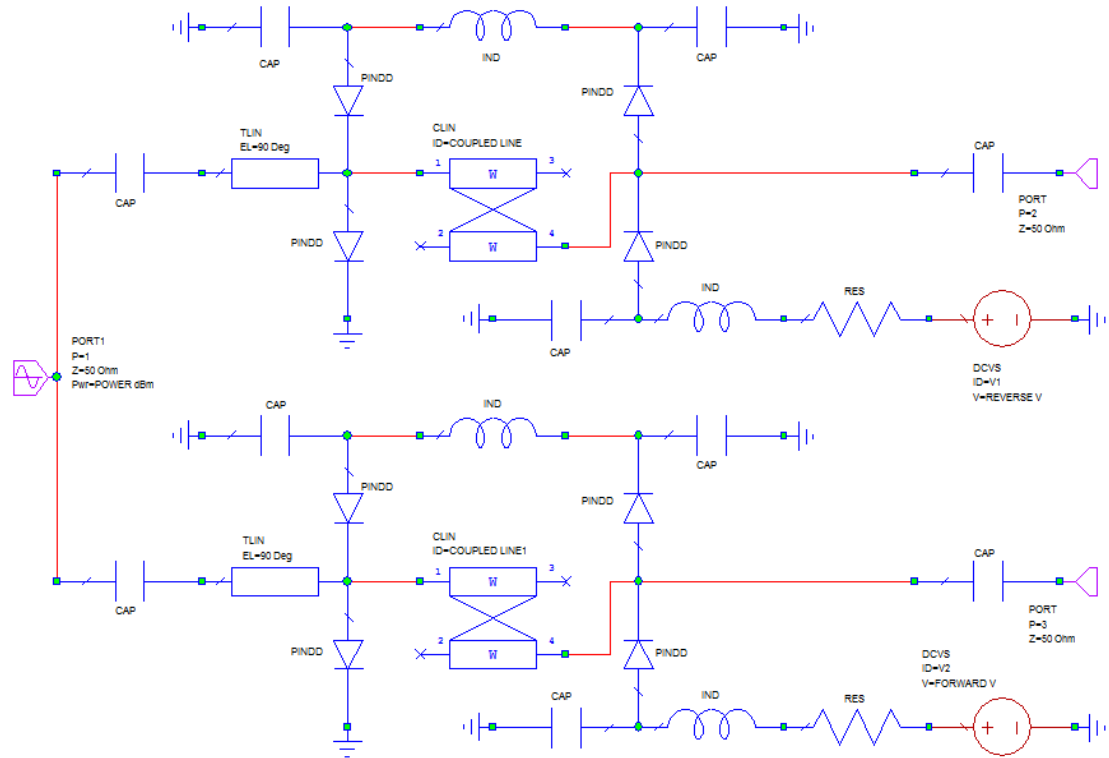


Figure 5.16: SPDT Switch with Increased Power Handling and Isolation with Low DC Current Consumption

The circuit in Figure 5.16 can be optimized for X-Band by adjusting the line lengths, widths and line spacing of coupled lines. The optimization done using ideal components of the simulation tool, the circuit has S-parameters as shown in Figure 5.17. Note that such a circuit has better than 14dB return loss at X-Band frequencies. Also, more than 70dB isolation can be obtained with only 20mA DC current. In such a circuit with increased isolation, the power dissipation capability of the PIN diodes closer to the junction is more critical than those closer to the output port since each diode closer to the junction carries half of the peak RF current but the others do not. One limitation of this structure is that PIN diodes in this circuit cannot be heat sunk as good as the designs in Chapter 3 since RF ground is provided by shunt capacitors to ground from one electrode of the PIN diodes.

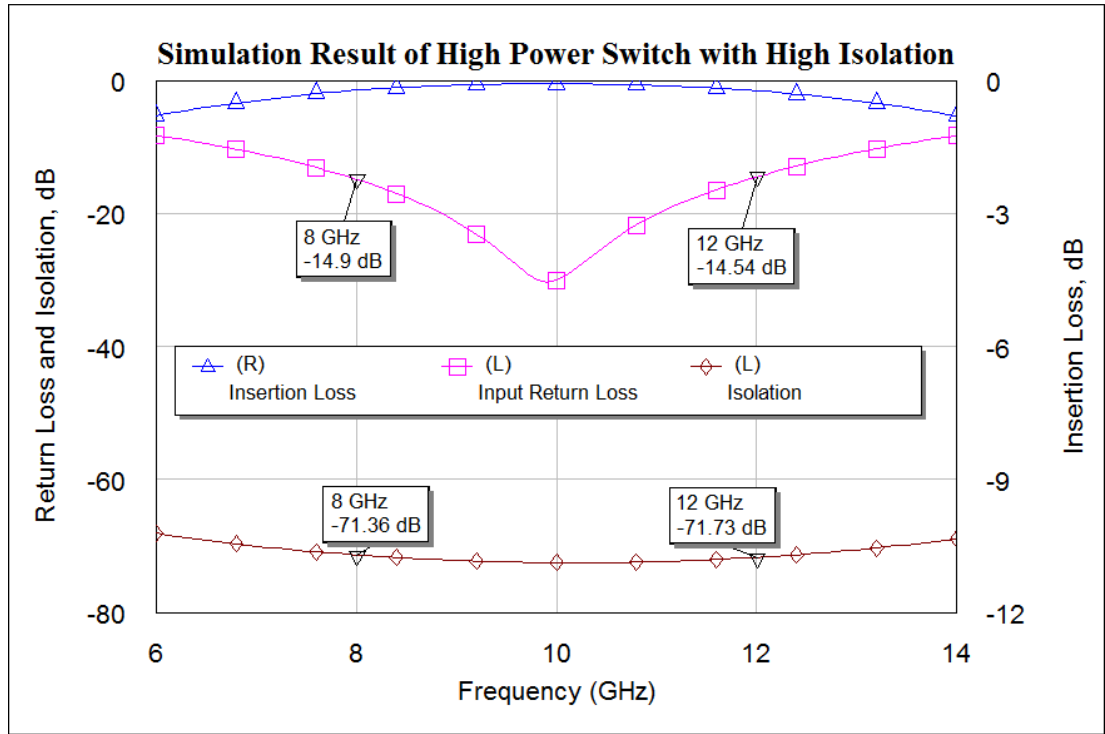


Figure 5.17: S-Parameters of SPDT Switch Given in Figure 5.16

Design of a high power switch with high isolation and low DC current consumption is introduced in this section. Considering the power handling analysis given in Section 5.3, this structure is expected to handle more power than the regular designs with one PIN diode at each arm. If this structure is used in a Tx/Rx switching application, sensitive receive line will be protected better since the isolation is higher.

CHAPTER 6

CONCLUSION

Microwave/RF switches are one of the most widely used components in radar and communication systems with their main purpose of choosing the desired path for the RF signal. Switches can be used for different functions, such as band select and Tx/Rx switching. Switches are evaluated by a number of specifications. Those are mainly insertion loss, return loss, isolation, switching speed and size. For radars detecting targets at long distance, ability to switch high power signals is also an important feature.

In this thesis study, SPDT PIN diode switches with different power handlings are designed and fabricated. The operating frequencies of all switches cover full X-Band. Power handlings of the designs are 9W, 70W and 80W CW. S-parameters, switching speeds and pulsed power handling of the switches are also measured. The products have maximum 0.9dB insertion loss and approximately 30dB isolation. In addition to designs, critical design rules are given. How to increase the power handling is analyzed. A design on increasing the power handling is done, fabricated and measured. Using the same PIN diodes 18W CW power handling is obtained with approximately same amount of temperature rise.

At the beginning of this thesis work, the studies on high power switching are investigated. Advantages and disadvantages of different switch types are analyzed and it is decided to construct PIN diode switches for the high power applications in this study. Similarly, the PIN diode switch topologies are evaluated with respect to their advantages and disadvantages on high power switching. All shunt topology is

chosen since the critical components can be better heat sunk. Also, all shunt topology has low insertion loss and good isolation within enough bandwidth to cover X-Band.

Second step was to choose the appropriate PIN diodes for the applications. Three different PIN diodes are chosen for different power handling levels. Each PIN diode is measured and characterized. Based on these measurements, three SPDT switches are designed for X-Band. These switches were expected to handle 9W, 70W and 80W CW signals. The power handling expectations are justified when the high power measurements are conducted. All switches have less than 0.9dB insertion loss, better than 15dB return loss and approximately 30dB isolation. Switching speeds are 70ns, 450ns and 1100ns respectively. An analysis related to establishing the minimum reverse bias [15] is investigated. Depending on the I-region thicknesses of PIN diodes, the switches are biased at only -5V. Although -5V is far less than the peak RF voltages at these power levels, appreciable amount of harmonic suppression is obtained. All these high power switches are assembled on a 7mm x 5mm carrier, which can be considered quite small when compared with their electromechanical counterparts.

Finally, failure mechanisms of PIN diodes at high power levels are given. Related critical design rules are given in order to draw attention on components whose probability of failure is ignored by many designers. An example of such component is the RF choke inductor. Keeping these failure mechanisms, it is mentioned about how to increase the power handling. Using the same PIN diodes as 9W CW switch, a switch with 18W CW power handling with approximately similar temperature rise is designed and fabricated. Inserting additional PIN diodes quarter wavelength away higher isolation can be obtained. Combining these two approaches, a high power switch with higher isolation is introduced. Since there are four PIN diodes in this structure, a method for decreasing the DC power consumption is shown. In this method, quarter wavelength transmission line is realized with coupled lines.

Especially for urgent needs in measurement setups, higher power switches can be realized using the PIN diodes in stocks. A future work can be the realization of such higher power switches with high isolation and low DC current consumption.

REFERENCES

- [1] Hindle, P., "The State of RF/Microwave Switches", *Microwave Journal*, Vol.53, No.11, November 2010, pp. 20-36.
- [2] Hiller, G.; Cory, R., "A High Power Solid State T-R Switch" *Electronica*, July/August 2009.
- [3] Shigematsu, T.; Suematsu, N.; Takeuchi, N.; Iyama, Y.; Mizobuchi, A., "A 6-18 GHz SPDT Switch Using Shunt Discrete Pin Diodes", *IEEE Int'l Microwave Symposium*, pp. 527-530 Vol.2, 1997.
- [4] Sherman, J., "A PIN Diode Switch that Operates at 100W CW at C-Band", *IEEE Int'l Microwave Symposium*, pp. 1307-1310 Vol.3, 1991.
- [5] Tenenholtz, R., "A 2000 Watt CW MIC 20-500MHz SPDT PIN Diode Switch Module", *IEEE Int'l Microwave Symposium*, pp. 252-254, 1981.
- [6] Bellantoni, J.V.; Bartle, D.C.; Payne, D.; McDermott, G.; Bandla, S.; Tayrani, R. & Raffaelli, L., "A Monolithic High Power Ka Band PIN Switch", *IEEE Microwave and Millimeter-Wave Monolithic Circuits Symposium*, pp. 47-50, 1989.
- [7] Kintigh, D.W. & Niblack, W.K., "High-Power 2-9 GHz Solid State Switch", *IEEE Int'l Microwave Symposium*, pp. 54-56, 1982.
- [8] Brown, E.; Snodgrass, D.; Hebeisen, M., "SPDT Switch MMIC Enables High-Performance Ka-band Tx/Rx Module", *Defence Electronics*, October 2007.
- [9] Ayasli, Y.; Mozzi, R.; Hanes, L.; Reynolds, L.D., "An X-Band 10W Monolithic Transmit-Receive GaAs FET Switch", *Microwave and Millimeter-Wave Monolithic Circuits*, vol.82, pp. 42-46, June 1982.
- [10] Schindler, M.J.; Kazior, T.E., "A High Power 2-18 GHz T/R Switch", *IEEE Int'l Microwave Symposium*, vol. 1, pp. 453-456, May 1990.
- [11] Janssen, J.; Van Heijningen, M.; Hilton, K.P.; Maclean, J.O.; Wallis, D.J.; Powell, J.; Uren, M.; Martin, T.; Van Vliet, F., "X-Band GaN SPDT MMIC with

- over 25 Watt Linear Power Handling”, *Microwave Integrated Circuit Conference EuMIC*, pp. 190-193, October 2008.
- [12] Campbell, C.F.; Dumka, D.C., “Wideband High Power GaN on SiC SPDT Switch MMICs”, *IMS 2010 Conference, Anaheim, CA*.
- [13] Skyworks Solutions, “Design with PIN Diodes”, APN1002, www.skyworksinc.com.
- [14] Agilent Technologies, “Understanding RF/Microwave Solid-State Switches and Their Applications”, Literature Number: 5989-7618EN, 2008.
- [15] Hiller, G.; Caverly, R., “Establishing the Minimum Reverse Bias for a PIN Diode in a High Power Switch”, *IEEE Transactions on Microwave Theory and Techniques*, vol. 38, no. 12, pp. 1938-1943, December 1990.
- [16] Hines, M. E., “Fundamental Limitations in RF Switching and Phase Shifting Using Semiconductor Diodes”, *Proceedings of the IEEE*, vol. 52, pp. 697-708, June 1964.
- [17] Goldfarb, M. E.; Platzker, A., “Losses in GaAs Microstrip”, *IEEE Transactions on Microwave Theory and Techniques*, vol. 38, pp. 1957-1963, December 1990.
- [18] Hiller, G.; Caverly, R., “The Reverse Bias Requirement for PIN Diodes in High Power Switches and Phase Shifters”, *IEEE MTT-S Int. Microwave Symp. Dig.*, May 1990.
- [19] Lucovsky, G.; Schwarz, R.; Emmons, R., “Transit Time Considerations in PIN Diodes”, *J. Appl. Phys.*, vol. 35, no. 3, pt. 1, p. 622, March 1964.
- [20] Caulton, M.; Rosen, A.; Stabile, P.; Gombar, A., “PIN diodes for Low Frequency, High Power Switching Applications”, *IEEE Transactions on Microwave Theory and Techniques*, vol. MTT-30, pp. 876-881, June 1982.
- [21] Sze, S. M., *Physics of Semiconductor Devices*, New York: Wiley-Interscience, 1981.
- [22] Wang, S., *Fundamentals of Semiconductor Theory and Device Physics*, Englewood Cliffs, NJ: Prentice Halls, 1989.
- [23] Caverly, R.; Hiller, G.; Caverly, R., “Distortion in Microwave and RF Switches by Reverse Biased PIN Diodes”, *IEEE MTT-S Int. Microwave Symp. Dig.*, vol. 3, pp. 1073-1076, June 1989.